The Roles and Mechanisms of Electro-Activated Liquid Chemicals on the Inactivation of the Abnormal Prion Protein of Chronic Wasting Disease

Livia Renaud

A thesis submitted to the University of Ottawa
in partial fulfillment of the requirements for the
Master of Science Degree in Cellular and Molecular Medicine

Department of Cellular and Molecular Medicine
Faculty of Medicine
University of Ottawa

Abstract

Transmissible spongiform encephalopathies (TSEs) are a group of fatal neurodegenerative diseases caused by the conversion of normal prion protein (PrP^{C}) into an abnormal, infectious form (PrP^{Sc}). These diseases affect various mammals, including Creutzfeldt-Jakob (CJD) disease in humans, bovine spongiform encephalopathy (BSE) in cattle, scrapie in goats and sheep, and chronic wasting disease (CWD) in cervids. This study investigated environmentally friendly electro-activated liquid chemicals (EALCs) as alternative prion disinfectants to the harsh chemicals conventionally used for decontamination. Brain homogenates from CWD-infected elk were treated with various EALCs (four catholytes, five anolytes, commercial CAC-717 and BrioHOCl), NaOH and bleach, all shown to be bactericidal. Treatment was followed by the quantitative detection of residual seeding activity of PrP^{Sc} by real-time quaking-induced conversion (RT-QuIC) and protein misfolding cyclic amplification (PMCA) assay. The results showed that Catholyte 4 and CAC-717 achieved 1,000- to 10,000-fold reductions in seeding activity, while NaOH and bleach eliminated detectable amplification. Other EALCs demonstrated variable efficacy depending on treatment concentration and sample type, with BrioHOCl and Anolyte 2 showing greater reductions on surface-bound PrP^{Sc} than in tissue homogenates. These findings support the potential of selecting EALCs as practical alternatives for prion decontamination.

Acknowledgments

First, thank you to my supervisor, Dr. Wandong Zhang, for taking me on as a student and allowing me to conduct this research. His continuous support and guidance were crucial in the successful completion of this thesis.

I would also like to express my deepest appreciation to the CFIA and Dr. Hongsheng Huang for allowing me the laboratory space and budget to conduct this work. Without him, neither this project nor this thesis could have come together.

I would also like to thank my thesis advisory committee, Dr. Marc-André Langlois, Dr. Hsiao-Huei Chen, and Dr. Gordon Mitchell, for their helpful feedback, suggestions, and support during each stage of this research.

Furthermore, there is a long list of CFIA OLF individuals who have been instrumental in the design, development, and execution of this project. Specifically, I would like to thank members from Dr. Mitchell Gordon and Dr. Jiewen Guan's laboratories, Maria Arifin, Tamara Morrill, William Pilot, and Andrei Soutyrine, for sharing their extensive knowledge and always answering my questions.

Lastly, I would like to thank all those who have contributed to my personal growth and development. To my mother, Elissa, thank you for your unwavering love and support at home. To my loved ones, friends, and extended support system: thank you for celebrating my successes, lifting me during setbacks, and helping me stay focused. Your love and spirit continuously pushed me to strive for my best.

Table of Contents

Abbreviations

Ab-I	Primary monoclonal antibody
Ab-II	Secondary antibody
AD	Alzheimer's disease
AEM	Anion exchange membrane
ALS	Amyotrophic lateral sclerosis
ASO	Antisense oligonucleotides
BHI	Brain heart infusion
BSC	Biosafety cabinet
BSE	Bovine spongiform encephalopathy
cBSE	Classical bovine spongiform encephalopathy
CD	Circular dichroism
CEM	Cation exchange membrane
CFIA	Canadian Food Inspection Agency
CFU	Colony-forming units
CJD	Creutzfeldt-Jakob disease
CL-2	Containment level - 2
CNS	Central nervous system
cryo-EM	Cryo-electron microscopy
CSF	Cerebrospinal fluid
CT	Cycle threshold
CWD	Chronic wasting disease
dH_2O	Distilled water
EALC	Electro-activated liquid chemical
EEG	Electroencephalogram
ELISA	Enzyme-linked immunosorbent assay
EUE	Exotic ungulate spongiform encephalopathy
fCJD	Familial CJD
FFI	Fatal Familial Insomnia
FSE	Feline spongiform encephalopathy
FT-IR	Fourier transform-infrared spectroscopy
GPI	Glycosylphosphatidylinositol
GSS	Gerstmann-Sträussler-Scheinker Syndrome
hGH	Human growth hormone
HOCl	Hypochlorous acid
IBH	Infected brain homogenate
iCJD	Iatrogenic CJD
IHC	Immunohistochemistry
LAS	Lysosomal-autophagy system
LB	Lysogeny broth
MBM	Meat and bone meal
MRI	Magnetic resonance imaging

NaOCl	Sodium hypochlorite
NaOH	Sodium hydroxide
NaPTA	Sodium phosphotungstic acid
NBH	Negative brain homogenate
NMR	Nuclear magnetic resonance
NSEP	National Scrapie Eradication Program
NTC	No-template controls
OD	Optical density
OLF	CFIA Ottawa Laboratory – Fallowfield
ORP	Oxidation-reduction potential
PBS	Phosphate-buffered saline
PK	Proteinase K
PMCA	Protein misfolding cyclic amplification
PPE	Personal protective equipment
PRNP	Prion protein gene
PrP KO	Prion protein knockout
PrP^{C}	Normal cellular prion protein
PrP^{Sc}	Misfolded, disease-associated prion protein
recPrP	Recombinant prion protein
RFU	Relative fluorescent units
RT-QuIC	Real-time quaking-induced conversion
sCJD	Sporadic CJD
SDS	Sodium dodecyl sulphate
SNPs	Single-nucleotide polymorphisms
SRM	Specified risk material
ssNMR	Solid-state nuclear magnetic resonance
SW	Steel wire
TAB	Transient amyloid binding
TgElk	Transgenic mice overexpressing elk PrP
ThT	Thioflavin T amyloid dye
TIRFM	Total-internal-reflection microscopy
TME	Transmissible mink encephalopathy
TMTC	Too many to count
TSE	Transmissible Spongiform Encephalopathy
T_{stdev}	Fixed fluorescence threshold
UK	United Kingdom
UPS	Ubiquitin-proteasome system
vCJD	Variant Creutzfeldt-Jakob disease

List of Tables

List of Figures

1.0. Introduction

1.1 The Prion Protein

Normal cellular prion protein (PrP^{C}) is found on cell membranes attached via a glycosylphosphatidylinositol (GPI) anchor and is most highly expressed and concentrated in neurons in the central and peripheral nervous systems. Stanley Prusiner first identified this protein while investigating the infectious agent responsible for several neurodegenerative diseases. He named it the prion protein (PrP) and discovered that it existed in two forms: a normal cellular protein (PrP^{C}) and a misfolded, disease-associated variant (PrP^{Sc}) (Prusiner, 1982). While the precise and complete role of PrP^{C} is not as well defined, its pathogenic, misfolded isoform, PrP^{Sc}, has been implicated in several mammalian diseases, known as transmissible spongiform encephalopathies (TSEs) (Wulf et al, 2017), and is the infectious agent of interest for this thesis.

1.1.1 Definition and Characteristics

PrP^{C} is defined as a normal, endogenous prion protein expressed in several peripheral tissues but primarily in the nervous system of all mammals (Ford et al, 2002), while PrP^{Sc} is the pathogenic form responsible for disease. Though all mammals express PrP^{C}, only certain species of some families (Hominidae, Bovidae, including subfamilies Caprinae and Bovinae, Cervidae, Felidae, and Mustelidae) may contract prion diseases (Imran & Mahmood, 2011). PrP^{Sc} possesses several characteristics that make it a unique protein and have contributed to understanding protein-based infectious agents (Hughes & Halliday, 2017). These characteristics include its ability to induce and catalyze the misfolding of PrP^{C} into PrP^{Sc} (Kupfer et al, 2009), its resistance to proteolytic degradation and most disinfectants (Concha-Marambio et al, 2014), its tendency to aggregate into amyloid fibrils (Soto & Pritzkow, 2018), and its capacity to cause transmissible neurodegenerative diseases across different species (Igel et al, 2023). These characteristics challenge traditional ideas of infectious diseases by showing that a misfolded protein, lacking genetic material, can cause disease and emphasizing the importance of protein structure in disease pathology.

1.1.2 Structure and Function of the Prion Protein

PrP^C is encoded by the prion protein gene (*PRNP*) and is composed of approximately 253-265 amino acid residues (depending on the host species strain), forming a 32-35 kDa protein that is represented as an unstructured N-terminus region and a structured C-terminus domain (Atkinson et al, 2016). The N-terminal domain comprises three regions: a polybasic region, an octapeptide repeat region comprised of an octapeptide sequence repeated five times, and the post-octapeptide repeat region (Hara & Sakaguchi, 2020). As demonstrated in Figure 1, the C-terminal domain of PrP^C is predominantly in the form of α-helices, as opposed to the rather unstructured N-terminus. The C-terminus is the primary contributor to the stability of the protein due to its GPI-anchor and contributes to maintaining its correct folding for the protein's normal function. PrP^{Sc} is a conformational isoform of normal PrP^C, meaning they share an identical amino acid sequence, and are believed to originate through a tertiary structural change. During the conversion, the α-helical core of PrP^{Sc} (42% α-helix, 3% β-sheet) condenses and is partially converted into β-sheets, resulting in PrP^{Sc} with a significantly altered structure (30% α-helix, 43% β-sheet), which can aggregate and form an amyloid fibril core (Wulf et al, 2017; Atkinson et al, 2016).

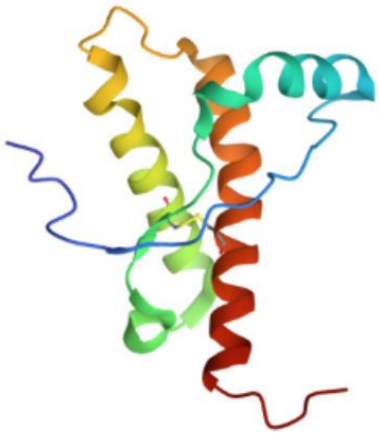

Figure 1. Nuclear magnetic resonance (NMR) ensemble of the Elk prion protein PrP^C from *Cervus canadensis nelsoni*. Image from the RCSB PDB (RCSB.org) of PDB ID 1XYW (Gossert, A.D., et al. (2005). Prion protein NMR structures of elk and of mouse/elk hybrids. *Proc.Natl.Acad.Sci.USA* 102: 646-650).

The function of PrP^{Sc} has been explored more extensively than that of PrP^{C}, which has been primarily examined as the precursor protein for prion diseases. Over the last few decades, the role of PrP^{C} has been explored not only for its role in prion disease but also for its involvement in normal cellular processes, including cell signalling, neuroprotection, and synaptic function (Westergard et al, 2007). PrP^{C} has been shown to interact with ion channels, receptors, and signalling molecules, contributing to synaptic transmission and neuronal excitability (Panes et al, 2021). Additionally, it plays a neuroprotective role by engaging stress-inducible proteins and activating pathways that mitigate oxidative stress, promoting neuronal survival under adverse conditions (Lo et al, 2007). Notably, the pathological implications of PrP^{C} extend beyond prion diseases. Contrary to its neuroprotective characteristics, in neurodegenerative conditions such as Alzheimer's disease (AD), PrP^{C} has been identified as a mediator of toxic signalling pathways triggered by β-amyloid oligomers, exacerbating synaptic dysfunction (Fulek et al, 2025). The protein is thought to have many other applications and roles within the body; however, further research is needed to fully understand the role of PrP^{C}.

Studies have worked to identify the roles of PrP^{C} through experiments using transgenic prion protein knockout (PrP KO) mice. Initially, though it appeared as the mice developed relatively typical, subtle neurophysiological defects and behavioural abnormalities have since been noted. Most notably, PrP KO demonstrated complete resistance to prion diseases. Originally designed to challenge the prion hypothesis, these knockout models ultimately provided strong evidence in its favour. When inoculated with infectious prions, all wild-type mice developed prion disease, whereas PrP KO mice remained unaffected, demonstrating that endogenous PrP^{C} is essential for contraction of the disease (Weissmann & Büeler, 2004). Although PrP KO mice resist prion diseases, the absence of endogenous PrP^{C} leads to physiological and behavioural abnormalities. Many studies have found abnormalities in PrP KO mice are more likely to have adverse cognitive effects, have difficulties with learning, social behaviour, and sleep regulation, show increased levels of anxiety and depression, and even have increased trouble with locomotion (Schmitz et al, 2014).

Overall, while research has provided valuable insight into the nature of PrP^{C} in both disease processes and normal physiological functions, many aspects of this protein remain unknown. Further studies are needed to fully characterize the functions of the PrP gene and the PrP^{C} protein.

1.2 Mechanisms of Pathogenic Prion Propagation

PrP^{Sc} propagation involves several important mechanisms, which are different from traditional pathogen replication due to the absence of nucleic acids. The process begins with the initial conformational conversion of PrP^{C} into PrP^{Sc} involving the conversion of alpha-helices in PrP^{C} into β-sheets in PrP^{Sc}. PrP^{Sc} then acts as a template, inducing the misfolding of other PrP^{C} molecules upon direct contact, which supports a chain reaction as more PrP^{C} molecules are converted into PrP^{Sc} (Kupfer et al, 2009). Misfolded PrP^{Sc} then aggregates into amyloid fibrils, which break into smaller fragments and act as seeds to convert additional PrP^{C} into PrP^{Sc}, further contributing to the amplification of infectious PrP^{Sc} (Soto & Pitzkow, 2018). Following exposure to PrP^{Sc}, it can be taken up by cells through endocytosis, and once inside the cell, PrP^{Sc} interacts with PrP^{C} in intracellular compartments, promoting further conversion. Prions can then spread to neighbouring cells via exocytosis or tunnelling nanotubes between cells (Alves et al, 2020). Inter-species propagation has also been reported, though only a few prion strains and species have demonstrated real-life evidence of this phenomenon (Houston & Andréoletti, 2018). Together, these mechanisms contribute to the self-propagating nature of prions, leading to the progressive accumulation of PrP^{Sc} and the subsequent progression of disease, resulting in neurodegeneration and eventually death.

1.2.1. PrP^{C} to PrP^{Sc} Conversion Models

The conversion of PrP^{C} to PrP^{Sc} is a crucial process in the progression of prion diseases and involves structural changes altering the conformation of PrP^{Sc} aggregates (Kupfer et al, 2009). As seen in Figure 2, two main theories exist to explain the conversion of PrP^{C} to PrP^{Sc}: the seeding/nucleation model and the template-assisted model (Abid & Soto, 2006). According to the seeded nucleation model, PrP^{C} and PrP^{Sc} isoforms naturally exist in equilibrium, with the correctly folded isoform being endogenously dominant.

Cellular production of more PrP^{C} may alter the equilibrium, encouraging the conversion of more PrP^{C} to PrP^{Sc} (Atkinson et al, 2016). The production of tiny aggregates of misfolded protein is the gradual and rate-limiting phase in the development of illness. Together, the aggregates, also called nuclei, attract and transform PrP^{C} to eventually create bigger fibrillar aggregates which convert further PrP^{C} inefficiently due to the limited number of exposed ends compared to their infectious isoform. For continued propagation, fibrils must fragment to generate new nuclei, or "seeds," which accelerate PrP^{Sc} conversion through fragmentation (Marrero-Winkens et al, 2020).

The template-assisted model describes that a conformational intermediate is formed during the interaction of PrP^{C} and PrP^{Sc} isoforms, which is catalyzed, and PrP^{C} is then given the refolding instructions contained within the original PrP^{Sc}. It has also been proposed that PrP^{Sc} possesses certain enzymatic properties capable of catalyzing the conformational change of PrP^{C}. According to the template-assisted model, the primary infectious unit is a monomer of PrP^{Sc}, which initially forms a PrP^{C}-PrP^{Sc} heterodimer that transitions into homodimeric PrP^{Sc} capable of interacting with other PrP^{Sc} molecules and forming large aggregates, though large aggregates are not necessary for prion replication (Abid & Soto, 2006).

While both models describe important aspects of prion conversion, the seed nucleation model focuses on the aggregation dynamics and the critical role of nucleation in PrP^{Sc} propagation, whereas the template-directed model primarily addresses molecular interactions and direct conformational templating.

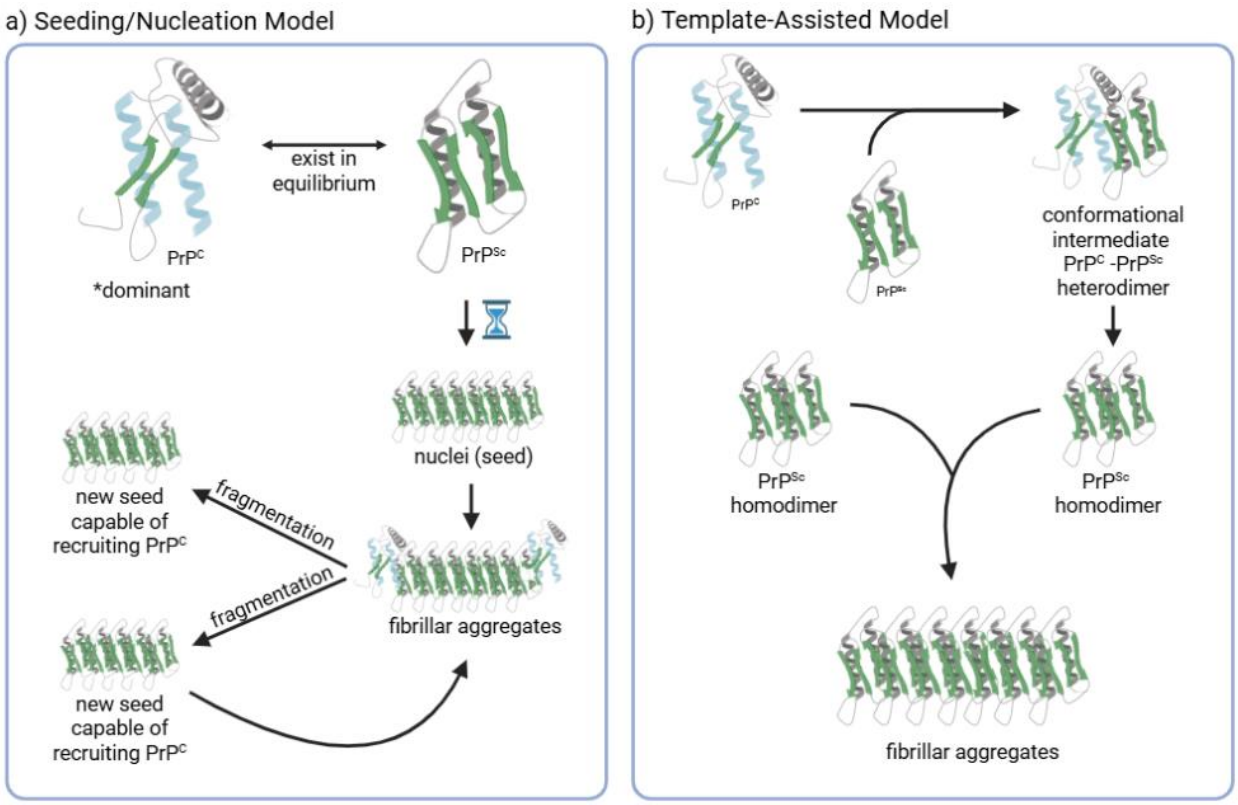

Figure 2. The main models hypothesized to be responsible for converting PrP^{C} to PrP^{Sc}. a) The seeding/nucleation model suggests that PrP^{C} and PrP^{Sc} naturally exist in equilibrium, with PrP^{C} being the more stable and dominant form. Over time, small aggregates of PrP^{Sc} (called seeds) can slowly form. Once formed, these seeds recruit additional PrP^{C} and convert it into PrP^{Sc}, leading to larger fibrillar aggregates. Fragmentation of these fibrils produces new seeds, allowing the process to continue and spread. b) The template-assisted model describes a more direct mechanism, where PrP^{Sc} interacts with PrP^{C} and guides its misfolding through a temporary intermediate structure. This interaction forms a PrP^{C}–PrP^{Sc} heterodimer, which transitions into PrP^{Sc} homodimers capable of further conversion. These newly formed PrP^{Sc} molecules may eventually cluster into larger aggregates, although large aggregates are not required for prion propagation.

1.2.2 PrP^{Sc} Aggregation Mechanisms

PrP^{Sc}'s characteristic loss of cellular PrP^{C} functions, and its ability to form aggregates, represent a fundamental aspect of its disease etiology. The increased β-sheet content of PrP^{Sc} demonstrates its conformational differences from its endogenous counterpart, PrP^{C}, making it prone to aggregation (Poggiolini et al, 2013).

Aggregation begins with nucleation which describes the spontaneous assembly of PrP^{Sc} monomers into small, unstable aggregates that act as seeds. These initial seeds are responsible for recruiting further PrP^{C} to PrP^{Sc}, and nucleation is often the rate-limiting step in the aggregation process, as this step can take years for some prion strains (Soto & Pritzkow, 2018). Once seeds form, oligomerization follows, with PrP^{C} being recruited and converted into PrP^{Sc}, leading to the growth of protofibrils. (Foliaki et al, 2020). Once protofibrils reach a certain size, they aggregate into larger structures called amyloid plaques, which can be deposited in tissues and disrupt healthy organs and cellular processes, especially in the central nervous system (CNS), causing neurodegenerative pathologies (Stefani & Rigacci, 2013).

The process of fragmentation also plays a crucial role in PrP^{Sc} propagation. Existing fibrils can fragment, generating new seeds or nuclei that can initiate and accelerate further aggregation. Fragmentation enhances the spread of prion aggregates within tissues and has been shown to increase the potential for cross-species transmission in cases of zoonotic prion diseases (Marrero-Winkens et al, 2020). Because PrP^{Sc} aggregates resist degradation, they accumulate over time, leading to cellular dysfunction and the progressive neurodegenerative symptoms characteristic of prion diseases (Hughes & Halliday, 2017).

1.2.3. PrP^{Sc} Stability

Endogenously, cellular protein control and degradation rely on two key pathways: the ubiquitin-proteasome system (UPS) and the lysosomal-autophagy system (LAS). The UPS degrades misfolded or damaged proteins by tagging them with ubiquitin and directing them to the proteasome for breakdown. The LAS is initiated by the delivery of proteins through several endolysosomal pathways into autophagosomes, which

fuse with lysosomes for degradation. Once within the lysosome, many enzymatic activities occur, including proteolytic enzymes capable of digesting PrP^{C} (Goold et al, 2015). Despite these functional and practical mechanisms for most endogenous proteins, PrP^{Sc} is resistant to both pathways due to its extreme molecular stability, which regulates its infectivity, persistence, and resistance to degradation. The increase in β-sheet structure promotes intermolecular hydrogen bonding, forming tightly packed amyloid-like aggregates that resist unfolding and proteolytic degradation (Wille & Requena, 2018).

This molecular stability has direct implications for prion disease transmission and strain diversity. Differences in glycosylation patterns and disulphide bond stability affect PrP^{Sc} aggregation kinetics and structural resilience (Bosques & Imperali, 2003). Prion strains with tighter β-sheet packing and lower susceptibility to fragmentation tend to be more persistent in the environment and within tissues. In contrast, strains that are more prone to fragmentation may replicate more efficiently, influencing disease progression and cross-species transmission (Cobb et al, 2013).

The stability of PrP^{Sc} is reflected in its resistance to proteinase K (PK) digestion, a technique commonly used to differentiate it from PrP^{C} which PK readily degrades. While the N-terminal region is more susceptible to PK digestion, the structured core of PrP^{Sc} (occasionally referred to as PrP 27-30, as this is the molecular weight range of the truncated protein after digestion) remains intact. Differences in PrP^{Sc} strain structure have been shown to influence the extent of PK resistance, with some strains exhibiting differing levels of sensitivity, but this protease-resistant fragment has been shown to retain infectivity and serves as a biochemical hallmark of prion diseases (Silva et al, 2015).

1.2.4. Prion Strains and Variants

Though all prion strains and variants are derived from the same protein, they are distinguished through unique biochemical and biophysical properties that affect the pathogenesis and clinical symptoms of the diseases they cause. Conformational variability of PrP^{Sc} is a determinant of strain diversity and has been proven using advanced in-vitro imaging technologies such as cryo-electron microscopy (cryo-EM) (Hoyt

et al, 2022) and solid-state nuclear magnetic resonance (ssNMR) (Manka et al, 2023). These studies have shown that the tertiary and quaternary structures differ distinctly from one prion strain to the next, proven through the differential arrangement and alignment of the β-sheet amyloid structure, affecting the overall stability and fold of the prion protein, therefore giving rise to unique strains (Prusiner, 2013). Total-internal-reflection microscopy (TIRFM) and transient amyloid binding (TAB) super-resolution microscopy have also been used to analyze fibril morphology, distinguishing strains and further showing differences in fibril diameter, length, elongation rate, and branching patterns exist between strains and affect the overall kinetics of the fibril (Sun et al, 2023). The evidence of prion strains affecting the molecular and clinical outcome of prion diseases has been compared to viral quasispecies. Viral quasispecies are a group of closely related but not identical viral particles that arise due to the high mutation rate of their genomes, while prion quasispecies have been hypothesized to describe a similar but not identical population of PrP^{Sc} conformations (Bartz, 2016). In conclusion, the biochemical and biophysical differences among prion strains highlight the complexity of this group of pathogens, suggesting that characterizing these variations is important for advancing our understanding of prion diseases and their treatment.

1.3 Transmissible Spongiform Encephalopathies – Pathogenic Prion Diseases

Transmissible spongiform encephalopathies (TSEs), also known as prion diseases, are a group of fatal mammalian neurodegenerative disorders largely believed to be caused by the accumulation of misfolded, pathogenic prion protein, PrP^{Sc}, in the CNS. These diseases include Creutzfeldt-Jakob disease (CJD) in humans, bovine spongiform encephalopathy (BSE) in cattle, and scrapie in sheep and goats (Bartz, 2016). Upon post-mortem investigation, the characteristic pathological features of TSEs include spongiform changes in brain tissue where vacuoles form due to neuronal loss and gliosis from misfolded PrP^{Sc} amyloid fibrils. The misfolding of PrP^{C} to PrP^{Sc} is unique as it is attributed to the self-propagating nature of this pathogen and its transmissibility, impacting the spread of disease within affected populations. Clinical manifestations vary depending on the type of TSE, host species, and the specific strain of PrP^{Sc}, but typically include rapidly progressive dementia, motor abnormalities, and in some cases, psychiatric symptoms

(Poggiolini et al, 2013; Eraña et al, 2020; Desai & Purzycki, 2023). Continued research in all aspects of prion biology and disease, from underlying molecular mechanisms to clinical therapeutic interventions, is an expanding field and is important for future work to combat these devastating diseases.

1.3.1 Historical Overview

The term "prion" was first coined by American neurologist and Nobel prize winner Stanley Prusiner in 1982 and is derived from Prusiner's description of the **pro**teinaceous **in**fectious particle responsible for the first described TSE, scrapie, a neurodegenerative and fatal disease affecting goats and sheep (Prusiner, 1982). In actuality, the evidence for the existence of prion diseases dates back centuries before Prusiner proposed his prion hypothesis. Scrapie was first documented in approximately 1732 in continental Europe during the Spanish scrapie epidemic and reported in an agricultural guide published in 1750 (Ness et al, 2023). Over the next two hundred years, research was done to understand how scrapie moved through flocks of animals, and by 1936 its transmissibility was conclusively demonstrated by Cuillé and Chelle, who showed that the disease could be experimentally transmitted to healthy sheep and goats through inoculation with infected brain material (Cuillé & Chelle, 1936).

The first human prion disease to be described, Creutzfeldt-Jakob disease (CJD), was noted in 1922, but at this time, the true cause of its symptoms remained unknown (Henry & Murphy, 2017). The first human prion disease to be formally recognized as a TSE was Kuru in 1957 by Dr. Carleton Gajdusek and Dr. Vincent Zigas and was the first TSE to be transmitted to chimpanzees in 1965, though at the time its pathogenic origin was unknown, and it was classified as a "slow unconventional virus disease" (Liberski et al, 2019). In 1968, another research group, Gibbs et al, successfully transmitted CJD to chimpanzees, sparking the idea that certain human neurodegenerative diseases, like scrapie in animals, were also transmissible and shared a common underlying agent. In 1971, Dr. Stanley Prusiner was introduced to a patient with CJD, which sparked his interest in "slow virus" diseases, leading to his prion hypothesis for which he later won the 1997 Nobel Prize in Medicine and Physiology (Stanley B. Prusiner - Biographica, 2024). Shortly after his Nobel Prize-winning ideas were proposed in 1982, curiosity about prions and TSEs

skyrocketed in popularity among researchers and the public due to the 1986 outbreak of BSE in Great Britain. By 1996, BSE was understood to be zoonotic and the cause of a new variant Creutzfeldt-Jakob disease (vCJD), leading to the death of 233 people and the slaughter of over 4.4 million cattle in the United Kingdom (UK) (Centres for Disease Control and Prevention, 2024). Since the early 2000s, ongoing prion research and diagnosis has grown and expanded greatly, though many characteristics of TSEs are dependent on the infected species and prion variant involved.

1.3.2 Human Prion Diseases

Human prion diseases are a group of rare, fatal neurodegenerative disorders caused by the accumulation of PrP^{Sc}, which induces PrP^{C} to adopt the same misfolded structure, leading to progressively fatal brain damage. The primary prion diseases in humans include Kuru, Creutzfeldt-Jakob Disease (CJD), variant Creutzfeldt-Jakob Disease (vCJD), Fatal Familial Insomnia (FFI), and Gerstmann-Sträussler-Scheinker Syndrome (GSS). Neuropathologically, prion diseases are marked by spongiform changes, neuronal loss, and gliosis in the brain (Soto & Satani, 2011). Clinical manifestations include rapidly progressive dementia, myoclonus, ataxia, visual disturbances, and behavioural changes. Unfortunately, there is no treatment or cure for any mammalian prion disease. Preventive strategies emphasize stringent infection control in medical settings and monitoring animal prion diseases to prevent zoonotic transmission. Research is focused on investigating prion propagation mechanisms, improving diagnostic methods, and exploring therapeutic interventions, with broader implications for other proteinopathies like Alzheimer's disease, Parkinson's disease, or amyotrophic lateral sclerosis (ALS) (Duyckaerts et al, 2019; McAlary et al, 2019).

1.3.2.1 Kuru

Kuru is a rare and fatal prion disease first reported in 1957 that was endemic to the native Fore people of Papua New Guinea. "Kuru" translates to "to be afraid" or "to shiver" in the native Fore language and describes the ataxia and involuntary tremors hallmarking the beginning stages of the disease (Gajdusek & Zigas, 1957). When Kuru was first discovered, it was thought to be a hereditary disease determined by a

single autosomal gene, dominant in women but recessive in men, as it occurred primarily in certain families and communities with a particular affinity for children and women. Shortly after its initial discovery, researchers came to understand that Fore kinship and social life involved a taboo custom: endocannibalism. This custom was deemed likely to be associated with the spread of Kuru as all parts of its victims (except for the gallbladder) were routinely consumed by family members (Liberski et al, 2019). At the time of Kuru's published description in 1957, TSEs had not yet been described, but the similarities between Kuru and scrapie were beginning to be noticed by researchers at the Rocky Mountain Laboratory after the transmission of Kuru to chimpanzees was successful (Hadlow, 2008). It is hypothesized that Kuru originated from the unlucky chance consumption of a single individual with sporadic CJD, and this hypothesis is supported by molecular and pathogenic similarities between the two diseases (Rossi et al, 2019). In the late 1950s and early 1960s, efforts to eliminate the practice of cannibalism were implemented by Australian administrators and missionaries. As cannibalism ceased, the incidence of Kuru dramatically declined (Alpers, 2008). However, Kuru has demonstrated a particularly long incubation period in certain individuals with incubation periods found to be as long as 56 years from the date the infection was acquired. It is estimated that Kuru's death toll is around 2,700 individuals, with the last confirmed kuru patient having died in 2005 (Alpers, 2005; 2008). After Kuru's publication in 1957, it would take 25 years for the infectious agent responsible for Kuru, prions, to be described in 1982 by Stanley Prusiner (Bonda et al, 2016). Kuru's distinct epidemiology and extended incubation period shed light on the significance of cultural traditions in the transmission of disease, as well as the detrimental effects of prion diseases.

1.3.2.2 Creutzfeldt-Jakob Disease (CJD)

Creutzfeldt–Jakob disease (CJD) was first described in Germany in 1922. It is a rare and progressive neurodegenerative prion disease with an incidence rate of only about one person per million globally every year, with about 350 cases diagnosed per year in the United States (Henry & Murphy, 2017; Sitammagari & Masood, 2024). The typical age of onset of symptoms in patients with CJD begins in their 70s and includes symptoms that are rather nonspecific and can be misdiagnosed as other common diseases

associated with aging, such as Alzheimer's disease or vascular dementia (Chitravas et al, 2011). Phenotypic variability of CJD symptoms is common, but classical illness features include neurological symptoms like dementia, along with impaired motor functions, generalized weakness, and akinetic mutism, alongside behavioural and psychiatric changes that progressively worsen over time (Katsikaki et al, 2021). There are three different modes of acquisition of CJD, each with its own associated biochemical and molecular profiles. Sporadic CJD (sCJD) descends from unknown, sporadic origins, and it is unclear as to why this disease affects certain individuals. Familial CJD (fCJD) is genetic and originates from several possible genetic mutations within the *PRNP* gene. Both iatrogenic CJD (iCJD) and variant CJD (vCJD) are acquired exogenously as they both originate from exposure to materials contaminated with CJD PrP^{Sc} (Centre for Disease Control and Prevention, 2024). The most common CJD diagnosed is sCJD accounting for roughly 85% of cases. Recently, Western blotting has been used as a classification tool for distinguishing between subgroups according to codon 129 methionine/valine polymorphisms of *PRNP* and profile of PrP^{Sc}, resulting in the distinction of six subtypes: MM1, MM2, MV1, MV2, VV1, and VV2, each with their own distinct set of molecular properties, disease progression timelines, and clinical manifestations (Bishop et al, 2010). Around 10-15% of CJD cases diagnosed are those of genetic origin, fCJD and typically present earlier in life than sporadic strains with onset ranging from about 30 to 70 years of age. Several mutations in the *PRNP* gene are associated with fCJD, including point mutations, insertions, and deletions that cause misfolded PrP^{Sc}. Mutations that are most associated with fCJD are E200K, D178N, and V210I (Kim et al, 2018; Zerr & Schmitz, 2021). Iatrogenic CJD (iCJD) is spread through medical procedures and represents an extremely small number of patients who have contracted the disease. Transmission of iCJD through medical interventions includes several documented routes. Early cases of iCJD have been linked to the use of cadaveric dura mater grafts, blood products, and human growth hormone (hGH), which were contaminated with prions from donors with undiagnosed CJD (Heath et al, 2006). Contaminated neurosurgical instruments that were inadequately sterilized have also been implicated in iCJD transmission, as PrP^{Sc} is notoriously difficult to inactivate and is not affected by hospital standard sterile disinfection procedures (Bonda et al, 2016). vCJD is the human form of BSE originating from consuming contaminated

beef products, which will be discussed in a subsequent heading. Overall, CJD is a rare yet deadly human prion disease with several forms that each present individual molecular, biochemical, and clinical characteristics.

1.3.2.3 Variant Creutzfeldt-Jackob Disease (vCJD)

Variant Creutzfeldt-Jakob disease (vCJD) presents several distinct characteristics distinguishing it from other forms of CJD. First identified in 1996 as a result of the consumption of BSE-contaminated beef and cattle products, vCJD is the only type of CJD that has been linked to zoonotic transmission with 233 cases reported worldwide as of 2021, most of which occurred in the UK (Centers for Disease Control and Prevention, 2024; National CJD Research and Surveillance Network, 2024). There have also been several documented cases of vCJD transmission through donated blood products where recipients of blood products from donors who later developed vCJD have contracted the disease themselves (USA Food and Drug Administration, 2022). With the average age of onset of symptoms being just 28, this form of CJD typically affects younger people. It frequently manifests with substantial psychiatric symptoms such as depression, anxiety, and behavioural changes, of which the symptoms are less common in other CJD variations. As opposed to the rapid neurological deterioration observed in sCJD, the disease course in vCJD typically lasts 14 months (Lizroth et al, 2015). Though a concrete diagnosis of vCJD requires post-mortem examination of neural tissues, medical professionals use several techniques to diagnose vCJD. Diagnostic methods such as EEG visualization or cerebrospinal fluid (CSF) 14-3-3 protein tests that prove to be useful for the diagnosis of sCJD have unfortunately not demonstrated comparable usability for vCJD, demonstrating variability between the forms of CJD (Connor et al, 2019). Genetic susceptibility to vCJD is significantly influenced by polymorphisms in *PRNP*, particularly at codon 129 which encodes either methionine (M) or valine (V). Individuals who are homozygous for methionine (MM genotype) at codon 129 are more susceptible to vCJD. Heterozygous (MV) or valine homozygous (VV) individuals are recognized to be less susceptible to vCJD, though it has not been shown that this phenomenon is due to a conferred resistance to infection and could be attributed to an extension in the incubation period (Pauly et al, 2022). The number

of diagnosed cases of vCJD continues to decline, which can be attributed to public health measures in the UK and worldwide (Watson et al, 2021). Thanks to modern science and food safety measures, the relative risk of contracting vCJD is extremely low, though it is important to continue research to further understand zoonotic prion diseases, improve detection and decontamination methods, and ensure that preventive measures remain in place for the sake of public health.

1.3.2.4 Fatal Familial Insomnia (FFI)

Fatal Familial Insomnia (FFI) is a rare, autosomal dominant prion disease characterized by a mutation in the *PRNP* gene at codon 178 (D178N substitution), producing a misfolded prion protein. First described in 1986 by Italian professor Elio Lugaresi (Lugaresi et al., 1986), by 1998, 40 families were recognized as carriers for FFI, most of which originated from European or Asian descent. In 2011, one additional family was discovered to be of Egyptian descent, though most new diagnoses are occurring in China, where the incidence rate of the disease has been increasing (Zhang et al, 2022). FFI causes progressively worsening neurodegeneration, especially in the dorsomedial nuclei of the thalami, which play an important role in regulating the circadian rhythm and various other autonomic functions. The median age onset of FFI is 48 and is marked by rapidly progressive and intractable insomnia resulting in a mean survival time of 13 months (Nafe et al, 2023). As the disease advances, patients experience a range of autonomic dysfunctions, including hyperhidrosis, tachycardia, hypertension, and psychological disturbances, which contribute to a dramatic decline in quality of life (Chu et al, 2022). The mutation responsible for FFI is a point mutation at codon 178, where an aspartic acid (D) is replaced by an asparagine (N), represented as D178N. For this mutation to induce FFI, a methionine must be present at position 129, as a valine in this position would rather induce fCJD (Gambetti et al, 1995). Unfortunately, FFI is no different from other TSEs in that there is no cure or treatment currently available and disease management usually is centered around improving quality of life.

1.3.2.5 Gerstmann-Sträussler-Scheinker Syndrome (GSS)

First described in 1936 in Austria (Zhao et al, 2019), Gerstmann-Sträussler-Scheinker Syndrome (GSS) is an uncommon, slowly progressing familial prion disease accounting for between 10% and 15% of cases of human TSEs. It is not unusual for individuals with GSS to have an autosomal dominant family history of unidentified illness causing death during the fifth or sixth decade, without receiving a definitive diagnosis until genetic testing is done. For this reason, and due to the phenotypic variability of the disease, it is thought that the number of GSS cases is likely underdiagnosed (Chen et al, 2023). As the disease progresses over the average five-to-six-year life expectancy, symptoms progress from impaired motor functions and ataxia to include psychological disturbances, parkinsonism, and usually dementia towards the end of life (Chen et al, 2024). GSS is an inherited prion disease linked to several mutations within the *PRNP* gene. The most common mutation associated with GSS is P102L (proline to leucine at codon 102), but as of late 2022, at least 15 less common mutations within the *PRNP* gene have been reported in more than 50 families affected by GSS including P105L, A117V, G131V, Y145stop, F198S, D202N, Q217R, and M232T (Chen et al, 2024). These mutations all result in the production of pathogenic PrP^{Sc} capable of forming aggregates responsible for the neurodegeneration characterizing this class of diseases. Currently, there is no treatment or cure found to be effective against GSS and early diagnosis via pre-mortem genetic testing is necessary to avoid misdiagnosis. Once a diagnosis of GSS has been issued, palliative care typically ensues as symptoms progress and focuses on improving quality of life (Chen et al, 2023).

1. 3. 3. Animal Prion Diseases

Though all TSEs originate from the misfolding of endogenous prion proteins into their pathogenic PrP^{Sc} isoforms, non-human TSEs and human TSEs differ in their host species, transmission dynamics, and epidemiology (Moreno & Telling, 2017). Animal TSEs include scrapie, BSE, chronic wasting disease (CWD), transmissible mink encephalopathy (TME), feline spongiform encephalopathy (FSE), and exotic ungulate spongiform encephalopathy (EUE) (Imran & Mahmood, 2011). While many prion disorders are often limited to a single or small group of closely related species, certain prions are not species-specific.

Prion protein sequences exhibit strong evolutionary conservation across mammalian species (Figure 3). This high level of conservation helps explain the fundamental similarities in prion biology across mammals (Prusiner, 1998).

Fears regarding the transmission of TSEs heightened after it was shown that BSE is zoonotic, has a broad host range, and can cross species barriers as transmissibility has been successful to several other mammals such as sheep, non-human primates including lemurs and macaques, cats and others (Marín-Moreno et al, 2020; Simmons et al, 2016). Commercial sanctions related to outbreaks of animal TSEs have resulted in billions of dollars of losses, as well as the loss of millions of individual animals (Petigara et al, 2011). These factors have led to the implementation of control or eradication initiatives in several nations, targeting TSEs affecting livestock to reduce and control the spread of these deadly diseases (Canadian Food Inspection Agency, 2023).

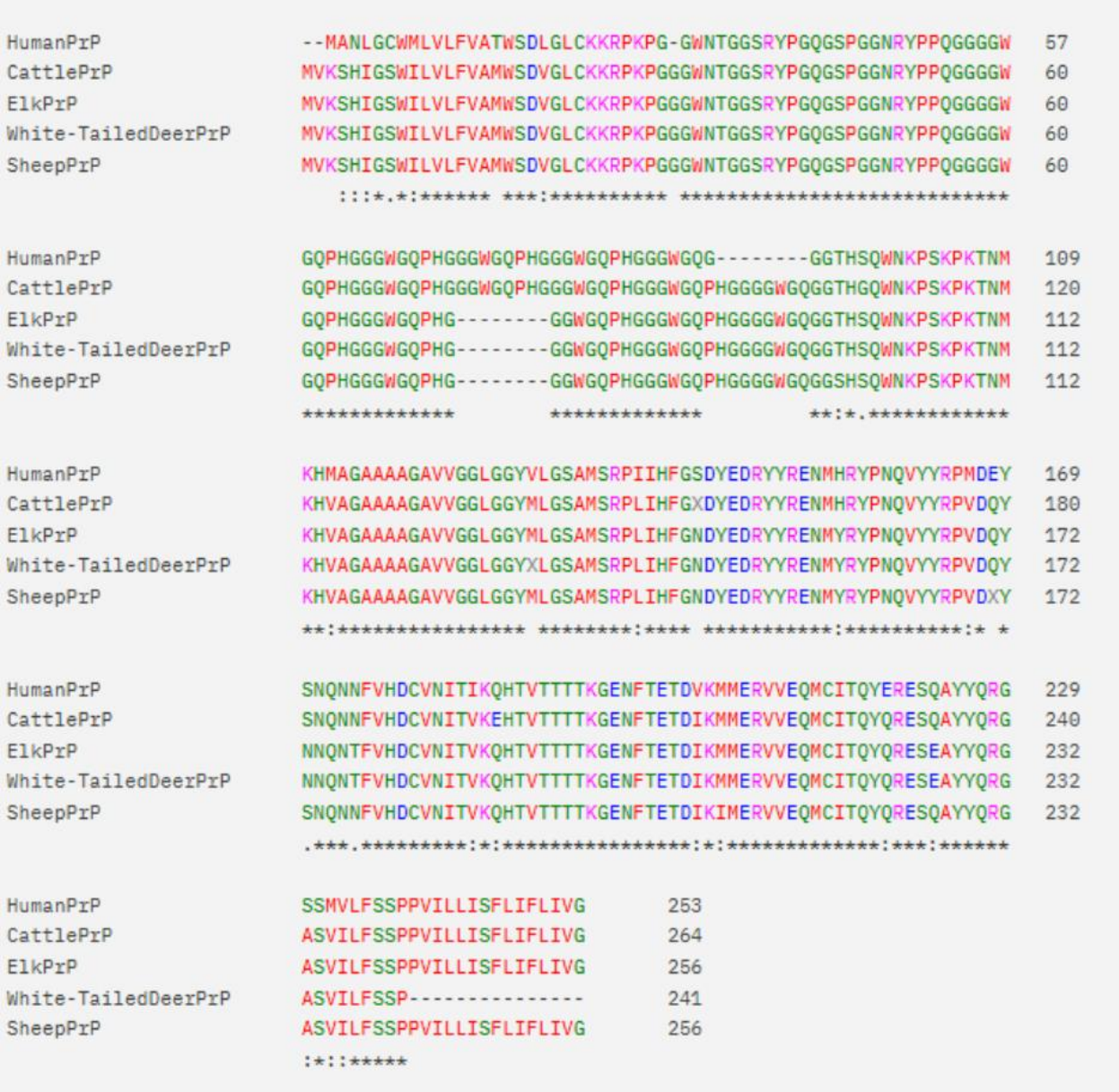

Figure 3. Clustal Omega multiple sequence alignment of the prion protein from human (*Homo sapiens*), cattle (*Bos taurus*), elk (*Cervus canadensis*), white-tailed deer (*Odocoileus virginianus*), and sheep (*Ovis aries*). Fully conserved residues are marked with an asterisk (*), conserved substitutions with a colon (:), and semi-conserved substitutions with a period (.).

1.3.3.1 Scrapie

Scrapie is one of the oldest documented TSEs, and affected species include wild and captive sheep (ovine) and goats (caprine). One of the most characteristic symptoms of scrapie is the development of incessant scratching which is responsible for the origins of the name of the disease (Henry & Schonburger, 2020). Two types of scrapie have been identified, classical and atypical scrapie, which have distinctly different epidemiologic findings and clinical symptoms. Classical scrapie was the first to be described, and it maintains traditional diagnostic criteria for prion disease, including a long incubation period, resistance to proteinases, high temperature, and formaldehyde treatment. Atypical scrapie was identified in 2003 and is considered a sporadic disease as no current evidence supports its natural transmission. Genetically modified transgenic mice and sheep have shown evidence of the ability to contract scrapie, but only under strictly controlled experimental conditions that are unrealistic to be found in nature (Acin et al, 2021). Interestingly, ovine genotypes play a large role in the susceptibility of the animal to contract classical or atypical scrapie and have been studied more extensively than caprine genotypes. The ovine *PRNP* gene contains three major polymorphic sites that are responsible for the susceptibility of the animal to classical scrapie: codons valine (V) 136, arginine (R) 154, and glutamine (Q) 171 (VRQ haplotype). Codon 171 is considered the polymorphic site with the most influence as sheep with QQ171 are at risk of developing classical scrapie, whereas RR171 sheep are predominantly resistant (Teferedegn et al, 2020; Acín et al, 2021).

On the other hand, resistance to classical scrapie after natural exposure is enhanced by polymorphic sites alanine (A) 136, histidine (H) 154, and arginine (R) 171. Regarding scrapie resistance, the five common haplotypes from least susceptible to most susceptible are ARR, AHQ, ARH, ARQ, and VRQ (Greenlee, 2019). To mitigate the risk of scrapie transmission through farmed sheep, breeding programs and regulations have been set to target selective breeding of scrapie-resistant genotypes, with some even enforced by law in certain countries. In Canada, the National Scrapie Eradication Program (NSEP) exists to eliminate scrapie from sheep flocks and goat herds to protect livestock and maintain confidence in Canada's sheep and goat industries. This program involves the identification of infected flocks and herds

through surveillance, implementing disease control measures where scrapie-positive animals are found, and delivering a Scrapie Flock Certification program (Canadian Food Inspection Agency, 2021; 2023). By understanding the scrapie agent and prioritizing genetic testing and selective breeding to enhance resistance, these efforts aim to eradicate scrapie, protect livestock health, and ensure the stability of the sheep and goat industries worldwide.

1.3.3.2 Bovine Spongiform Encephalopathy (BSE)

BSE, commonly known as "mad cow disease," is a TSE affecting cattle typically noticed through symptoms such as nervous or aggressive behaviour, abnormal posture and coordination, decreased milk production, and weight loss. Due to the lethal and transmissible characteristics of prion diseases such as BSE, they pose a great agricultural and economic threat in many countries worldwide (Canadian Food Inspection Agency, 2023). In Canada, the discovery of BSE-positive cattle in May 2003 led to 34 countries banning the import of ruminants and ruminant products from Canada (Le Roy & Klein, 2005), contributing to economic loss in the billions, particularly for provinces that rely on agricultural exports such as Alberta (Petigara et al, 2011). BSE presents in two different forms: atypical and classical (C-BSE), which differ in epidemiology and pathogenesis. Atypical BSE usually presents in older cattle and is without a common source of infection, indicating that it is likely a sporadic form of the disease. Atypical BSE is subdivided into two distinct strains: H-type and L-type, named for the higher (H) and lower (L) molecular mass of the protease-resistant PrP^{Sc} fragments detected in these forms (Dudas & Czub, 2017). These strains are also distinguished by different patterns of PrP^{Sc} deposition in the brain, suggesting distinct pathways of neurodegeneration (Corona et al, 2017). Typically, both strains of atypical BSE present with depressed symptoms such as dullness, drooping head posture, lethargy, and decreased nervousness (Konold et al, 2012). Contrarily, C-BSE is considered to have an exogenous origin as it is associated with ingesting feed contaminated with meat and bone meal (MBM) derived from prion-infected sources, though its precise origin remains unknown. C-BSE is distinguished by changes in behaviour and lack of coordination, increased nervousness and fearfulness, decreased milk production, and progressive wasting. The histopathological characteristics

include neuronal and neuropil vacuolation, glial response, and the total absence of inflammatory lesions (Canadian Food Inspection Agency, 2023). With a known, dangerous zoonotic potential, C-BSE is responsible for the human variant Creutzfeldt-Jakob disease (vCJD), and as of May 2024, there have been 233 instances of vCJD recorded globally of which the intake of beef products infected with BSE has been positively linked (U. S. Centers for Disease Control and Prevention, 2024). To control the spread of BSE and consequently vCJD, several measures, such as the implementation of feed bans, surveillance programs, and culling of suspected positive cases, were taken in afflicted countries and internationally that proved successful as the number of vCJD diagnosis and classical BSE cases now have such a low incidence rate that the World Organisation for Animal Health reports the disease as negligible and estimates the number of diagnoses will soon approach zero cases per million bovines (Canadian Food Inspection Agency, 2013; World Organization for Animal Health, 2023). In all, the discovery of BSE was an important step in understanding prion diseases and the complexity of experiencing epidemics of such pathogens leading to enhanced biosafety methods, improved regulatory measures, and a greater awareness of the mechanisms underlying neurodegenerative disorders.

1.3.3.3 Chronic Wasting Disease (CWD)

Chronic wasting disease (CWD) is a TSE affecting members of the *Cervidae* family, such as deer, elk, and moose, that was first noted in North America but can now be found worldwide. CWD was first identified in Colorado in 1967 in captive farmed mule deer (*Odocoileus hemionus hemionus*) and one black-tailed deer (*Odocoileus hemionus columbianus*) but is now found in both wild and captive animals in 34 U.S states, four Canadian provinces, Finland, Norway, South Korea, and Sweden (United States Geological Survey, 2024; Williams & Young, 1980). CWD was first identified in Canada in 1996 on an elk farm in Saskatchewan. Since then, it has spread extensively throughout the province and into neighbouring Alberta, affecting captive and wild moose, deer, and elk populations. In addition, cases of CWD have been detected in wild deer in British Columbia and Manitoba. In eastern Canada, the disease has only been reported on a

single red deer farm in Quebec, which was promptly depopulated. To date, there is no evidence of transmission to wild populations in the region (Canadian Food Inspection Agency, 2024).

CWD maintains an average incubation period of approximately 16 months until the onset of clinical symptoms including weight loss and overall decrease in body condition, hypersalivation, ataxia, recumbent posture, and behavioural changes. In captive cervids affected by CWD, symptoms may be noted by farmers and caretakers, but identification of sick animals is more difficult in wild populations, and in some regions, CWD prevalence is up to 18.8% in animals sampled through surveillance programs (Environment and Protected Areas, 2024). In members of the *Cervidae* family, *PRNP* is a highly conserved gene that significantly influences the susceptibility, incubation period, and progression of CWD in different cervid species (Moazami-Goudarzi et al, 2021). Notable species-specific single-nucleotide polymorphisms (SNPs) include codon 96 (glycine to serine, G96S) in white-tailed deer (*Odocoileus virginianus*), codon 132 (methionine to leucine, M132L) in elk (*Cervus canadensis*), and codon 226 (glutamine to lysine, Q226K) in mule deer. Certain *PRNP* polymorphisms, such as the S96 variant in white-tailed deer and the L132 variant in elk, have been linked to a lower incidence of CWD infection (Ishida et al, 2020; Moore et al, 2018). While animals with protective alleles may exhibit slower disease progression and milder clinical symptoms, those with susceptible alleles typically experience rapid disease onset and severe neurological symptoms (Arifin et al, 2021). *PRNP* genotype can also affect neuropathological variations, such as the location and amount of PrP^{Sc} deposition and spongiform alterations in the brain (Otero et al, 2019). To date, there is no research proving direct evidence of CWD transmission to humans. Potential zoonotic transmission remains a concern, particularly in the United States as the expanding range of CWD continues to include more of the nearly six million deer harvested by hunters each year (Groveman et al, 2024; NDA Staff, 2024), as experimental studies have shown that CWD prions can convert human PrP in vitro, suggesting a theoretical risk (Barria et al, 2018). In recent years, the number of CWD-positive animals and increasingly expanding affected areas has revealed that the spread of the disease continues at a rampant rate (United States Geological Survey, 2024), emphasizing the importance of ongoing efforts to control the

spread, enhance surveillance, develop effective management strategies, and conduct further research to better understand the mechanisms underlying this devastating prion disease.

1.3.3.4 Transmissible mink encephalopathy (TME)

Transmissible mink encephalopathy (TME) is a rare disease of captive-farmed mink (*Neovison (Mustela) vison*) that was first noted in 1947 and described in detail by Burger and Hartsough in 1965 (Liberski et al, 2009). Six outbreaks of TME have been documented across North America between 1947 and the last reported outbreak in 1985, several of which were linked to contaminated feed, classifying TME as a foodborne TSE (Baron et al, 2007). Initially, TME was thought to originate from infected sheep by-products in mink feed, but the 1985 Stetsonville, Wisconsin outbreak showed infected mink were fed fresh meat from sick dairy cattle instead of ovine products. Other outbreak records support the link between downer cattle meat and TME, and studies suggest TME in transgenic mice resembles L-type BSE rather than H-type or classic BSE, supporting the theory that TME originates from a rare TSE in cattle. Experimental transmission of TME to sheep with VRQ/VRQ genomes via intracerebral inoculation further supports L-BSE as its origin. These findings imply L-BSE zoonosis may exist in the form of TME, warranting continued concern over exposure to L-BSE and TME agents, which likely share a common source (Hamir et al, 2006; Liberski et al, 2009; Cassman et al, 2019).

1.3.3.5 Feline spongiform encephalopathy (FSE)

Feline spongiform encephalopathy (FSE) is a TSE affecting captive, domestic, and wild cats in the family *Felidae*. The first documented cases emerged from the UK in 1990, shortly after the UK's BSE outbreak, when five domestic cats exhibited progressive ataxia, aggression, and altered sensory responses (Wyatt et al, 1991). Post-mortem analysis using western blotting and strain typing of brain homogenates from affected cats and cows confirmed the FSE agent's relation to BSE (Lezmi et al, 2003). This similarity suggests that FSE is a foodborne TSE originating from BSE-contaminated meat in feed (Hilbe et al, 2009). FSE remains rare, with only 87 confirmed cases in the UK and a few others worldwide (Lezmi et al, 2003). Following

strict measures like banning meat and bone meal (MBM) in animal feed, FSE incidence has significantly declined (Animal and Plant Health Agency, 2023). While BSE is linked to human vCJD, FSE's zoonotic potential is unproven, though cross-species prion transmission remains a concern (Mathiason et al, 2013).

1.3.3.6 Exotic Ungulate Spongiform Encephalopathy (EUE)

Exotic ungulate spongiform encephalopathy (EUE) is a TSE affecting captive Bovidae ruminants in zoos. During the UK's 1990s BSE outbreak, EUE was diagnosed in six greater kudu (*Tragelaphus strepsiceros*), six elands (*Taurotragus oryx*), and several other species, including Arabian oryx, Ankole cattle, and bison throughout the UK (Imran & Mahmood, 2011). Common symptoms across species included ataxia, tremor, weight loss, and eventual death (Cunningham, 1991). Investigations linked EUE cases to ruminant-derived meat and bone meal (MBM) in feed. Experimental transmission of EUE to mice using greater kudu brain homogenates produced neuropathology like BSE, further supporting the suggestion that the diseases have shared origins (Kirkwood & Cunningham, 1994). Greater kudu, however, can sustain horizontal transmission, comparable to scrapie and CWD (Sigurdson & Miller, 2003). In 1998, the last death of a positive animal occurred, and since the EU implemented a ban on animal-derived proteins in animal feeds, new cases of EUE have ceased to emerge (Imran & Mahmood, 2011).

1.3.4 Fungal Prions

A fascinating area in prion biology involves fungal prions, which have been primarily studied in yeast and filamentous fungi. Fungal prions, unlike their mammalian counterparts, do not cause disease in humans or animals and primarily function as non-pathogenic, epigenetic elements that regulate cellular processes. Fungal prions demonstrate the ability to replicate themselves by inducing a conformational change in normal, soluble proteins into the aggregated, amyloid state and transmit from cell to cell, leading to heritable changes in phenotype. Many prion proteins isolated from fungi appear to form very ordered amyloid fibrils enriched in β-sheets that are quite like the aggregates typically observed in mammalian prion diseases, though their biological consequences are very different (Wickner et al, 2007). Important fungal prions

include [PSI+], [URE3], and [PIN+]. The self-propagating nature of the translation termination factor protein Sup35p results in [PSI+] prions and in this form sequesters it into aggregates, decreasing its availability and causing stop codon read-through. Under some circumstances, this may provide an evolutionary advantage by generating phenotypic variety and enabling the selective appearance of latent genetic variation (McGlinchey et al, 2011; True et al, 2000). In its aggregated form, the Ure2p protein, which is involved in nitrogen catabolite regulation, is also recognized to be the [URE3] prion. In nitrogen-limited conditions, the ability of the cell to use a wider variety of nitrogen sources can be beneficial since the prion form [URE3] inactivates Ure2, resulting in the activation of nitrogen catabolic genes (Chen et al, 2011; Wickner et al, 2007). The [PIN+] (also referred to as [RNQ+]) prion affects the Rnq1p protein, which facilitates the formation of other prions, including [PSI+] through the overproduction of Sup35. [PIN+] is therefore considered a "prion-inducing" factor as it can influence the prion-forming propensity of other proteins (Serio, 2018). While both fungal and mammalian prions propagate through templated protein misfolding, the species barrier between them appears absolute, with no evidence that fungal prions can influence or interact with mammalian PrP (Chen et al, 2007). To better understand human prion illnesses and other amyloid-related disorders, fungi that produce prions offer useful model systems for exploring the fundamental mechanisms of prion formation, propagation, and transmission. Understanding fungal prions holds promise for biotechnological uses, including creating prion-based synthetic biology inheritance systems, modifying commercial yeast strains in a heritable way, and improving their usefulness in various biotechnological procedures.

1.3.5 Prions in the Environment

Infectious PrP^{Sc} prions are deposited into the abiotic environment through various interactions, tissues, and bodily fluids, posing a great concern for public health and ecological authorities due to their long persistence and transmissibility (Pritzkow et al, 2021). PrP^{Sc} remains extremely resistant to inactivation and degradation, even in extremely harsh conditions, and can transmit disease (Concha-Marambio et al, 2014). The most common route of transmission for TSEs is oral transmission, and once replicated within intestinal lymphoid

tissues, prions can be expelled through saliva, mucus, urine, feces, blood, milk, birthing materials, skin, antler velvet, and more (Saunders et al, 2012). Contaminated tissues from infected animals, such as those from the brain and spinal cord during decomposition, have high concentrations of PrP^{Sc} and are released into the nearby surroundings. These prions bind strongly to soil particles, with a particularly strong bond to clay, which protects them from microbial degradation and environmental factors, enhancing their longevity and infectious potential (Wyckoff et al, 2016). Clay-rich soils have a major impact on prions' environmental dynamics, mostly via the adsorption of PrP^{Sc}, defense against degradation, and changes to mobility and bioavailability (Schramm et al, 2006). The prions are efficiently anchored to soil particles by the adsorption process, which also involves hydrophobic and hydrogen bonding interactions between the positively charged peptides and negatively charged mineral surfaces. This protection is essential for the prolonged persistence of PrP^{Sc} particles in the environment since it hinders their denaturation into non-infectious fragments (Johnson et al, 2006). Prions bound to clay particles also remain bioavailable, posing a risk to animals that ingest soil while foraging and grazing. This route of exposure is particularly relevant in regions where prion diseases, such as CWD in cervids, are prevalent (Kuznetsova et al, 2014). Scavengers, predators, and parasites, including birds, coyotes, cougars, ticks, and other animals, may unintentionally help spread infectious prions across greater distances when they consume the remains of animals infected with prion disease and excrete prions in their urine and feces, further contaminating new areas (Jennelle et al, 2010; Inzalaco et al, 2023). It is also believed that rainfall can wash prions from the decomposing carcass into nearby bodies of water, spreading contamination over a wider area. This environmental contamination could create hotspots of infection, posing a risk to other animals that graze or drink in these areas, perpetuating the cycle of prion disease transmission (Miles et al, 2011). Misfolded PrP^{Sc} existing in the environment has also been found to interact with both mycorrhizal and non-mycorrhizal plants, and it is hypothesized that they may accumulate and translocate PrP^{Sc} within tissues, therefore acting as a vector of disease transmission (Carlson et al, 2023). Beyond mere surface binding, plants absorb prions through their root system through various soil compositions and mineral contents, which bind to the cell walls of cells in the aerial tissues and remain infectious for long periods. This presents an unquantifiable long-term risk to

other animals in the environment and presents the possibility of inducing further infectious prion diseases, though the extent to which is not yet fully determined (Pritzkow et al, 2015). As non-human TSEs affect many animal species farmed for various reasons (meat and milk production, fur, fiber, or hide farming, etc.), it is not unsurprising that farming materials and equipment have been implicated in the harbour and spread of PrP^{Sc} particles found to be capable of infecting new herds of animals, particularly regarding scrapie and CWD. Salt licks are a commonly used tool across Europe and North America in wildlife management and livestock farming and when prion-infected animals use salt licks, their saliva and other bodily fluids contaminate these surfaces. As other animals subsequently use the same salt licks, they encounter these infectious prions, resulting in horizontal transmission of the disease (Plummer et al, 2018). Another method of prion transmission that has proven responsible for infection is aerosolization as dust particles. This can occur through activities that disturb contaminated soils, bedding, or feed, such as agricultural operations, livestock movements, and wildlife activity. Once airborne, these prion-laden dust particles can be inhaled or ingested by susceptible animals, leading to new infections (Denkers et al, 2013; Gough et al, 2015). Studies have also pointed to shared feeding and watering stations as a source of horizontal transmission between sick and healthy animals, and that these contaminated materials stay infectious for extended periods. Studies have shown that prions can bind to a variety of materials, including metals such as stainless steel and plastics used commonly to manufacture feed troughs and buckets, and even drinking from a water trough used by scrapie-infected flocks was sufficient to transmit infection to clean sheep in a clean building (Konold et al, 2015). Complicating the control process of TSEs in both natural and agricultural environments is the uncertainty of the precise mechanism of transmission between individuals and the length of time TSEs can persist in the environment, as previously discussed. For example, cervids contracted with CWD contain sufficient prions in their blood and saliva to transmit the disease to other cervids, but CWD prions existing in the environment are also attributed to infection (Mathiason et al., 2009). A previous study found that scrapie prions are highly persistent and can be found in environments like soil and hay feeds for as long as 16 years after the initial infected animals were removed and the environment was disinfected (Georgsson et al., 2006). The environmental persistence of prions presents an ever-

changing, complicated challenge for management and decontamination efforts in natural and agricultural settings that requires the cooperation of many different parties. Therefore, the continuous efforts of many governmental, scientific, and industrial parties are critical to mitigate and lessen the spread and effects of prions throughout the environment.

1.4. The Species Barrier

An important aspect of prion diseases and their transmission between individuals is the "species barrier," which refers to the varying degrees of difficulty prions encounter when crossing from one species to another. This barrier is influenced by several factors such as the molecular and structural compatibility of prion proteins between species. Despite the inherent resistance posed by the species barrier, certain conditions can facilitate cross-species transmission, posing significant challenges to disease control and public health (Manson & Diack, 2016). Understanding these mechanisms behind the species barrier is essential for developing strategies to manage and mitigate certain risks associated with prion diseases and contaminated spaces.

1.4.1 The Prion Species Barrier

Evidence of the species barrier has been extensively examined through various prion strains and host types. While prion transmission within the same mammalian species is generally efficient given the right conditions, a species barrier usually affects transmission between species. This barrier results in rare transmission with prolonged incubation periods before the onset of neurodegenerative symptoms after prion inoculation (Igel et al, 2023). Several factors have been found to affect the ability of PrP^{Sc} to transmit between host species. The primary determinant of the species barrier of prion diseases is the amino acid sequences of the potential prion proteins of the two species involved. Higher homology between sequences usually results in a lower species barrier. For example, BSE prions have historically been linked to human infection, resulting in vCJD, due to considerable similarity between bovine and human PrP sequences (Manson & Diack, 2016). Species-specific polymorphisms of the host PrP gene also exist to prevent prion

diseases from transmitting between individuals. As previously discussed, a well-documented instance of this is the methionine/valine polymorphism at codon 129 of the human *PRNP*. This polymorphism significantly influences the risk of an individual contracting vCJD. Individuals homozygous for methionine (M/M) at codon 129 are more susceptible to developing vCJD upon exposure to BSE prions from contaminated sources, compared to heterozygous (M/V) individuals, who have a reduced risk due to genetic incompatibilities (Pauly et al, 2022). The structural plasticity of certain regions in the prion protein, such as the β2-α2 loop of scrapie, BSE, and CWD prions, has also been shown to influence the species barrier phenomenon. Studies examining the structural makeup of the PrP^{C} to PrP^{Sc} conversion have uncovered that the β2-α2 loop maintains variable flexibility, and this flexibility affects the initial binding of PrP^{C} to PrP^{Sc} (Šulskis et al, 2023). Species-specific differences in the loop's conformation can either facilitate or hinder the binding process, further contributing to the species barrier. For example, the loop in cervids differs structurally from that in cattle, which may explain the relative resistance of certain cervid species to BSE prions (Kurt et al, 2014). Strain-specific characteristics of the host's PrP^{C}, the route of transmission, and post-translational modifications of PrP^{C}, including glycosylation and sialylation status, also shape the species barrier and influence strain selection (Igel et al, 2023).

1.4.2 Prion Zoonosis

Prion zoonosis refers to the transmission of prion diseases from animal hosts to humans. The species barrier in prion transmission significantly impacts the risk of human zoonotic diseases and is crucial for understanding the potential for cross-species prion adaptation. To date, the only known animal prion disease with demonstrated zoonotic potential is C-BSE in cattle, leading to human vCJD. There is no evidence to suggest that typical or atypical scrapie, atypical BSE, or CWD are naturally capable of transmitting disease to humans. However, extreme caution should still be exercised regarding these diseases as their invariably fatal outcome has been demonstrated under strict laboratory conditions in some non-human primates and human PrP transgenic mice, demonstrating possible zoonotic potential (Houston & Andréoletti, 2018). The zoonotic potential of CWD has been followed closely since its recent increase in spread across geographical

distribution in North America and Europe, and is of particular concern to many researchers, hunters, and the public. Experimental transmission studies of CWD have shown their infectious potential in certain species of primates, namely squirrel monkeys (*Saimiri sciureus*) who show a high oral attack rate of 92% with an average incubation period of 68 months post-inoculation (Race et al, 2009). Although non-human primates are not perfect models to represent human susceptibility to prion diseases, they corroborate the results that emerge from research examining human PrP transgenic mice, in vitro studies and epidemiological evidence to suggest that though the risk of CWD zoonosis is currently believed to be low but cannot be ruled out as impossible (Wang et al, 2021; Saunders et al, 2012). One of the most concerning aspects of prion zoonosis is the long incubation period of the disease before the onset of symptoms, which can extend several decades in humans, combined with the lack of a robust immune response, making early diagnosis and intervention difficult (Houston & Andréoletti, 2018; Alpers, 2005). Ongoing research into animal prion diseases and their affiliated zoonotic potential is extremely important for understanding the mechanisms of interspecies prion propagation, developing effective diagnostic and therapeutic strategies, mitigating the risks of future zoonotic epidemics, and ensuring the safety of the public through improved management of cultivated and wildlife populations.

1.5. Detection and Diagnosis of Prion Diseases

Traditionally, diagnosis and quantification of TSE in animals is based on herd history, clinical signs, pathological observations, and immunodetection of abnormal PrP^{Sc} via immunohistochemistry, Western blot, and ELISA on brain and lymphoid tissues (Moudjou et al., 2020; Gavier-Widén et al, 2005). However, challenges arise as there is generally a low quantity of PrP^{Sc} in peripheral tissues and body fluids, the bioassays are expensive, and lots of time and labour are required. This challenge has inspired the need for rapid artificial amplification and replication of PrP^{Sc} from seed in-vitro to a detectable level by more sensitive testing methods. Cell-free assays for the in vitro conversion of normal PrP^{C} to PrP^{Sc}, which mimics the in vivo process, such as protein misfolding cyclic amplification (PMCA) (Eraña et al, 2020; Moudjou et al., 2020) and the real-time quaking-induced conversion (RT-QuIC) (Kang et al., 2017), have emerged

as useful methods (Moudjou et al., 2020). PMCA is a technique in which PrP^{Sc} replication occurs much faster than normal due to several consecutive cycles of incubation and sonication. This technique is advantageous as it can detect even extremely low concentrations of PrP^{Sc}, down to as little as one attogram for some prion species, and the products of PMCA are usually highly infectious (Eraña et al., 2020; Moudjou et al., 2020). The RT-QuIC assay is another method to assess for PrP^{Sc} also utilizing movement to encourage seeding of PrP^{Sc} through multiple rounds of agitation and incubation. A notable difference between PMCA and RT-QuIC is that PMCA mimics the natural process of prion replication. It involves cycles of incubation and sonication to amplify small amounts of PrP^{Sc} by converting PrP^{C} into the misfolded form, while RT-QuIC uses shaking or quaking to induce PrP^{Sc} to convert recombinant PrP^{C} into the misfolded state. RT-QuIC technology has improved significantly since its development in 2001 and is now used as a key diagnostic tool when diagnosing TSEs such as CJD as it can detect minute amounts of PrP^{Sc} in cerebrospinal fluid (Orrú et al, 2015). Importantly, these two assays correlate with infectivity (Moudjou et al., 2020; Orrú et al., 2015; Kang et al., 2017), and the measurement of the reduction of PrP^{Sc} is crucial for the determination of the effects of any decontamination process for PrP^{Sc}. European and certain national medical agencies have recently implemented guidelines for prion inactivation of non-disposable medical material and encourage or request the use of these cell-free assays to predict the value of the validated PrP^{Sc} decontamination methods (Moudjou et al., 2020).

Diagnosing prion disease in humans relies on clinical evaluation, electroencephalogram (EEG), magnetic resonance imaging (MRI), CSF 14-3-3 protein detection, *PRNP* genetic testing, and definitive brain biopsy or autopsy. Due to the similarity of prion disease symptoms to other neurological diseases, it is common for a definitive diagnosis of prion disease to be unobtainable until a post-mortem examination can be performed (Desai & Purzycki, 2023). For example, a positive diagnosis for vCJD must entail neuropathological examinations, immunohistochemical analyses, Western blot for proteinase-resistant PrP^{Sc}, or confirmation of the presence of scrapie-associated fibrils (Connor et al, 2019). To date, the only

versatile confirmation method for positive TSE infections, regardless of host species or TSE type, is the presence of partially protease-resistant and aggregated isoform PrP^{Sc} (Eraña et al., 2020).

1.6. Decontamination of PrP^{Sc} and Treatment Approaches for Prion Diseases

The increasing quantity of research on prion diseases has increased awareness of the critical need for efficient management and mitigation techniques. The challenges in early diagnosis of prion disease, their resistance to standard decontamination techniques, and the recognition that they are universally incurable stresses the importance of ongoing research in these fields (Bechtel & Geshwind, 2013).

1.6.1 Current Decontamination Methods

One of the challenges when working with TSEs is their unique ability to resist most conventional forms of pathogen inactivation. This characteristic was discovered after vaccines derived from sheep CNS tissues were administered to other sheep flocks to eradicate the looping-ill virus, which only allowed those sheep to develop scrapie. These vaccines had been certified virus-free, but given that the affected sheep developed scrapie, it was not possible that the scrapie prion protein was destroyed during decontamination efforts (Giles et al, 2008). Over the years, tremendous efforts have been made to investigate effective ways to inactivate abnormal prions (Sakudo et al, 2011; McDonnell & Burke, 2003; Taylor, 2000) The first attempts to inactivate PrP^{Sc} were conducted in the 1960s using ionizing and ultraviolet radiation, but there was no impact on prion infectivity. This failed decontamination method also led researchers to the idea that PrP^{Sc} is a nucleic acid-free agent due to the nonresponse to nucleic acid-specific wavelengths, which was proven to be true in later years (Prusiner, 1998).

TSE-infected livestock carcasses are a concerning biohazard, and it has been shown that composting can reduce the quantity of infectious PrP^{Sc} in tissues after only a few months. During composting the internal temperature of the carcasses quickly rises to above 60°C then drops to ambient temperature (Huang et al, 2007), but microbes found in the gut of sheep have been shown to have an impact on the degradation of PrP^{Sc} at room temperature and an increased impact at 60°C. This method may be effective, but there are

many barriers including the requirement for deep land space, the length of time decomposition takes, and only being able to use this method post-mortem which suggests different decontamination methods must be explored (Huang et al, 2010).

Chemical decontamination using sodium hydroxide (NaOH) (combined with autoclaving) (Giles et al, 2008), sodium hypochlorite (bleach) (Williams et al, 2019), hypochlorous acid (HOCl) (Hughson et al, 2016), sodium dodecyl sulphate (SDS) (Peretz et al, 2006), and electrically charged disinfectant CAC-17 have all been shown to have some level of disinfectant against $PrP^{Sc.}$ Physical methods rely primarily on heat and irradiation. Standard autoclaving at 121 °C is often insufficient for PrP^{Sc} inactivation, but extended sterilization cycles at 134 °C for ≥18 minutes, especially when combined with detergents such as SDS or acidic conditions, significantly reduce infectivity (Sakudo et al, 2020). Other approaches include incineration (>1000 °C) (Brown et al, 2004), alkaline hydrolysis of tissues (Murphy et al, 2009), and emerging technologies like non-thermal plasma (Sakudo et al, 2022) or vaporized hydrogen peroxide (Sakudo et al, 2020). However, in a clinical setting, these methods can be very damaging to equipment and may not be practical for frequent use (Sakudo et al, 2020). For this reason, it is important that ongoing efforts attempting to inactivate or decontaminate prions not only focus on effectiveness but also on practicality and safety for widespread use.

1.6.2. Current Treatments and Challenges in Treatment

Currently, there is no effective treatment against TSEs and ante-mortem diagnosis of TSEs proves difficult due to the ambiguous and varied nature of the accompanying symptoms and the slow progression of the diseases they cause (Eraña et al., 2020). As prions are distinctly resilient compared to other pathogens, conventional antiviral or antibacterial treatments are ineffective; therefore, alternative therapeutic techniques are being investigated (Sakudo, 2020). The generation of small oligomer modulator molecules that either stabilize PrP^{C} or prevent it from transforming into PrP^{Sc} is one potential field of study of recent interest. In preclinical settings, compound anle138b is one example of a small molecule that has been found to slow disease progression for other amyloidogenic neuropathies such as Parkinson's in mouse models,

and has demonstrated the ability to inhibit PrP^{C} conversion, indicating potential use as therapeutic or preventative treatments (Levin et al, 2014). Another avenue of treatment that has been investigated is the use of antisense oligonucleotides (ASOs) that can be designed to *PRNP* mRNA leading to degradation of mRNA through RNase H-mediated cleavage or preventing its translation into protein. This results in a reduction of endogenous PrP^{C} levels, therefore lowering the risk of its conversion to the disease-causing PrP^{Sc} (Raymond et al, 2019). Inspired by the understanding of molecular chaperones and their role in maintaining and propagating fungal prions in *Saccharomyces cerevisiae* (Rikhvanov et al, 2007), scientists have investigated the use of other molecular chaperones for mammalian prion diseases. In 2019, researchers managed to design a molecular chaperone, (N,N′-([cyclohexylmethylene]di-4,1-phenylene)bis(2-[1-pyrrolidinyl]acetamide)), that was successful in not only delaying the progression of psychological symptoms and neurological damage but also reduced the number of biomarkers associated with disease in the CSF of male cynomolgus macaques (*Macaca fascicularis*) infected with BSE (Yamaguchi et al, 2019). Unfortunately, while research on animal models continues to explore the use of anti-prion treatments, there are no treatments currently approved for use in humans and clinical settings, and care plans for patients with prion diseases consist of hospice care, typically focusing on improving the remaining quality of life (De Vries et al, 2021). Overall, while considerable progress has been made in the understanding of prion diseases, the development of effective treatments for humans remains in the experimental stages, with research focusing on overcoming various biological, chemical, and technical challenges associated with these illnesses.

Treating prion diseases poses several challenges due to their uniquely resistant properties and unclear mechanisms. One of the main challenges associated with terminal prion illnesses is the latent appearance of symptoms leading to late-stage diagnosis, in which case treatment would be too delayed to be optimally effective. Most people diagnosed with prion diseases do not get a correct diagnosis until approximately two-thirds of the way through the disease, or about the point at which symptoms of cognitive decline and behavioural abnormalities due to irreversible neurological damage begin (Bechtel & Geschwind, 2013).

Treatment of human prion diseases is further complicated as more than 60 genetic alterations of TSEs have been documented, each with distinct molecular features resulting in potentially unique clinical presentations and specialized treatments (Eraña et al., 2020). Previous research using neuronal and fibroblastic cell cultures has demonstrated that prions are also subject to accumulating mutations under selective pressures, such as environmental changes or drug exposure. This leads to the emergence of different prion mutants that can outcompete others depending on the conditions. The findings challenge the idea that prion strains are stable and suggest they can undergo mutation and selection, posing challenges in creating a universal treatment (Li et al, 2010). Also posing challenges to the treatment and control process of animal TSEs is the uncertainty of the precise mechanism of transmission between individuals, and the length of time TSEs can persist in the environment, as previously discussed. Treating the natural environment in which prions are present is not currently possible. While conventional chemical decontamination methods such as concentrated NaOH or concentrated bleach are effective, these chemicals are very hazardous and damaging to the environment and can therefore not be used to treat environmentally bound prions (Sakudo, 2020). The strong resistance of prions to traditional decontamination methods and treatments, their strain characteristics and ability to mutate, and their environmental challenges emphasize the complexity associated with treating pathogenic PrP^{Sc} prions. Though scientists have yet to uncover the answers to the mysterious mechanisms of prions, these factors reinforce the importance of ongoing research into the decontamination of the prion protein and the treatment of the diseases they cause for the betterment of human and animal health.

1.6.3. Prevention and Control

Prevention and control of prion diseases is a challenge that typically requires response and cooperation from several parties, such as farmers, hunters, government agencies, healthcare agencies, food processing industries, and scientists. The BSE outbreak of the 1980s and 1990s fundamentally changed the world's understanding of prion diseases and reshaped strategies for their prevention and control. The crisis and its zoonotic link to vCJD in humans brought to light significant gaps in knowledge of these pathogenic proteins,

prompting significant changes in policy, regulation, and scientific research worldwide (Canadian Food Inspection Agency, 2013). As previously discussed, preventing the spread of TSEs such as BSE, TME or EUE is based on the exclusion of specified risk material (SRM) from animal feed. In Canada, mammalian proteins, including SRM, have been banned from ruminant feed since 1997, and since 2007, it has been prohibited from being included in any animal food or being used in fertilizers (Canadian Food Inspection Agency, 2023). Surveillance programs can also be credited for preventing the prions from infecting non-infected animals and spreading them from contaminated to unaffected areas. These programs are usually specific to the TSE or the infected species, but they are all designed to track, detect, and monitor prion diseases early, which permits the isolation of infected animals to prevent their spread (Watson et al, 2021; Houston & Andréoletti, 2018). Surveillance efforts also focus on preventing the geographic spread of prion diseases by monitoring animal trade and movement, imposing restrictions on exporting animals from regions where prion diseases are endemic and implementing environmental monitoring in affected areas. In addition to the ban on SRM, in Canada, measures have been taken to ensure that animal TSEs, particularly CWD, remain under control and to minimize introduction and spread into new areas. For example, Canada's *Health of Animals Act* dictates that all suspected cases of TSE noticed from wild animal populations (e.g., hunters encountering CWD) and farmed populations (e.g., CWD in cervids, BSE in cattle, and scrapie in sheep or goats) must be reported to the Canadian Food Inspection Agency (CFIA). Canada maintains strict national chronic wasting disease herd certification programs for farmed cervids, with the focus on disease prevention and risk management and further requires that all farmed cervids over the age of 12 months that are slaughtered in Yukon, Alberta, Saskatchewan, Manitoba, Ontario, and Quebec are tested for CWD and that any animal testing positive for CWD is forbidden to be allowed into the commercial food chain (Canadian Food Inspection Agency, 2024).

The prevention of prion diseases varies significantly depending on whether the disease is acquired or genetic, with acquired TSEs such as CWD, BSE, iCJD, and Kuru being primarily prevented through measures that minimize exposure to contaminated tissues or biological materials (Pritzkow et al, 2021;

Watson et al, 2021). In contrast, for genetic prion diseases such as fCJD, FFI, or GSS, prevention focuses on genetic counselling and research into therapies that may slow or halt disease progression (Goldman & Vallabh, 2022). To err on the side of caution, it is recommended that animals suspected of prion disease be culled, including others of the group that could have possibly been exposed as well. Unfortunately, no current therapies have proven successful enough at preventing the development of genetic prion disease to be used regularly in clinical settings, though clinical trials are constantly ongoing (Zerr & Schmitz, 2021). Public awareness and education play a vital role in reducing risky behaviours that could lead to prion transmission, particularly in hunting communities and regions where consumption of high-risk animal parts is common. However, surveys have found that hunters who are more knowledgeable about CWD are more likely to decrease their harvest rate, potentially contributing to increased CWD prevalence as fewer animals are being hunted (Vaske et al, 2006). Overall, the search for effective measures to prevent the spread and development of prion diseases continues, driven by ongoing research into diagnostic techniques, potential therapies, and enhanced surveillance methods.

1.6.4. Need for Development of Environmentally Friendly Prion-Inactivating Chemicals

As discussed in the previous section, the current methods for the decontamination of prions may be effective, but they are typically either very impractical for large-scale use (such as the incineration of farming infrastructure and soil after a TSE outbreak) or very harsh and therefore not practical either. For this reason, environmentally friendly prion-inactivating chemicals are of interest for decontaminating materials contaminated with PrP^{Sc}.

Electro-activated liquid chemicals (EALCs) represent a promising alternative, offering strong decontamination potential while minimizing environmental and material damage. EALC solutions, generated through the electrochemical activation of water and salt-based precursors, can be tailored to exhibit antimicrobial (Liato et al, 2017) and protein-disrupting properties (Hughson et al, 2016; Sakudo et al, 2020), making them an attractive candidate for prion decontamination. Unlike conventional disinfectants, EALCs degrade into non-toxic byproducts, reducing long-term ecological impact (Iram et al, 2021).

Additionally, their adaptability for in situ applications on various surfaces, including steel, soil, and agricultural equipment, enhances their practicality for large-scale use (Thorn et al, 2012). Developing EALCs as a prion-inactivating solution could provide a practical and sustainable alternative to harsh decontamination methods. By balancing efficacy with environmental safety, these chemicals have the potential to be implemented in real-world settings where traditional treatments are impractical, helping to reduce prion contamination risks more feasibly and responsibly.

1.7. Statement of Rationale

Prion diseases, or TSEs, are fatal neurodegenerative disorders caused by the accumulation of the misfolded prion protein, PrP^{Sc}, in the central nervous system. PrP^{Sc} is extremely stable and can spread through contaminated feed, bodily fluids, shared environments, and contact with infected surfaces, including medical and laboratory equipment. In environmental settings, particularly in soil and on surfaces such as stainless steel or plastic, PrP^{Sc} can persist in an infectious state for more than 15 years. Its resistance to heat, enzymatic degradation, and conventional disinfectants, makes decontamination especially challenging.

Addressing contamination from CWD has become increasingly important, especially where infected carcasses, tissues, equipment, or materials like soil and manure may still harbour infectivity. The CFIA has recognized this as a high-priority research need through its TSE control program (Objective 1119), which calls for the development of safe and effective methods to destroy prions in potentially contaminated environments, including on farms, in abattoirs, and on transport equipment. While chemicals like sodium hydroxide and bleach are effective, their corrosive and hazardous nature makes them difficult to apply safely outside of controlled settings. This creates a gap where there is a pressing need for practical, environmentally friendly alternatives suitable for real-world use.

This study aims to help fill that gap by exploring the potential of EALCs to inactivate PrP^{Sc} from CWD-infected brain tissue and contaminated surfaces. By using RT-QuIC and PMCA, this research aims to determine whether EALCs can serve as more sustainable options to traditional disinfectants.

In addition, the bactericidal efficacy of EALCs was evaluated using two representative bacterial species: Gram-positive *Listeria monocytogenes* and Gram-negative *Pseudomonas aeruginosa*. The preliminary results may also support the effects of EALCs on the abnormal prions. The details are explained in the Appendices.

Identifying effective, field-compatible decontaminants has important implications for controlling the spread of CWD and reducing the environmental burden of prion contamination. This research contributes to the broader goal of developing practical and scientifically validated solutions for abnormal prion inactivation, with potential applications in wildlife, agricultural, and biosafety settings.

1.8. Hypothesis

It is hypothesized that the if the selected EALCs are applied to CWD PrP^{Sc} sourced from both brain homogenates and on contaminated surfaces, seeding activity of abnormal prions will be significantly reduced or eliminated as measured by RT-QuIC and PMCA. This effect is expected to be comparable to that achieved by conventional disinfectants such as sodium hydroxide and bleach, but with the added advantages of environmental safety and suitability for practical application in TSE-contaminated areas.

2.0. Materials and Methods

2.1. Selection and Characterization of Electro-Activated Liquid Chemicals (EALCs)

A comprehensive literature search was conducted to identify potentially relevant chemicals and relevant studies on PrP^{Sc} inactivation. Databases such as PubMed, Google Scholar, University of Ottawa Library, and ScienceDirect were explored using keywords such as “prion,” “inactivation,” “disinfection,” “electro-activated,” “chronic wasting disease,” and “environmentally friendly” to refine the search. The literature of interest was primarily focused on articles published after the year 2010, although it was necessary to include several published before that date. As a result of the literature search, two chemicals were selected to be used as positive controls due to their well-established effectivity for the destruction of prions (Taylor, 1993): household bleach (Clorox, 8.25% sodium hypochlorite) and 2N NaOH (Thermo Fisher Scientific).

Two more commercially available electro-activated liquid chemicals were selected for their previous use in environmentally friendly geared settings: CAC-717 (Santa Mineral Co., Ltd. Tokyo, Japan) and BrioHOCl (Briotech Inc., Woodinville, WA, USA). As this project is in collaboration with Laval University, they were responsible for providing several EALCs that have shown promise for their bactericidal effects. Nine EALCs (four catholytes and five anolytes) were therefore shipped to the CFIA Ottawa Laboratory – Fallowfield (OLF) from Laval University.

2.1.1. Chemical Procurement and Preparation

All the chemicals previously discussed in Section 2.1 were procured to OLF and stored in their original manufacturing packaging, light-blocked, and at room temperature.

The nine EALCs from Laval University were prepared by Dr. Mohammed Aider using a three-compartment electro-activation reactor. The central compartment was separated from the anodic compartment by an anion exchange membrane (AEM) and from the cathodic compartment by a cation exchange membrane (CEM) (Figure 4). This configuration was essential to prevent interference between the acidic and alkaline environments generated in the anodic and cathodic compartments, respectively. Electro-activation was performed using a direct electric current intensity of 800 mA for 60 minutes.

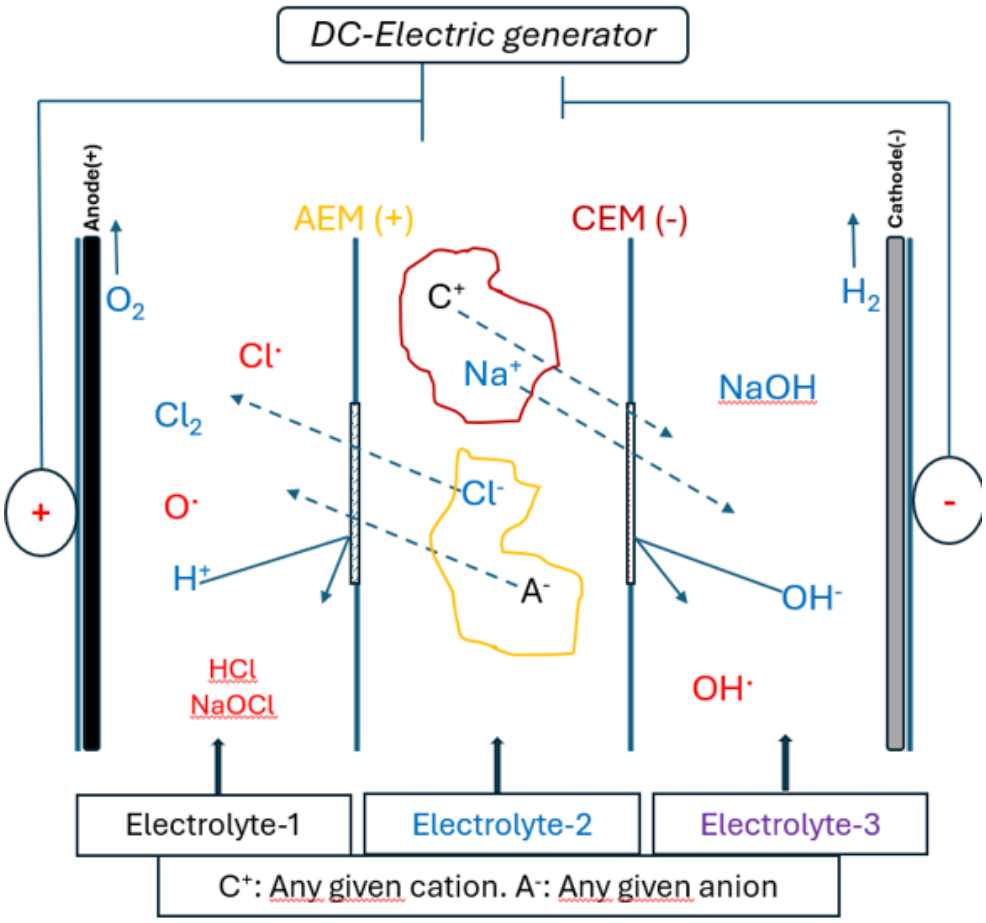

Figure 4. Representation of the Electro-Activation Reactor System. The diagram illustrates the three-compartment electro-activation reactor used for generating the EALCs used in this study. The system consists of an anodic compartment (left), a central compartment, and a cathodic compartment (right), separated by an anion exchange membrane (AEM) and a cation exchange membrane (CEM), respectively. Ion migration, electrochemical reactions, and the formation of oxidative and reductive species are shown, highlighting the generation of Cl_2, NaOCl, NaOH, and other reactive components under the influence of a direct electric current.

2.1.2. Composition of EALCs

The four catholytes and five anolytes were composed of the following:

Catholyte 1: Electro-activated solution containing Na+ ions which electro-migrated from the central compartment. The initial cathodic compartment was filled with water. The central compartment was initially filled with 2 M NaCl solution.

Catholyte 2: Electro-activated solution containing 0.1 M CaCl2 solution and $Ca2^{+}$ ions which electro-migrated from the central compartment. The cathodic compartment was initially filled with 0.1 M CaCl2 solution. The central compartment was initially filled with 1 M CaCl2 solution.

Catholyte 3: Electro-activated solution containing 0.2 M NaCl and Na^{+} ions which electro-migrated from the central compartment. The cathodic compartment was initially filled with 0.2 M NaCl solution. The central compartment was initially filled with 2 M NaCl solution.

Catholyte 4: Electro-activated solution containing 0.1 M KCl solution and K+ ions which electro-migrated from the central compartment. The initial cathodic compartment was filled with 0.1 M KCl solution. The central compartment was initially filled with 2 M KCl solution.

Anolyte 1: Electro-activated solution containing Cl- ions which electro-migrated from the central compartment. The initial anodic compartment was filled with water. The central compartment was initially filled with 2 M NaCl solution.

Anolyte 2: Electro-activated solution containing NaCl and Cl- ions which electro-migrated from the central compartment. The initial anodic compartment was filled with a 0.1 M NaCl solution. The central compartment was initially filled with 2 M NaCl solution. The cathodic compartment was initially filled with water + 3 mL of 2M NaCl.

Anolyte 3: Electro-activated solution containing CaCl2 and Cl- ions which electro-migrated from the central compartment. The initial anodic compartment was filled with a 0.1 M CaCl2 solution. The central

compartment was initially filled with 1 M CaCl2 solution. The cathodic compartment was initially filled with 0.1 M CaCl2 solution.

Anolyte 4: Electro-activated solution containing 0.1 M sodium acetate solution and Cl- ions which electro-migrated from the central compartment. The initial anodic compartment was filled with 0.1 M sodium acetate solution. The central compartment was initially filled with 2 M NaCl solution. The cathodic compartment was initially filled with a 0.1 NaCl solution.

Anolyte 5: Electro-activated solution containing 0.1 M KCl solution and Cl- ions which electro-migrated from the central compartment. The initial anodic compartment was filled with a 0.1 M KCl solution. The central compartment was initially filled with 2 M KCl solution. The cathodic compartment was initially filled with 0.1 KCl solution.

2.2. Preparation of Prion-Contaminated Materials

Materials and methods regarding bactericidal testing will be discussed in the Appendices.

2.2.1. Cervid Tissue Collection

CWD-positive and negative brain tissues were collected from two Elk (*Cervus canadensis*) individuals originating from cervid farms in Saskatchewan, Canada, which were euthanized due to CWD suspicion and sent to the CFIA's Ottawa Fallowfield Laboratory for testing. Tissues that were sent for testing include obex and lymph nodes, and the results of CWD status were determined via ELISA and immunohistochemistry (IHC). Tissues were then stored at -80°C.

2.2.2. Preparation of Chronic Wasting Disease (CWD) Brain Homogenate

Obex tissues were initially received as coarse homogenates of pure samples and were further homogenized in grinding tubes containing quarter inch grinding beads using a Precellys 24 Tissue Homogenizer (Bertin, Paris, France) to form 15% w/v (0.30 g of raw brain homogenate into 2 mL buffer = 150 mg/mL) homogenates in sterile phosphate buffered saline (PBS).

2.2.3. Preparation of Steel Wire for PrP^{Sc} Binding Assays

Stainless steel wire (Thermo Fisher Scientific), 0.51mm in diameter, was cut into segments 5 mm in length. Wires were initially rinsed with distilled water and air-dried in a biosafety cabinet (BSC) overnight. Dried wires were then stored in sterile 1.5 mL tubes at room temperature until use.

2.2.4. PrP^{Sc} Sorption onto Steel Wire: Incubation and Washing Protocols

To establish a positive control gradient, ten-fold serial dilutions (10^{-2} to 10^{-8}) were generated from a 15% brain homogenate solution prepared in PBS. Wire segments were submerged in each dilution and incubated at room temperature for one hour while rotating at 18 rpm. After incubation, wires were washed three times by brief vortexing in 1 mL PBS, then air-dried overnight in a sterile Petri dish.

2.3. Treatment of PrP^{Sc} Contaminated Samples with EALCs

2.3.1. Treatment Conditions and Exposure Time

EALCs were evaluated for their ability to degrade or inactivate PrP^{Sc} in contaminated samples. Treatment conditions, including concentration and exposure times, were optimized to assess the efficacy of EALCs under various conditions. Experiments were designed to simulate both controlled laboratory conditions and environmental scenarios relevant to prion decontamination. For each treatment condition, a minimum of 8 replicates were used in at least 2 independent experiments.

EALCs were used at their original stock concentrations, and various dilution ratios were tested to determine both the minimum effective dose and the potential for concentration-dependent prion degradation. Specifically, brain homogenate was treated with EALCs at ratios of 1:1, 1:50, 1:100, 1:200, 1:500, and 1:1000 (v/v, brain homogenate: EALC). Control groups included CWD-negative and positive untreated samples, vehicle controls (PBS-treated), and positive controls treated with either 2N NaOH (Thermo Fisher Scientific) or 40% bleach (3.3% sodium hypochlorite) (Clorox® Germicidal Bleach, 8.25% concentration).

To ensure adequate distribution, samples were mixed with the EALCs via reverse pipetting followed by gentle vortexing for approximately three seconds. All samples were exposed to treatment solutions for a standardized duration of one hour at room temperature. These exposure conditions were selected based on preliminary optimization experiments and existing literature on chemical prion decontamination (Herzog et al, 2025).

To determine the efficacy of the selected EALCs in inactivating PrP^{Sc} bound to stainless steel, each wire was placed in a sterile 1.5 mL microcentrifuge tube and fully submerged in 1 mL of EALC solution, ensuring complete contact, and allowed to incubate at room temperature for one hour. Following treatment, wires were carefully removed and immediately processed for post-treatment washing (Section 2.4.2). Controls included untreated wires, phosphate buffered saline (PBS) "mock"-treated wires, and wires exposed to conventional decontamination agents such as 2N NaOH and 40% bleach for comparison.

2.3.2. Sample Recovery and Post-Treatment Washing of Steel Wire

To ensure the removal of residual EALCs from the steel wire, a standardized washing protocol was used. Each wire was transferred to a fresh 1.5 mL microcentrifuge tube containing 1 mL of sterile PBS and subjected to three sequential washes. Washing was performed by gently vortexing the tubes for three seconds per wash, followed by removal of the supernatant. For each wash, fresh PBS was used. After the third and final wash, the wires were air-dried at room temperature overnight.

2.3.3. Controls and Validation of Treatments

To ensure any effects and reductions in PrP^{Sc} seeding activity were due to the EALCs and no other confounding factors, a series of controls were included in all experiments.

Untreated PrP^{Sc}-contaminated wires were included as a baseline to compare the natural behaviour of PrP^{Sc} throughout the duration of our assays of interest. To account for potential effects seen due to solution-based incubation for both brain homogenate and steel wire samples, vehicle controls were included where samples were incubated in PBS alone under identical conditions (one hour at room temperature). This allowed for

differentiation between spontaneous aggregate formation, chemical degradation, and any non-specific protein removal due to liquid exposure and washing steps.

To evaluate how effective EALCs are at reducing the seeding activity of PrP^{Sc} compared to established methods for prion decontamination, samples were treated with traditional prion-inactivating agents such as 2N NaOH and 40% bleach.

2.4. Real-Time Quaking-Induced Conversion (RT-QuIC) Assay

RT-QuIC was used to assess the seeding activity of PrP^{Sc} following EALC treatment. This assay detects prion-induced conversion of recombinant prion protein (recPrP) into amyloid fibrils, producing a measurable increase in fluorescence over time.

2.4.1. RT-QuIC Reaction Components and Reagent Preparation

RT-QuIC master mix was prepared to allow each well to contain 300 mM NaCl, 1 mM EDTA, 10 µM ThT, 0.1 mg/mL recPrP, and 50 mM Na2PO4 (pH 7.38–7.4). The reaction master mix (95 µL) was added to each well of a black-walled, clear-bottom 96-well plate.

2.4.2. Sample Preparation and Seeding Conditions

PrP^{Sc}-positive samples treated with EALCs were compared to all previously described controls (Section 2.4.3). Samples were subjected to 10-fold serial dilutions in 0.05% SDS and 5 µL of diluted sample was added to the master mix contained within each well. Once added, the sample was mixed five times by reverse pipetting, and the plate was covered with sealing tape.

2.4.3. RT-QuIC Assay Conditions

RT-QuIC reactions were conducted at 42°C in a BMG FLUOstar Omega plate reader (BMG Labtech, Ortenberg, Germany). Each cycle lasted approximately 15 min, with seven repeats of a one-minute shake at 700 rpm (double orbital) and a one-minute rest, followed by a one-minute reading. ThT fluorescence

measurements were taken every cycle at a gain of 1000, excitation of 450 nm, and emission of 480 nm. RT-QuIC ran for a maximum of 80 hours.

2.4.4. Fluorescence Detection and Threshold Calculations

The assay data was exported from Mars data analysis software (BMG Labtech) and processed in Microsoft Excel (Microsoft 365) and RStudio (version 2024.02.29). The cycle threshold (CT) was defined as the time when the ThT signal of a reaction surpassed a fixed threshold based on background fluorescence (T_{stdev}), which was calculated using the average baseline or fourth cycle reading of all the reactions in relative fluorescent units (RFU) plus ten standard deviations.

In our study, we adopted the 33-hour optimal assay duration for RT-QuIC detection of CWD in white-tailed deer obex tissues, as established by Yilmaz et al. (2024). T_{stdev} was determined to maximize sensitivity and specificity in their optimization of the RT-QuIC assay. We used this 33-hour time point as cutoff criteria for classifying replicates as positive. Specifically, replicates that crossed the CT within 33 hours were considered true positives. Replicates that crossed the CT after 33 hours were not classified as true positives, as they may represent background noise or non-specific amplification, consistent with the findings of Yilmaz et al (2024). This approach allowed us to maintain consistency with validated assay parameters and ensure the reliability of our CWD detection results.

2.5. Protein Misfolding Cyclic Amplification (PMCA) Assay

PMCA was used to amplify PrP^{Sc} from CWD-positive, EALC-treated samples to assess the persistence of seeding activity following EALC treatment. This technique relies on cyclic sonication and incubation to promote the conversion of normal PrP^{C} into its misfolded and infectious form (Figure 5).

2.5.1. PMCA Reaction Setup

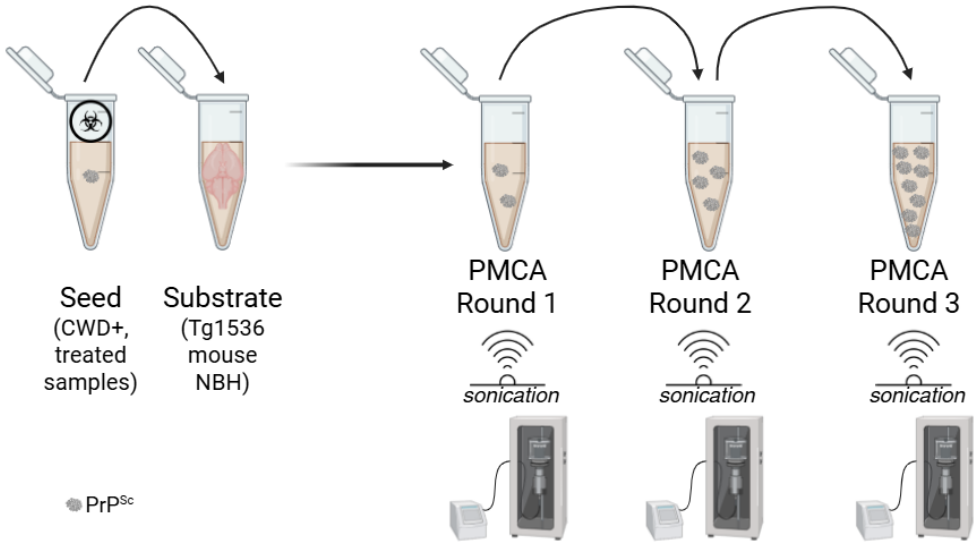

Figure 5. Schematic representation of the PMCA assay. A small amount of PrP^{Sc}-positive seed or experimental sample is added to normal, healthy PrP^{C} substrate derived from TgElk mouse brain homogenate. The sample then undergoes round one of cyclic amplification in a sonicator programmed to deliver repeated bursts of high-frequency ultrasonic waves. After round one of amplification, 8 µL is taken and diluted into fresh substrate to begin the next round. This process is repeated multiple times (e.g., three rounds shown here) to amplify even trace amounts of PrP^{Sc}. In this study, each round involved 39 cycles of sonication, each including a 40-second sonication burst (~200 W) followed by a 30-minute incubation period, totaling 26 minutes of sonication time per round.

2.5.2. Preparation of Normal Brain Homogenate as a Substrate

Normal brain homogenate (NBH) used as the substrate for PMCA was prepared from healthy, non-infected transgenic mice overexpressing elk PrP (Tg1536 line). These TgElk mice express cervid PrP^{C} approximately 2.5-fold higher than endogenous murine PrP (LaFauci et al, 2006). The Tg1536 line was originally developed by Dr. Debbie McKenzie's group at the University of Alberta, Canada, and provided courtesy of their laboratory for this study.

Perfused brains were harvested from Tg1536 mice and homogenized into a 10% (v/v) solution in Soto's conversion buffer (PBS containing 150 mM NaCl, 1.0% Triton X-100, and Complete™ protease inhibitor mixture) by manual homogenization with a Potter-Elvehjem PTFE pestle and glass tube at 4 °C. Homogenates were centrifuged at 1000 rpm for 1 minute to remove insoluble debris and stored in 500 µL aliquots at -80°C until use. Freeze-thaw cycles were minimized to prevent protein degradation.

2.5.3. PMCA Sample Preparation

PMCA sample preparation began with 10-fold serial dilutions of the sample of interest in 10% NBH done in 1.5 mL tubes. Serial dilutions examined for our purpose were mainly 10^{-2} to 10^{-4}. An aliquot of 20 µL from the initial serial dilutions was reserved and frozen at -80°C to be examined as the "pre-PMCA" sample. This acts as a control for non-amplified reactions. In 0.2 mL microcentrifuge tubes, 8 µL of each serially diluted sample was added to 72 µL of NBH and carefully mixed by reverse-pipetting. Each tube was then individually sealed using parafilm wrap and given a five-minute bath in 2% bleach before being rinsed and loaded into the microtubule holder and placed in the horn of the sonicator.

2.5.4. Cyclic Sonication and Incubation Conditions

Cyclic sonication, combined with incubation, is a crucial step in the PMCA protocol, as it generates mechanical and thermal forces that facilitate the conversion of Pr^{PC} into PrP^{Sc}. Sonication was performed with a Misonix Q700 sonicator (QSonica, Newtown, USA) set up with a horn and a disk-shaped rack adaptor for processing a large number of samples in microtubes. The sonicator and associated horn were placed within an incubator set at 37°C to mimic physiological conditions that optimize prion conversion in-vivo. The sonicator was programmed to perform 40-second bursts of power at approximately 200 watts, with 30-minute incubation intervals, for a cumulative total sonication time of 26 minutes per PMCA round. A water bath was used to regulate temperature and prevent overheating during amplification. After each PMCA round, sample tubes were decontaminated in 2% bleach for five minutes before being rinsed and placed at -80°C.

2.5.5. PMCA Rounds and Sample Collection

PMCA is performed in serial rounds, where 8 µL of the amplified product from one round serves as the seed for the next. In this study, PMCA was conducted for up to four rounds. At the start of each passage, samples from the previous round were retrieved from −80°C storage and thawed. An 8 µL aliquot was then diluted into 72 µL of NBH to initiate the next round. Additionally, a 20 µL aliquot from each round was collected in a 1.5 mL microcentrifuge tube for later analysis by western blot.

2.5.6. Validation of Amplification Efficiency

Analysis of PMCA products through Western blot was used to confirm successful PrP^{Sc} amplification.

2.6. Western Blot Analysis of PrP^{Sc}

Western blot analysis was used to evaluate the effectiveness of EALCs against PrP^{Sc} in PMCA-amplified samples. This technique relies on SDS-PAGE to separate proteins by molecular weight, followed by transfer of the proteins to a PVDF membrane for immunodetection. The RIDA® monoclonal antibody P4 (Cedarlane), which specifically targets the N-terminal epitope 93WGQGGSH99 (ovine numbering) of the prion protein (Harpaz et al, 2023), was used to detect PrP^{Sc}. By comparing banding patterns and signal intensities, the technique enables qualitative and semi-quantitative examination of prion amplification and the effects of EALC treatments on PrP^{Sc} stability.

2.6.1. Sodium Phosphotungstic Acid (NaPTA) Precipitation for PrP^{Sc} Enrichment

To enhance the detection of PrP^{Sc} by western blot, samples underwent sodium phosphotungstic acid (NaPTA) precipitation before electrophoresis. NaPTA precipitation was carried out as described by Huang et al, 2005. Briefly, 15% CWD-positive (enzyme-linked immunosorbent assay [ELISA] optical density [OD] ≥ 3.5) and 15% CWD-negative (ELISA OD < 0.1) brain homogenate samples were thawed and treated with each EALC at the respective treatment ratio for one hour at room temperature. Aliquots containing 20 µL of untreated CWD-positive and CWD-negative brain homogenates were reserved as positive and

negative controls for both the PMCA assay, as well as assay controls for subsequent western blots. After treatment, 100 µL of the sample was combined with 100 µL of a 4% sarkosyl solution and incubated at 37°C for 30 minutes. Next, 24 µL of NaPTA was added to the sample to achieve a final concentration of 0.3%, followed by incubation at 37°C for 120 minutes while shaking at 400 rpm. The sample was then centrifuged at 16,249 x g for 30 minutes, and the supernatant was discarded. The pellet was resuspended in 20 µL PMCA Soto's conversion buffer for subsequent PMCA analysis or in distilled water (dH_2O) for direct western blotting. Samples were stored at -80°C for future use.

2.6.2. Sample Preparation, SDS-PAGE, and Transfer to Membrane

For proteinase K (PK) treatment, 1 mg/mL stock solution was prepared by dissolving 1 mg of dry PK (Sigma Aldrich) in 1 mL storage buffer, which contained 12.1 mg Tris base, 8 mL dH_2O, 1.1 mg CaCl2, and 5 mL glycerol, adjusted to pH 7.5. For each sample, 2 µL of this stock was added to 20 µL of the sample to achieve a final PK concentration of 100 µg/mL. The mixture was incubated at 37°C for 60 minutes. Following PK treatment, 20 µL of XT sample buffer (Bio-Rad) and 4 µL of XT reducing agent (Bio-Rad) were added to the sample, which was then heated at 95°C for five minutes to inactivate PK. The samples were either processed immediately or stored at -20°C for up to 24 hours.

For electrophoresis, Criterion™ XT Bis-Tris Protein Gels were placed in a Criterion™ cell. The upper and lower chambers of the cell were filled with 60 mL and 800 µL of XT MOPS migration buffer, respectively, and each well of the gel was gently rinsed with migration buffer. Each well was loaded with 10 µL of the sample, along with 10 µL of diluted kaleidoscope prestained standard and MagicMark. The gel was run for 50-55 minutes at 200V at room temperature. For protein transfer, a piece of 0.2 µm PVDF membrane was prepared by cutting it to the size of the gel, labelling it, and soaking it in ethanol, water, and transfer buffer. After electrophoresis, the gel was equilibrated in a transfer buffer, and a gel sandwich was assembled by stacking an extra thick filter stack, membrane, gel, and filter stack in the Trans-Blot® Turbo™ Transfer system. The cassette was loaded into the blotting system and the transfer was run at 25V for five minutes.

2.6.3. Immunoblotting with P4 Antibody

After protein transfer, the cassette was removed from the bay, and the membrane was carefully extracted for development. First, the membrane was quickly fixed in ethanol, followed by a five-minute rinse in dH_2O and immediately incubated in blocking buffer (5% non-fat milk) for 30 minutes at room temperature or overnight at 4°C. The blocking solution was then discarded, and the membrane was incubated with primary monoclonal antibody (Ab-I) P4 (RIDA®, Cedarlane) diluted 1:5000 in wash solution 1 (10 mM PBS, 0.1% Tween-20) for 60 minutes at room temperature on a rocker plate under medium agitation. After rinsing twice, the membrane was incubated with secondary antibody (Ab-II) goat anti-mouse polyclonal serum conjugated with horseradish peroxidase (Bio-Rad) diluted 1:5000 in wash solution 1. After rinsing three more times with wash solution 1, the membrane was rinsed a final time in wash solution 2 (4 mM PBS). Excess liquid was drained from the membrane, which was then placed in a plastic folder and evenly saturated with 2 mL of Clarity Western ECL substrate. The membrane was incubated in a dark cabinet for five minutes to allow for signal development. Chemiluminescent images were captured using the ChemiDoc™ Touch Imaging System under optimized exposure settings.

2.6.4. Detection and Image Analysis

Images were taken from the ChemiDoc™ and analyzed using the ImageLab software (Bio-Rad, version 6.1.0.07).

2.7. Statistical and Data Analysis

2.7.1. RT-QuIC Data Processing and Interpretation

Raw fluorescence data (ThT RFU) generated from RT-QuIC were exported from the MARS software and analyzed using RStudio (Version 2023.12.1), Microsoft Excel (Version 2502), and GraphPad Prism (Version 10.4.1). T_{stdev} for positive amplification was defined using a fixed fluorescence threshold set at 10 standard deviations above the mean baseline. The CT value was calculated for each well and used as a quantitative measure of seeding activity. Data was visualized as amplification curves and frequency of

positive replicates per treatment condition. Comparative analyses were conducted across dilutions and treatment groups to assess PrP^{Sc} inactivation.

2.7.2. Western Blot

Western blot band intensities were assessed qualitatively by comparing the signal's presence or absence, banding pattern shifts, and intensity differences relative to positive (PBS-treated) and negative (CWD-negative) controls. Samples showing reduced or absent PrP^{Sc} bands after PK digestion were interpreted as evidence of partial or complete inactivation. Semi-quantitative interpretation (e.g., “strong,” “moderate,” “faint,” or “no signal”) was used when comparing treatment efficacy across multiple rounds of PMCA.

2.7.3. Statistical Analysis

Statistical analyses were conducted to evaluate the efficacy of EALC treatments in reducing PrP^{Sc} seeding activity, as measured primarily by RT-QuIC. All statistical analysis were performed using GraphPad Prism (version 10.4.1), and a p-value < 0.05 was deemed statistically significant.

For RT-QuIC data, raw ThT RFU values were exported from MARS software and processed in Microsoft Excel and RStudio (version 2023.12.1) to determine the time at which each reaction crossed T_{stdev} (resulting in a respective CT value). Before statistical testing, each dataset was assessed for normality using the Shapiro–Wilk test. Since the data did not meet normality assumptions, non-parametric analyses were employed, such as the Mann-Whitney U-test. This was used to assess pairwise comparisons between treatment and control groups. In addition to the CT value comparisons, the proportion of positive RT-QuIC replicates per treatment was calculated. This type of categorical data was analyzed using Fisher’s exact test, as sample sizes were small, and some expected frequencies were below the threshold required for other statistical methods.

Due to the qualitative nature of Western blotting, statistical tests were not applied to those data. Instead, treatment effects were interpreted based on a visual comparison of band presence, intensity, and patterns

between EALC-treated samples and controls. Emphasis was placed on assessing PrP^{Sc} degradation following PK digestion, particularly across multiple PMCA rounds.

2.8. Safety and Decontamination Procedures

2.8.1. Biosafety Level 2 (BSL-2) Containment Measures

All experiments involving infectious prion materials were conducted under biosafety containment level 2 (CL-2) conditions in compliance with CFIA institutional biosafety regulations and National Canadian biosafety standards for handling prion diseases. Upon entering the lab, it was required to always wear personal protective equipment (PPE), such as a disposable gown, double gloves when working with positive samples, and designated lab shoes. All work with infectious materials was performed in designated CL-2 work areas, which included BSCs (Class II). Surfaces and equipment were routinely decontaminated using a freshly made 20% bleach solution with a contact time of 10 minutes before and after handling prion-contaminated samples to prevent contamination.

2.8.2. Prion Decontamination Strategies

Although this study is interested in exploring EALCs for prion decontamination across different environmental surfaces, existing prion decontamination protocols must be used to maintain a contamination-free environment. To achieve this, a freshly prepared 20% (v/v) bleach solution in dH_2O was utilized. The bleach solution was applied to surfaces using a wash bottle and allowed to remain for 10 minutes to ensure adequate contact time. Following treatment, any residual bleach was removed using a paper towel dampened with dH_2O. To decontaminate any metal or glass instruments such as forceps or tweezers, homogenization tools, and containers, a designated basin containing 20% bleach was used. The instruments and tools were fully submerged in this basin and left to incubate at room temperature for one hour. After the decontamination period, the instruments were thoroughly rinsed with dH_2O and left to dry before further use.

2.8.3. Handling and Disposal of Infectious Waste Materials and Methods

Due to the nature of prions and their resistance to classical decontamination methods, all waste produced in the CL-2 TSE lab at OLF must be disposed of through incineration. This includes all tissue samples, regardless of prion status (positive or negative), as well as liquid waste generated during experimental procedures such as Western blot, and solid laboratory waste, including packaging materials, gloves, pipette tips, paper, and tubes.

To manage all solid waste, there are several biohazard step-on waste bins situated in each work area. These bins are lined with autoclavable biohazard waste bags. All waste from the lab is deposited into these bags, including the small biohazard bags kept within the BSC. Once a week, all waste is collected from the labs and placed into a larger incineration barrel which is then transported to be disposed of through incineration.

3.0 Results

3.1. Evaluation of the Effects of EALC Treatment on PrP^{Sc} in Brain Homogenate

Following initial bactericidal testing (see appendices in Section 7.0), selected EALCs were evaluated for their ability to reduce the seeding activity of PrP^{Sc} derived from CWD-positive elk brain homogenate. Using RT-QuIC, this section presents experimental results comparing the seeding amplification from untreated, mock-treated, and chemically treated brain homogenate.

3.1.1. Seeding Activity of Untreated and Mock-Treated Controls

Untreated and mock-treated CWD-positive and negative brain homogenate samples were used to establish the baseline seeding activity to which the EALC treatments are compared. PBS was selected as the mock-treatment control because it is physiologically inert, does not alter prion structure or seeding properties, and serves to replicate the dilution steps applied during EALC treatment.

As stated in the Materials and Methods, homogenates from CWD-positive and negative cervid brain tissues were homogenized to 15% w/v (150 mg/mL) in sterile PBS. Samples mock-treated with PBS were

subjected to a one-hour incubation at each indicated volume used for EALC treatment ratios. Each sample was plated in quadruplicate, and two independent experiments were conducted to confirm the results. Results show the average of these replicates, including their standard errors. Each plate also contained quadruplicate samples of standard controls to ensure assay efficacy. These standard controls were 10^{-4} dilutions of CWD-positive and negative homogenate in 0.05% SDS, along with no treatment control wells containing only master mix.

Serial dilutions examined via RT-QuIC confirmed that the assay can sensitively and selectively detect prion seeds in elk brain homogenate (Figure 6). CWD-positive brain homogenate generated sigmoidal ThT fluorescence curves and measurable CT values across six $\log_{10}$ dilutions (10^{-3} through 10^{-8}), whereas all reactions seeded with CWD-negative brain homogenate or no-template controls (NTC) did not amplify at any point during the 75-hour run. Notably, the 10^{-2} dilution of brain homogenate resulted in fully inhibited amplification, which will be further discussed in Section 4.2.1. Mean CT values rose from approximately 6 hours at 10^{-3} to approximately 46 hours at 10^{-8} (Table 1). This inverse correlation indicated a dose-dependent relationship. No CT value could be produced for samples at or beyond the 10^{-9} dilution, but low-amplitude ThT curves were still visible. Though still present, these low amplitude curves do not qualify as positive due to failing to cross the fluorescence threshold (T_{stdev}) within the 75-h run and true amplification appearing in fewer than half of replicate wells, and while conditions vary between testing facilities, criteria such like this has been used in the past to verify positivity (Burgener et al, 2022; Holz et al, 2022).

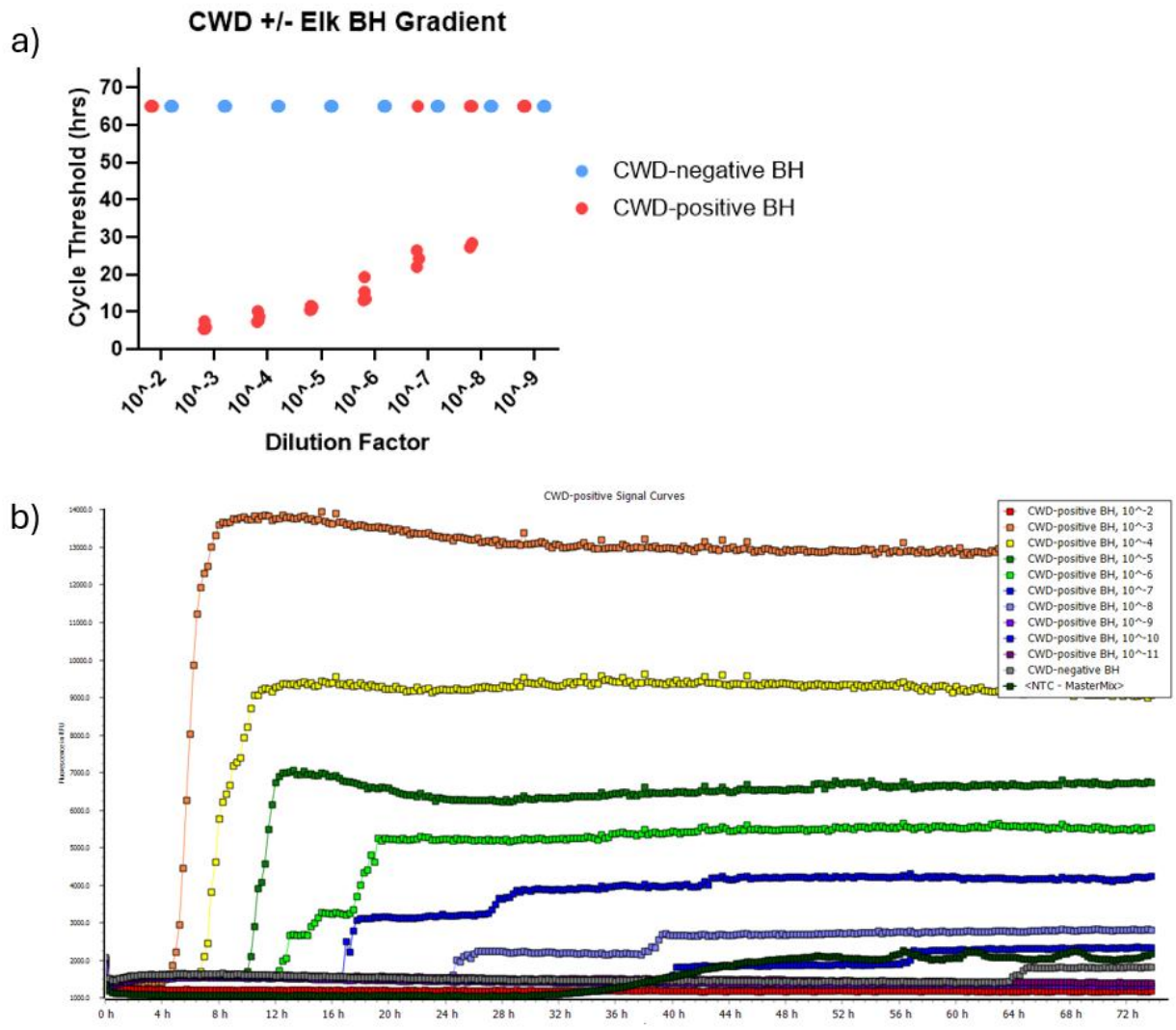

Figure 6. The seeding activity of serially diluted elk CWD-positive and negative brain homogenates as measured by RT-QuIC. a) Relationship between serial sample dilutions (n = 4, 10^{-2} to 10^{-9}, containing approximately 1.50 x 10^{-2} g/mL to 1.50 x 10^{-9} g/mL of brain tissue, respectively) of 15% elk CWD positive (red) and negative (blue) brain homogenates seeded RT-QuIC reactions. The seeding activity was detectable in positive CWD sample dilutions 10^{-3} through 10^{-8} with the CT values increasing as seed concentration decreased, reflecting the expected dilution-dependent delay. Negative brain homogenate produced no detectable signal at any dilution. b) Corresponding ThT fluorescence, as measured in relative fluorescence units (RFU), curves over 75 hours for the same dilution series but including higher dilutions 10^{-10} and 10^{-11}. Higher-concentration positive samples reached maximal fluorescence within the first 8 h,

whereas more dilute samples exhibited progressively right-shifted and lower amplitude curves. All negative controls and NTCs remained at baseline throughout the run.

To establish a baseline seeding response curve, untreated CWD-positive elk brain homogenate was serially diluted from 10^{-2} to 10^{-9} and seeded into RT-QuIC reactions. Each dilution was tested in quadruplicate (n = 4). Mean CT values (hrs) and standard error are reported in Table 1, along with the number of positive replicates per dilution.

Table 1. RT-QuIC CT values for a 10-fold serial dilution gradient of CWD-positive elk brain homogenate.

Sample	Dilution	Mean CT Value (hrs)	Standard Error (±)	Number of positive replicates
CWD-positive elk brain homogenate	10^{-2}	65.000	0.000	0/4
	10^{-3}	6.050	0.379	4/4
	10^{-4}	8.468	0.500	4/4
	10^{-5}	11.002	0.199	4/4
	10^{-6}	15.294	1.099	4/4
	10^{-7}	34.401	7.931	3/4
	10^{-8}	46.397	8.321	2/4
	10^{-9}	65.000	0.000	0/4

To verify that no factors such as sample handling methods or the dilution of the sample during the treatment itself compromised the detectable seeding activity via RT-QuIC, mock-treatments were prepared by mixing 15% CWD-positive or negative elk brain homogenate with sterile PBS across a range of dilutions (Figure 7). Although each treatment dilution starts with a different brain homogenate-to-chemical ratio (e.g., 2:1 (v/v) gives 10 % brain homogenate, 1:1 (v/v) gives 7.5 % brain homogenate, 1:1000 (v/v) gives 0.015 % brain homogenate), it was important to ensure the same concentration of PrP^{Sc} brain homogenate was included in each final RT-QuIC well. To achieve this, brain homogenate was treated at the indicated ratios of PBS and allowed to incubate for one hour at room temperature. After treatment, an aliquot of each sample is diluted into RT-QuIC reaction buffer (0.05% SDS) to result in a universal final concentration of 0.01% brain homogenate (v/v), regardless of starting concentration. At this concentration, 0.01% brain

homogenate (v/v) contains the same amount of PrP^{Sc} as the 10^{-4} dilution factor as seen in Figure 6. After normalizing every sample to a final concentration of 0.01 % brain homogenate, all replicates at all PBS treatment ratios (but one replicate seen after the 2:1 treatment) seeded with CWD-positive elk brain homogenate crossed T_{stdev} with a mean CT of approximately 10 hrs, which further supports the similarity to the CT recorded for the 10^{-4} untreated positive control.

a)

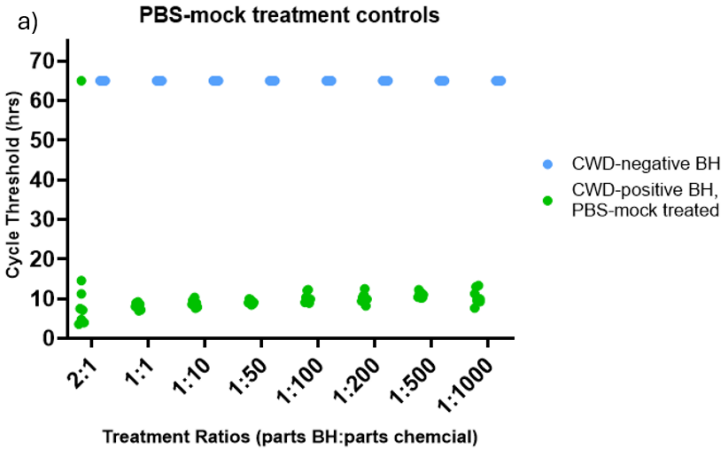

b)

	Mean CT Value (hrs)	Standard error	Number of positive replicates
2:1	7.518	1.542	7/8
1:1	8.220	0.288	8/8
1:10	8.830	0.313	8/8
1:50	9.127	0.181	8/8
1:100	10.189	0.464	8/8
1:200	10.143	0.443	8/8
1:500	11.033	0.257	8/8
1:1000	10.440	0.692	8/8

Figure 7. Effect of PBS mock-treatment on RT-QuIC detection of seeding activity of CWD-positive elk brain homogenate. CWD-positive elk brain homogenate (n = 8) was incubated for 1 hour with PBS at the indicated brain homogenate: PBS ratios (2:1 to 1:1000 [v/v]) and then diluted to a standard 0.01 % brain homogenate (equivalent to the 10^{-4} untreated dilution or containing 1.50 x 10^{-4} g/mL brain tissue) before RT-QuIC. a) Individual CT values for eight technical replicates are shown for mock-treated CWD-positive and CWD-negative brain homogenate controls. Positive samples are clearly distinguished from negative controls, and CT values trend linearly across dilutions. b) Summary table showing the mean CT value, associated standard error (±), and number of positive replicates for each tested ratio.

3.1.2. Reduction in RT-QuIC Seeding Activity Following EALC Exposure

Across all experiments, the PBS mock-treated controls amplified reliably between replicates (Figure 7). Negative controls included on each plate were 10^{-4} dilutions of CWD-negative elk brain homogenate to act as assay controls, and no positives were detected from any sample. Samples treated with various EALCs,

and the standard chemicals used for decontamination (2N NaOH and 40% Bleach) showed varying levels of success after the one-hour treatment. Samples were run in quadruplicate and were taken from two independent experiments to verify accuracy. Log reductions were estimated from the linear regression of CT versus 10-fold dilutions of untreated brain homogenate ($R^2 = 0.97$).

Treatment with each catholyte resulted in elevated CT values at most treatment ratios compared to PBS-treated positive brain homogenate (Table 2), suggesting there is, at a minimum, some partial reduction in seeding activity after treatment with these EALCs. For catholytes 1-3, modest CT increases were seen for most treatment ratios, except for the 1:100 (v/v) treatment ratios of Catholyte 1 and 2, and the 1:10 (v/v) treatment ratio of Catholyte 3 (Table 2) which proved statistically insignificant ($p > 0.05$) as assessed via the Mann-Whitney U-test. Of all catholytes, catholyte 4 showed the strongest inhibitory effect on PrP^{Sc} seeding activity with several treatments, particularly at the 1:1000 (v/v) ratios (mean CT = 23.247 ± 1.201 hrs), where seeding was noticeably reduced and mean CT value were comparable to those found between the 10^{-6} and 10^{-7} serial dilution of untreated brain homogenate as seen in Figure 8, or approximately a 1000-fold reduction in activity. As Catholyte 4 at the 1:1000 (v/v) treatment ratio was the catholyte that showed the most drastic and consistent effect on PrP^{Sc}, it was further selected for simulation testing and mechanistic assessment.

Across most treatment ratios, exposure to each anolyte solution varied in its impact on seeding activity compared to the PBS-treated controls. As seen in Table 2, CT was most increased from ~10 hrs to ~18 hrs when elk CWD PrP^{Sc} brain homogenate was treated with a 1:1000 (v/v) treatment ratio of Anolyte 2 (mean CT = 18.403 ± 0.945 hrs). Under these conditions, seeding activity was comparable to the 10^{-6} serial dilution of untreated brain homogenate as seen in Figure 8, or approximately a 100-fold reduction in activity. This is the only anolyte that shows such a dramatic effect, as all others show CT values much more like those of the PBS controls (Figure 7), meaning little to no reduction of seeding activity took place under most conditions. Interestingly, some samples treated with anolytes had CT values lower than those of the PBS controls and were statistically significant in doing so (notably 1:100 (v/v) treatment ratio using Anolyte 3:

$p < 0.05$, Mann-Whitney U test), meaning the opposite intended effect of the chemicals was taking place and PrP^{Sc} seeding and aggregation was happening rapidly (up to 39% faster as in the case of the 1:100 (v/v) treatment ratio using Anolyte 3). This may reflect matrix effects from the EALCs that enhance nucleation, though more investigation is needed into this mechanism. In the same manner that Catholyte 4 was selected from all catholytes for further investigation, Anolyte 2 was selected from the anolytes to be used in further experiments due to its comparatively strong inhibitory effect on PrP^{Sc} seeding activity, particularly at higher treatment ratios, while maintaining consistent RT-QuIC amplification across replicates.

After treatment with BrioHOCl (Figure 8, k), CT values are relatively similar to those of the PBS controls. The 1:10 (v/v) treatment produced 7/8 positive replicates, but one replicate failed to amplify and caused an increase in the mean of this condition. Interestingly, a similar pattern is observed with BrioHOCl treatment as with some anolytes, in which CT values appear lower than those of the controls, and at the 1:500 (v/v) ratio, treated samples are statistically significantly lower than PBS-treated samples. The only sample presenting the statistical significance of reduction of seeding activity for BrioHOCl is the 1:1000 (v/v) treatment, and it is right at the cutoff of significance with a p-value of 0.0449. CAC-717 shows a much more distinct concentration effect. For ratios 1:1 and 1:10 (v/v) treated with PBS, samples are similar to PBS-treated samples and do not show a statistically significant difference. 1:50 and 1:100 (v/v) treatments result in slight increases in seeding activity, with seeding activity and CT values comparable to those found between the 10^{-5} serial dilution of untreated brain homogenate, as seen in Figure 8 or approximately a 10-fold reduction in activity. Higher treatment ratios of 1:500 and 1:1000 (v/v) produced much higher CT values, with the 1:500 treatment reducing seeding activity by approximately 500-fold and the 1:1000 (v/v) treatment reducing seeding activity by approximately 10,000-fold. 2N NaOH and 40% bleach were completely effective at eliminating seeding activity from all samples at all treatment dilutions.

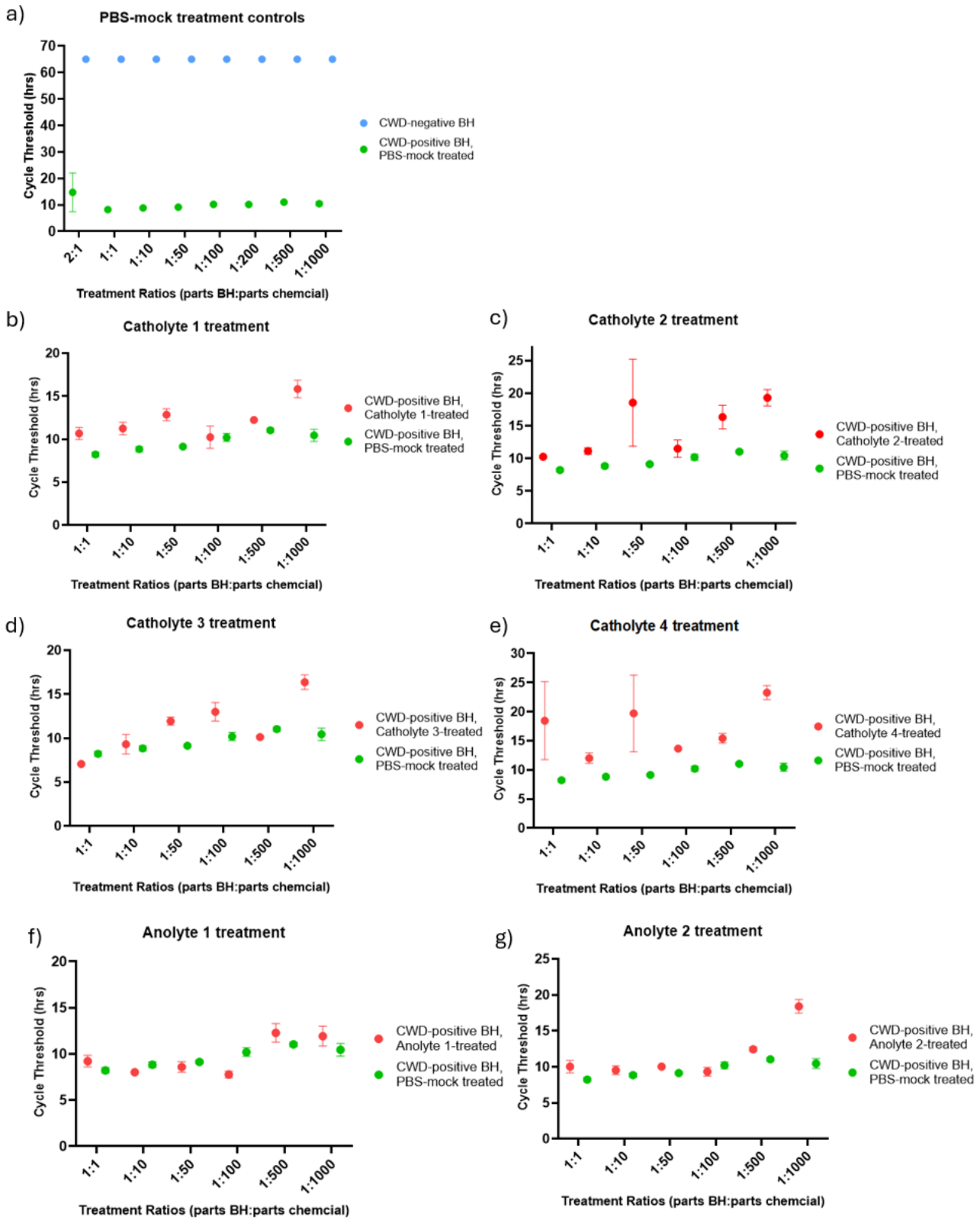
a)
PBS-mock treatment controls
Cycle Threshold (hrs)
Treatment Ratios (parts BH:parts chemcial)
2:1
1:1
1:10
1:50
1:100
1:200
1:500
1:1000
CWD-negative BH
CWD-positive BH, PBS-mock treated
b)
Catholyte 1 treatment
CWD-positive BH, Catholyte 1-treated
CWD-positive BH, PBS-mock treated
c)
Catholyte 2 treatment
CWD-positive BH, Catholyte 2-treated
CWD-positive BH, PBS-mock treated
d)
Catholyte 3 treatment
CWD-positive BH, Catholyte 3-treated
CWD-positive BH, PBS-mock treated
e)
Catholyte 4 treatment
CWD-positive BH, Catholyte 4-treated
CWD-positive BH, PBS-mock treated
f)
Anolyte 1 treatment
CWD-positive BH, Anolyte 1-treated
CWD-positive BH, PBS-mock treated
g)
Anolyte 2 treatment
CWD-positive BH, Anolyte 2-treated
CWD-positive BH, PBS-mock treated

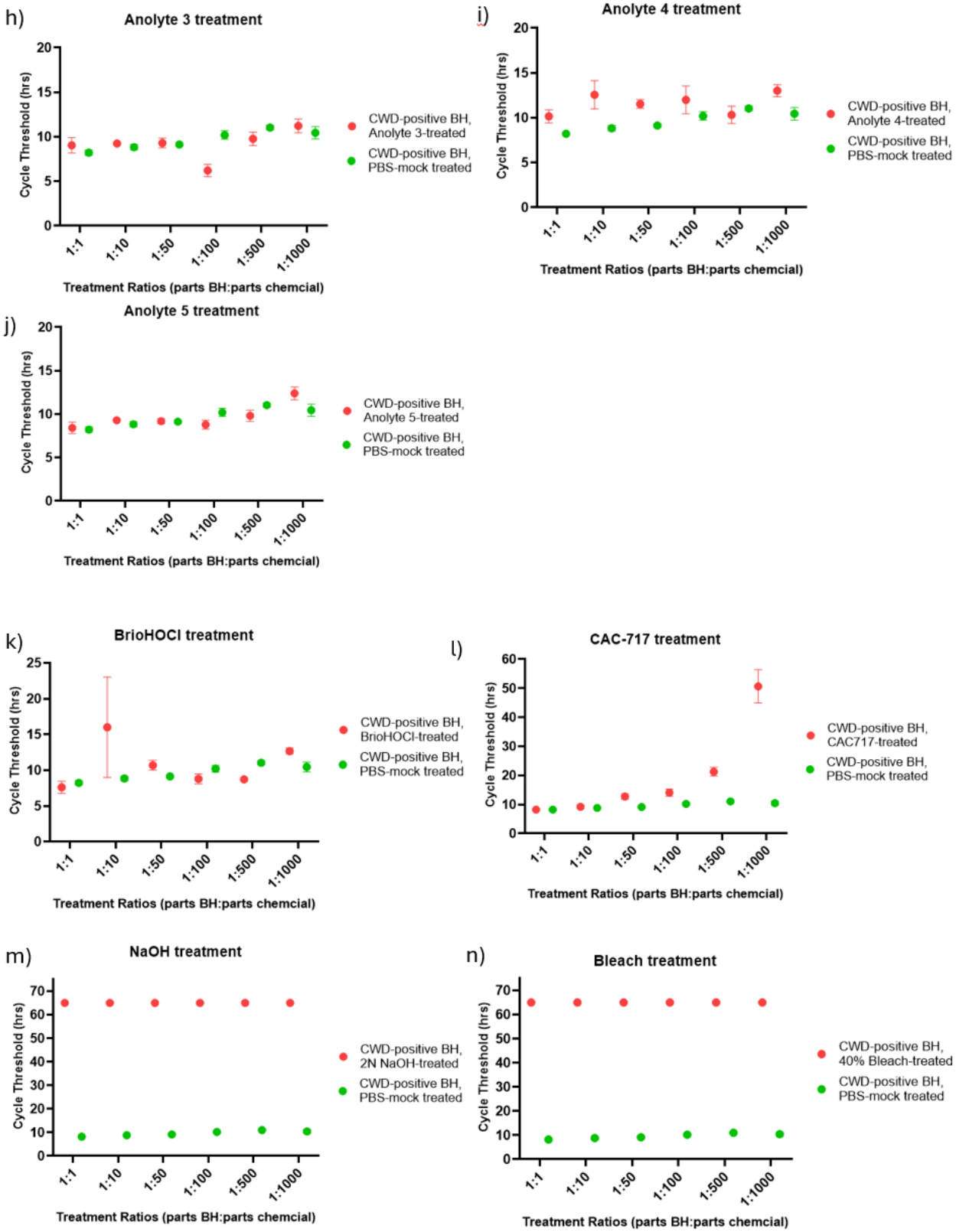
h)
Anolyte 3 treatment
Cycle Threshold (hrs)
Treatment Ratios (parts BH:parts chemcial)
CWD-positive BH, Anolyte 3-treated
CWD-positive BH, PBS-mock treated
i)
Anolyte 4 treatment
Cycle Threshold (hrs)
Treatment Ratios (parts BH:parts chemcial)
CWD-positive BH, Anolyte 4-treated
CWD-positive BH, PBS-mock treated
j)
Anolyte 5 treatment
Cycle Threshold (hrs)
Treatment Ratios (parts BH:parts chemcial)
CWD-positive BH, Anolyte 5-treated
CWD-positive BH, PBS-mock treated
k)
BrioHOCl treatment
Cycle Threshold (hrs)
Treatment Ratios (parts BH:parts chemcial)
CWD-positive BH, BrioHOCl-treated
CWD-positive BH, PBS-mock treated
l)
CAC-717 treatment
Cycle Threshold (hrs)
Treatment Ratios (parts BH:parts chemcial)
CWD-positive BH, CAC717-treated
CWD-positive BH, PBS-mock treated
m)
NaOH treatment
Cycle Threshold (hrs)
Treatment Ratios (parts BH:parts chemcial)
CWD-positive BH, 2N NaOH-treated
CWD-positive BH, PBS-mock treated
n)
Bleach treatment
Cycle Threshold (hrs)
Treatment Ratios (parts BH:parts chemcial)
CWD-positive BH, 40% Bleach-treated
CWD-positive BH, PBS-mock treated
1:1
1:10
1:50
1:100
1:500
1:1000

Figure 8. Effects of selected EALCs and conventional decontaminants on CWD-positive elk brain homogenate as quantified via RT-QuIC. a - n) CWD-positive elk brain homogenate was incubated for 1 hour with each respective chemical at the indicated brain homogenate: chemical ratios (1:1 to 1:1000 [v/v]) and then diluted to a standard 0.01 % brain homogenate (containing 1.50×10^{-4} g/mL brain tissue) before RT-QuIC. Mean CT values from 8 replicates of each treated sample are plotted for each condition (red) along with the PBS mock-treated control sample (green). CWD-negative brain homogenate controls (blue) are only shown in the first panel.

Table 2. RT-QuIC CT values following a 1-hour treatment of CWD-positive elk brain homogenate with selected EALCs and conventional decontaminants.

Chemical Treatment	Treatment Ratio (parts brain homogenate: parts chemical [v/v])	Mean CT Value (hrs)	Standard Error (±)	Number of positive replicates
PBS mock-treatment	1:1	8.220	0.288	8/8
	1:10	8.830	0.313	8/8
	1:50	9.127	0.181	8/8
	1:100	10.189	0.464	8/8
	1:500	11.033	0.257	8/8
	1:1000	10.440	0.692	8/8
Catholyte 1	1:1	10.654	0.698	8/8
	1:10	11.237	0.742	8/8
	1:50	12.842	0.695	8/8
	1:100	10.223	1.289	8/8
	1:500	12.225	0.378	8/8
	1:1000	15.839	1.023	8/8
Catholyte 2	1:1	10.260	0.343	8/8
	1:10	11.125	0.495	8/8
	1:50	10.260	6.676	7/8
	1:100	11.125	0.684	8/8
	1:500	16.331	1.800	8/8
	1:1000	19.290	1.233	8/8
Catholyte 3	1:1	7.052	0.153	8/8
	1:10	9.300	1.114	8/8
	1:50	11.927	0.458	8/8
	1:100	12.993	1.052	8/8

	1:500	10.114	0.155	8/8
	1:1000	16.367	0.837	8/8
Catholyte 4	1:1	18.437	6.696	8/8
	1:10	12.002	0.905	8/8
	1:50	19.692	6.578	7/8
	1:100	13.643	0.590	8/8
	1:500	15.414	0.821	8/8
	1:1000	23.247	1.201	7/8
Anolyte 1	1:1	9.215	0.634	8/8
	1:10	8.017	0.246	8/8
	1:50	8.581	0.575	8/8
	1:100	7.764	0.366	8/8
	1:500	12.271	0.998	8/8
	1:1000	11.917	1.082	8/8
Anolyte 2	1:1	10.013	0.855	8/8
	1:10	9.518	0.606	8/8
	1:50	10.017	0.515	8/8
	1:100	9.312	0.594	8/8
	1:500	12.433	0.325	8/8
	1:1000	18.403	0.945	8/8
Anolyte 3	1:1	9.042	0.879	8/8
	1:10	9.244	0.331	8/8
	1:50	9.297	0.540	8/8
	1:100	6.205	0.684	8/8
	1:500	9.764	0.744	8/8
	1:1000	11.219	0.761	8/8
Anolyte 4	1:1	10.156	0.732	8/8
	1:10	12.553	1.563	8/8
	1:50	11.530	0.480	8/8
	1:100	11.982	1.543	8/8
	1:500	10.315	0.957	8/8
	1:1000	13.015	0.666	8/8
Anolyte 5	1:1	8.414	0.651	8/8
	1:10	9.283	0.150	8/8
	1:50	9.189	0.276	8/8
	1:100	8.784	0.516	8/8
	1:500	9.812	0.639	8/8
	1:1000	12.382	0.718	8/8
BrioHOCl	1:1	8.220	0.288	8/8
	1:10	8.829	0.313	8/8

	1:50	9.127	0.181	8/8
	1:100	10.189	0.464	8/8
	1:500	11.033	0.257	8/8
	1:1000	10.440	0.692	8/8
CAC-717	1:1	8.205	0.643	8/8
	1:10	9.203	0.624	8/8
	1:50	12.727	0.951	8/8
	1:100	14.076	1.230	8/8
	1:500	21.255	1.492	8/8
	1:1000	50.640	5.727	2/8
2N NaOH	1:1	65	0	0/8
	1:10	65	0	0/8
	1:50	65	0	0/8
	1:100	65	0	0/8
	1:500	65	0	0/8
	1:1000	65	0	0/8
40% Bleach	1:1	65	0	0/8
	1:10	65	0	0/8
	1:50	65	0	0/8
	1:100	65	0	0/8
	1:500	65	0	0/8
	1:1000	65	0	0/8

CWD-positive brain homogenate was incubated for 1 hour at room temperature with each chemical at the indicated brain homogenate: chemical ratio, then diluted to 0.01% and seeded into RT-QuIC reactions. Each condition was tested in quadruplicate across two independent experiments (n = 8). The mean CT value and standard error are shown for each treatment ratio. RT-QuIC wells per treatment were scored positive when their fluorescence crossed T_{stdev} within the 33-h cutoff period.

3.1.3 Assessment of Treatment Replicability and Variability

RT-QuIC yielded high technical consistency between replicates and experiments when using CWD-positive, EALC-treated brain homogenate. As seen in Table 3, PBS-treated controls demonstrated high levels of amplification across all dilutions, and always remained positive (8/8 positives), confirming the integrity of treatment and RT-QuIC methods, while negative control brain homogenate remained devoid of

PrP^{Sc} seeding activity (0/8 positives). For each of these treatments, Clopper–Pearson 95% confidence intervals ranged from 63.1–100.0 % (for 8/8 positives) or 0.0–36.9 % (for 0/8 negatives), indicating statistical uncertainty due to the small sample size, but supporting the qualitative outcomes of the replicates.

As seen in Table 3, all four examined catholytes, all five anolytes, and BrioHOCL demonstrated the same level of replicability as the PBS-treated positive control, producing 100% positivity and showing no detectable reduction in the number of wells classified as positive by RT-QuIC. In contrast, conventional disinfectants, 2N NaOH and 40% Bleach, eliminated all replicates of PrP^{Sc} seeding activity (0/8 positives, $p < 0.001$ vs. PBS-treated positive control, Fisher's exact).

CAC-717 was the only chemical that displayed intra-treatment variability, with only 2 of 8 (25%) wells generating sufficient amplification to cross T_{stdev} within the 33-hour positivity cutoff period. This represents a significant reduction compared with the positive control ($p = 0.00699$, Fisher's exact). The confidence interval for the CAC-717 1:1000 (v/v) treated PrP^{Sc} ranged from 3.2–65.1 %, reflecting the appearance of reduced seeing activity and the variability of positivity between samples. This likely reflects the differences in how well the treatment worked across samples, or the persistent survival of a small number of prion seeds after treatment.

Table 3. RT-QuIC seeding replicability after a 1-hour treatment of CWD-positive elk brain homogenate at the 1:1000 (v/v) brain homogenate: chemical treatment ratio.

Chemical Treatment	Number of RT-QuIC positive wells	Number of RT-QuIC negative wells	Percent Positivity %	Difference in significance from Pos Control	CI Lower (95%	CI Upper (95%)
CWD-negative, PBS mock-treatment	0	8	0%	-	0	36.9
CWD-positive, PBS mock-treated	8	0	100%	-	63.1	100
Catholyte 1	8	0	100%	No difference	63.1	100
Catholyte 2	8	0	100%	No difference	63.1	100

Catholyte 3	8	0	100%	No difference	63.1	100
Catholyte 4	8	0	100%	No difference	63.1	100
Anolyte 1	8	0	100%	No difference	63.1	100
Anolyte 2	8	0	100%	No difference	63.1	100
Anolyte 3	8	0	100%	No difference	63.1	100
Anolyte 4	8	0	100%	No difference	63.1	100
Anolyte 5	8	0	100%	No difference	63.1	100
BrioHOCL	8	0	100%	No difference	63.1	100
CAC-717	2	6	25%	Significant decrease, p = 0.0070	3.2	65.1
40% Bleach	0	8	0%	Significant decrease, p = 0.000155	0	36.9
2N NaOH	0	8	0%	Significant decrease, p = 0.000155	0	36.9

Eight technical replicates were treated with either EALCs or conventional disinfectants, and RT-QuIC wells per treatment were scored positive when their fluorescence crossed T_{stdev} within 33 h. Percent positivity was calculated as (positive wells ÷ 8) x 100. Uniform 8/8 or 0/8 outcomes suggest high intra-assay agreement, whereas mixed positivity outcomes (e.g., 2/8) reveal variability between treated samples. The difference in significance for each chemical compared to the PBS-treated positive control was calculated using a two-tailed Fisher's exact test. P-values listed are those < 0.05, indicating a statistically significant reduction in positive replicates.

3.2. Evaluation of EALC Treatment of PrP^{Sc} Sorbed onto Steel Wire

EALCs were further tested on steel wire artificially contaminated with CWD PrP^{Sc} to simulate environmental contamination scenarios. This section outlines the development and validation of a steel wire sorption model, allowing the assessment of EALC efficacy on a solid surface similar to those found in field conditions. The experiments began with optimization of the wire preparation and washing protocol to ensure consistent PrP^{Sc} binding and removal of possible inhibitors. RT-QuIC was then used to confirm the

presence and detectability of PrP^{Sc} bound to steel. Finally, the efficacy of each EALC in inactivating steel-bound prions was evaluated, providing insight into their potential for use in decontaminating reusable equipment and infrastructure.

3.2.1. Evaluation of Wire Preparation and Washing Protocol

To establish a reliable protocol for preparing PrP^{Sc}-contaminated steel wire, several wire pre-treatment and washing conditions were evaluated to minimize non-specific background interactions while preserving surface-bound seeding activity (Figure 9). Stainless steel wires were cut into 5 mm segments, rinsed with distilled water, and left to dry until use. To evaluate whether the steel wire material itself had any influence on RT-QuIC assay performance, control experiments were performed using uncontaminated wires that had not been exposed to any elk brain homogenate. These blank wires were processed through the same washing protocol and then directly added to RT-QuIC wells. In addition, the final PBS wash solutions from these control wires were also tested independently in RT-QuIC to assess for any presence of inhibitory or stimulatory contaminants. No amplification was observed in the blank wires or their corresponding washes ($n = 4$), indicating that the wire material did not interfere with ThT fluorescence, recombinant substrate stability, or overall assay performance. These results confirmed that any subsequent seeding activity observed in test conditions was attributable specifically to PrP^{Sc} sorbed to the wire surface, not due to artifacts from the wire or residual wash contaminants.

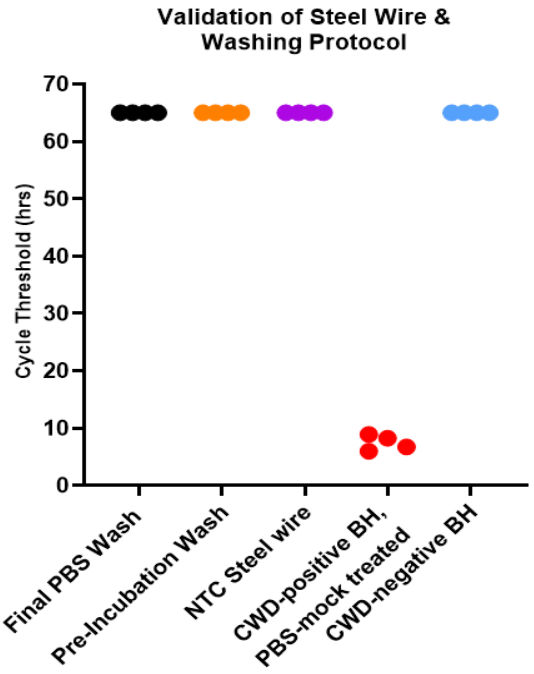

Figure 9. RT-QuIC assessment of steel wire preparation and washing protocol controls. RT-QuIC reactions seeded with the final PBS wash and pre-incubation wash solutions showed no amplification over 65 hours. Uncontaminated steel wires (NTC Steel wire) also produced no signal, indicating no background interference from the wire material. In contrast, strong amplification was observed in wells seeded with CWD-positive elk brain homogenate (POS elk BH), while no amplification was observed from CWD-negative brain homogenate (NEG elk BH).

With the washing protocol validated and the background signal eliminated, subsequent experiments focused on confirming the ability of RT-QuIC to detect PrP^{Sc} bound to steel wire following exposure to infectious brain homogenate.

3.2.2. Confirmation of PrP^{Sc} Binding Controls to Steel Wire Using RT-QuIC

Before assessing the effects of EALC treatments on PrP^{Sc}-contaminated steel wire, a preliminary experiment was conducted to confirm the successful adsorption of prion seeds to steel wire segments and to determine the sensitivity of RT-QuIC in detecting wire-bound PrP^{Sc}. To evaluate the relative amount of PrP^{Sc} retained on the wire under our experimental conditions, a gradient series of wires were prepared using

serial dilutions of the starting brain homogenates (ranging from 10^{-2} to 10^{-8}) and each applied to replicate wires, followed by a mock treatment with PBS for one hour at room temperature, and washed before being placed directly into RT-QuIC reaction wells (Figure 10). RT-QuIC was then performed under the same conditions previously used for Section 3.2.

Amplification was observed for PBS mock-treated steel wires, which served as a control to simulate the submersion and incubation steps used for chemical treatment of the steel wires without introducing any inactivating effects. This confirmed that the chemical treatment process itself did not drastically affect PrP^{Sc} retention. Compared to untreated brain homogenate controls, PBS mock-treated wires showed higher CT values. For dilutions 10^{-2}, 10^{-3}, and 10^{-4}, amplification maintained within the 33-hour T_{stdev} cutoff.

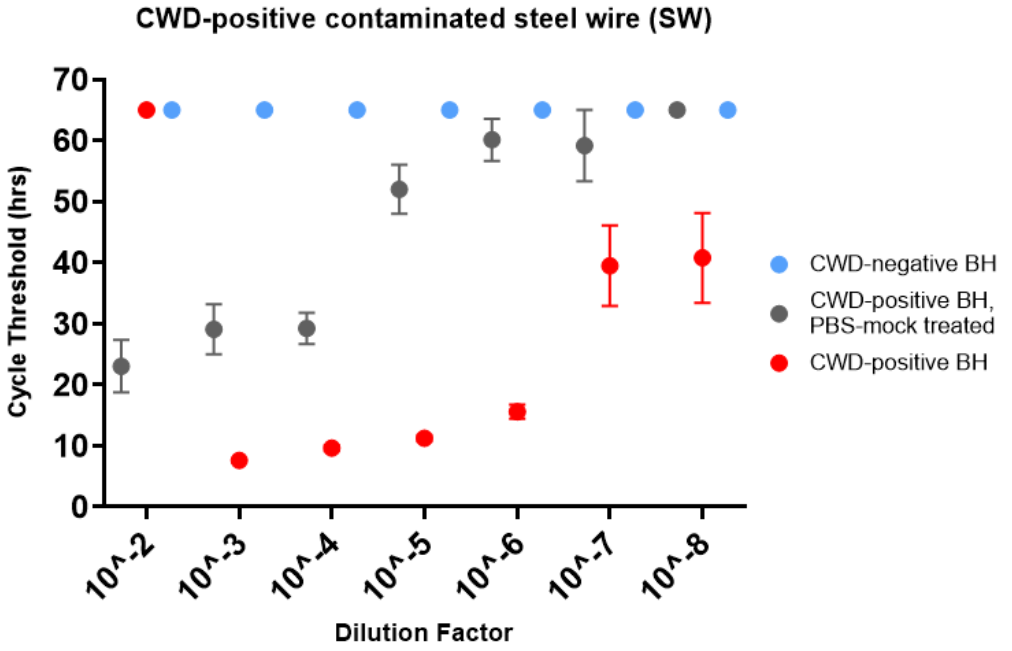

Figure 10. RT-QuIC detection of PrP^{Sc} seeding from steel wires exposed to a 10-fold gradient of CWD-positive elk brain homogenate. Steel wires (n = 8) were incubated for 1 hour in serial 10-fold dilutions (10^{-2} to 10^{-8}) of CWD-positive elk brain homogenate, mock-treated in PBS for 1 hour, washed, and transferred directly to RT-QuIC reactions to assess the retention of surface-bound PrP^{Sc}. Amplification was observed across dilutions 10^{-2} to 10^{-4}, with increasing CT values at lower concentrations. Amplification

was highly delayed after the 33-hour positivity cutoff for samples incubated in 10^{-5} through 10^{-7} dilutions. No amplification was detected throughout the assay for samples incubated in 10^{-8}, resulting in a final CT of 65 hours. Controls included untreated brain homogenate dilutions (POS elk BH) and CWD-negative brain homogenate (NEG elk BH). Wires incubated with CWD-negative brain homogenate did not produce any amplification. Each point represents the mean CT value (n = 8), with error bars indicating the standard error of the mean.

To more accurately assess RT-QuIC detection of PrP^{Sc} seeding from contaminated steel wires, the mean CT values and their associated standard errors were calculated, and the number of positive replicates per dilution was recorded in Table 4. As expected, the number of positive RT-QuIC replicates declined with increasing dilution. At 10^{-2} and 10^{-3}, all or almost all eight replicates crossed T_{stdev} within the 33-hour positivity threshold (8/8 and 7/8, respectively). The number of positive replicates decreased as dilution increased, and only three replicates amplified at 10^{-5} (3/8), while no seeding was detected within the positivity cutoff period for 10^{-6} or 10^{-8} (0/8 each), and only one replicate of the 10^{-7} sample produced a CT value within this time. This trend suggests that RT-QuIC is a viable method to detect PrP^{Sc} seeding activity once sorbed to steel wire from an original CWD-positive elk brain homogenate up to the 10^{-5} dilution, though with lower reliability at higher dilutions.

In addition to the reduced number of positive replicates at lower concentrations, greater variability in amplification was also observed among steel wire replicates compared to untreated brain homogenate samples. This was reflected in higher standard error values across all dilutions tested, particularly between 10^{-2} and 10^{-4}, where the standard error ranged from ~2.5 to 4 hours (Table 4). This variability may stem from differences in PrP^{Sc} sorption efficiency across wires or amplification ability throughout the assay.

Table 4. RT-QuIC detection of PrP^{Sc} seeding activity from steel wires contaminated with serial dilutions of CWD elk brain homogenate.

	Dilution	Mean CT Value (hrs)	Standard Error (±)	Number of positive replicates
PrP^{Sc} contaminated steel wire	10^{-2}	23.035	4.276	8/8
	10^{-3}	29.092	4.076	7/8
	10^{-4}	29.245	2.552	6/8
	10^{-5}	52.021	3.999	3/8
	10^{-6}	60.131	3.451	0/8
	10^{-7}	59.159	5.841	1/8
	10^{-8}	65.000	0.000	0/8

Steel wires were incubated in 10-fold serial dilutions of CWD-positive brain homogenate, washed, and used to seed RT-QuIC reactions. The mean CT values, their respective standard errors, and the number of positive replicates (n = 8) are reported for each dilution. Amplification was observed consistently at higher PrP^{Sc} concentrations, while lower concentrations produced longer CT values and fewer positive wells. No positive replicates were recorded from any wires exposed to wires incubated in 10^{-6} or 10^{-8} dilutions of brain homogenate.

Overall, multiple positive replicates at higher brain homogenate dilutions support the conclusion that PrP^{Sc} retains its seeding activity following sorption to steel surfaces, validating the model for subsequent decontamination studies.

3.2.3. EALC Efficacy Against PrP^{Sc} Contaminated Steel Wire

For subsequent testing of EALC efficacy against PrP^{Sc} sorbed to steel wire, brain homogenate dilutions of 10^{-2} (1.50×10^{-2} g/mL brain tissue), 10^{-3} (1.50×10^{-3} g/mL brain tissue), and 10^{-4} (1.50×10^{-4} g/mL brain tissue) were selected for wire contamination. These dilutions were chosen based on earlier gradient testing (Section 3.3.2), which demonstrated reliable and consistent RT-QuIC detection at these concentrations, with all replicates (8/8) showing amplification at 10^{-2}, 7/8 replicates positive at 10^{-3}, and 6/8 replicates positive at 10^{-4}. Mean CT values for these dilutions also crossed T_{stdev} below the 33-hour positivity threshold,

indicating concrete PrP^{Sc} seeding activity. Importantly, dilutions beyond 10^{-4} showed a steep decline in positive replicates, making them less suitable for treatment evaluation. By selecting dilutions with defined seeding activities, it was possible to evaluate EALC effects across a small range while maintaining confidence that any differences in signals after treatment reflect a reduction of PrP^{Sc} activity rather than a detection error.

Catholyte 4 and Anolyte 2 were both successful in decreasing the seeding activity of PrP^{Sc}, particularly at lower concentrations. Compared to PBS-treated controls, wires treated with Catholyte 4 resulted in a noticeable but incomplete reduction of PrP^{Sc} seeding activity (Table 5). Amplification was still observed with the 10^{-2} dilution, although CT values were higher than those of PBS controls. The delayed amplification beyond the 33-hour T_{stdev} suggests that while seeding activity was substantially suppressed, residual PrP^{Sc} may still retain the ability to induce fibril formation. The presence of residual activity warrants further investigation, especially to determine its potential implications for residual infectivity of PrP^{Sc} from environmental surfaces. Anolyte 2 showed a similar inactivation pattern to Catholyte 4 but with slightly milder effects. Though CT values were delayed relative to PBS controls, residual seeding activity was measurably higher than the negative controls, indicating that Anolyte 2 was unable to eliminate the ability of PrP^{Sc} to convert PrP^{C} into PrP^{Sc} even after sorption to stainless steel surfaces.

Treatment of contaminated steel wires with BrioHOCl suppressed almost all detectable PrP^{Sc} seeding activity, with CT values relatively comparable to those of negative controls. However, some replicates did show evidence of low levels of amplification. CAC-717-treated samples also showed slight evidence of residual seeding activity even after a 1-hour treatment. Though CT values for CAC-717-treated samples were below the negative control at 65 hours, they were still significantly reduced compared to the PBS controls. Interestingly, BrioHOCl being more effective than CAC-717 at reducing CT values of PrP^{Sc}-contaminated steel wire is the inverse effect seen with brain homogenate-treated samples (Figure 11).

Unsurprisingly, treatment with both 2N NaOH and 40% bleach led to a complete loss of detectable PrP^{Sc} activity on steel wire. RT-QuIC assays showed no amplification across all dilutions, with CT values remaining at the 65-hour maximum.

From these results, there is a clear hierarchy of inactivation efficacy present depending on the EALC or commercial chemical used. Treatment with 2N NaOH, 40% bleach, and BrioHOCl was all around the most effective chemical for reducing the seeding activity of PrP^{Sc}-contaminated steel wires, followed by Catholyte 4, CAC-717, and Anolyte 2, which, while they were still effective, managed to maintain seeding.

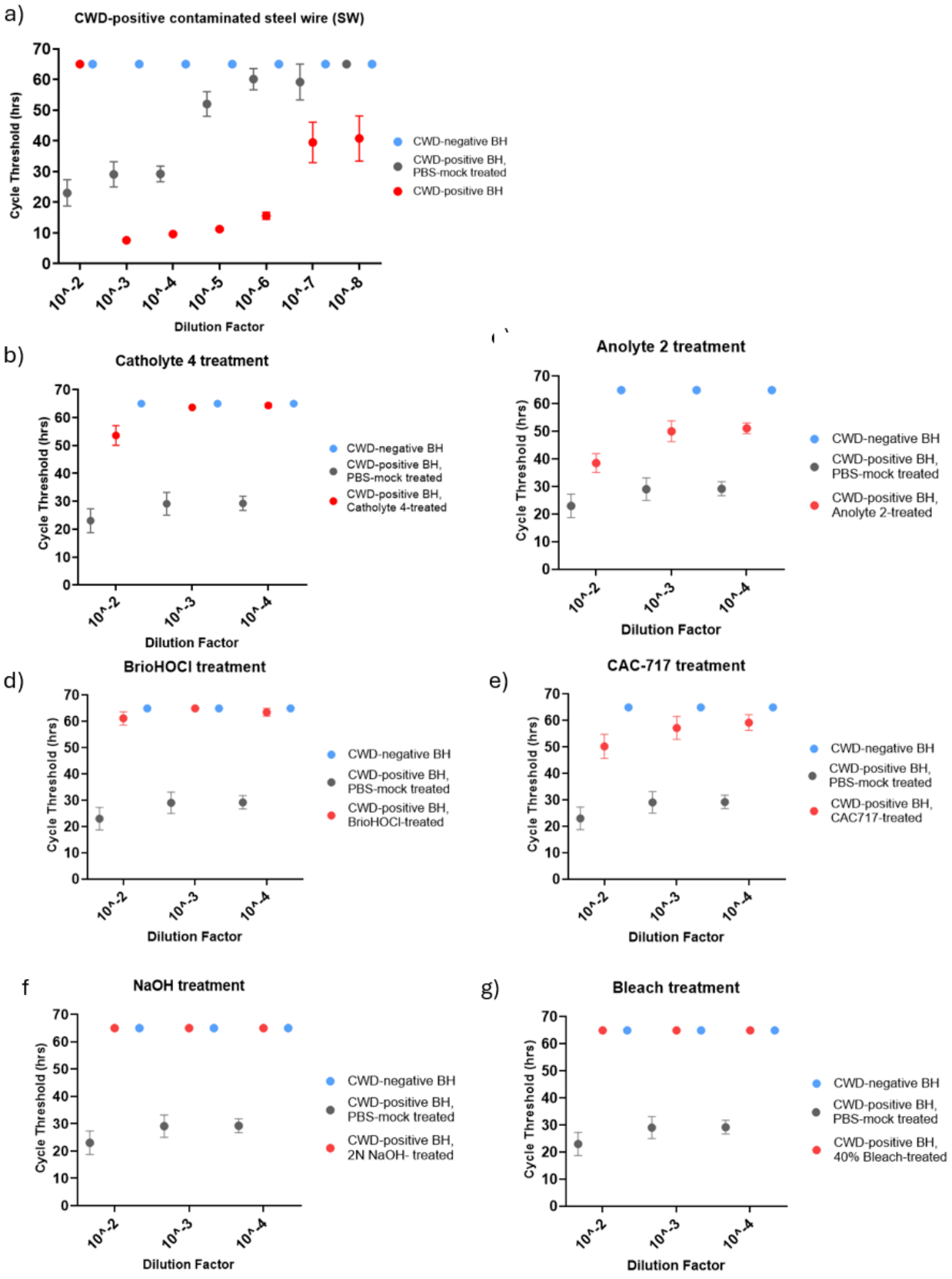
a)
CWD-positive contaminated steel wire (SW)
Cycle Threshold (hrs)
Dilution Factor
10^-2
10^-3
10^-4
10^-5
10^-6
10^-7
10^-8
CWD-negative BH
CWD-positive BH, PBS-mock treated
CWD-positive BH
b)
Catholyte 4 treatment
CWD-positive BH, Catholyte 4-treated
c)
Anolyte 2 treatment
CWD-positive BH, Anolyte 2-treated
d)
BrioHOCl treatment
CWD-positive BH, BrioHOCl-treated
e)
CAC-717 treatment
CWD-positive BH, CAC717-treated
f
NaOH treatment
CWD-positive BH, 2N NaOH- treated
g)
Bleach treatment
CWD-positive BH, 40% Bleach-treated

Figure 11. RT-QuIC analysis of PrP^{Sc} seeding activity on steel wires contaminated with CWD-positive elk brain homogenate (10^{-2} to 10^{-4}) following treatment with selected EALCs and commercial chemicals. a - g) Mean CT values and their associated SEM of steel wires (n = 8) were calculated following a 1-hour incubation in 10^{-2}, 10^{-3}, or 10^{-4} serial dilutions of CWD-positive elk brain homogenate and treated for 1-hour with either Catholyte 4, Anolyte 2, BrioHOCl, CAC-717, 2N NaOH, or 40% household bleach. PBS-treated wires served as mock-treated controls. Following treatment, wires were washed with PBS, dried, and placed directly into RT-QuIC wells to assess bound PrP^{Sc}. The seeding activity was consistently detectable across PBS-treated controls. In all chemical-treated samples, CT values were dramatically reduced, and in some cases, eliminated.

RT-QuIC analysis of PrP^{Sc}-contaminated steel wires revealed dramatic differences in inactivation efficacy across chemical treatments, as summarized in Table 5. PBS mock-treated samples consistently produced consistent seeding activity at all dilutions, with CT values crossing T_{stdev} before the 33-hour positivity threshold and many positive replicates. These samples served as references for statistical comparisons.

Catholyte 4 treatment of contaminated steel wire led to delayed amplification at all dilutions, with no replicates crossing T_{stdev} before the positivity threshold as the PrP^{Sc} concentration decreased. Mean CT values for all dilutions were significantly higher than PBS controls ($p < 0.05$, Mann-Whitney U test). Fisher's exact tests also confirmed significantly fewer positive ($p < 0.05$) replicates than PBS at all dilutions, supporting a partial but incomplete inactivation effect. Anolyte 2 produced a similar trend to Catholyte 4. Though similar, RT-QuIC CT values after Anolyte 2 treatment were faster than Catholyte 4 and more positive replicates were observed. All dilutions maintained statistical significance, and Fisher's exact test showed a significant decline in the number of positive wells even though some replicates produced amplification before the 33-hour cutoff.

BrioHOCl treatment nearly eliminated all detectable seeding activity from steel wire samples. CT values were at or very close to the 65-hour assay maximum across all dilutions, with only isolated amplification events observed, and these values were not within the range to be considered positive. Mann-Whitney U

tests showed significant differences from PBS at 10^{-2} ($p = 0.0007$), 10^{-3} ($p = 0.0004$), and 10^{-4} ($p = 0.0004$). Fisher's exact tests indicated significantly fewer positive replicates than PBS at all three dilutions (all $p < 0.001$), supporting strong inactivation efficacy for this sample type.

CAC-717 also produced delayed CT values and reduced amplification. Although seeding activity was detected in some replicates, average CT values were significantly higher than PBS controls at all examined dilutions of brain homogenate used to contaminate the steel wire ($p < 0.05$, Mann-Whitney U test). Fisher's exact tests confirmed significantly reduced positivity rates ($p < 0.001$).

All CT values for 2N NaOH and 40% Bleach were fixed at the 65-hour mark, meaning no amplification occurred. These results were significantly different from PBS controls at the 10^{-2}, 10^{-3}, and 10^{-4} (all $p = 0.0004$, Mann-Whitney U test; all $p = 0.0002$, Fisher's test), confirming complete inhibition of PrP^{Sc} seeding activity.

Table 5. RT-QuIC CT values following a 1-hour treatment of PrP^{Sc}-contaminated steel wires with selected EALCs and conventional decontaminants.

Chemical	The Dilution Factor of Brain Homogenate used to contaminate SW	Mean CT Value (hrs)	Standard Error (±)	Number of positive replicates
PBS mock-treatment	10^{-2}	23.035	4.276	8/8
	10^{-3}	29.092	4.076	7/8
	10^{-4}	29.245	2.552	6/8
Catholyte 4	10^{-2}	53.592	3.542	1/8
	10^{-3}	63.637	0.705	0/8
	10^{-4}	64.326	0.674	0/8
Anolyte 2	10^{-2}	38.565	3.387	3/8
	10^{-3}	50.089	3.797	1/8
	10^{-4}	51.159	2.002	0/8
BrioHOCl	10^{-2}	61.222	2.557	0/8
	10^{-3}	65.000	0.000	0/8
	10^{-4}	63.552	1.448	0/8
CAC-717	10^{-2}	50.286	4.587	1/8

	10^{-3}	57.257	4.310	1/8
	10^{-4}	59.261	3.001	0/8
NaOH	10^{-2}	65.000	0.000	0/8
	10^{-3}	65.000	0.000	0/8
	10^{-4}	65.000	0.000	0/8
Bleach	10^{-2}	65.000	0.000	0/8
	10^{-3}	65.000	0.000	0/8
	10^{-4}	65.000	0.000	0/8

Steel wires (SW) were contaminated through a 1-hour incubation with CWD-positive elk brain homogenate at the indicated dilution (10^{-2} to 10^{-4}), treated for 1 hour with each chemical, washed, dried, and transferred directly into RT-QuIC reaction wells. PBS-treated wires served as mock-treated controls. Each treatment condition was tested in eight technical replicates (n = 8). The mean CT value, standard error, and number of RT-QuIC positive replicates are reported for each treatment and dilution. RT-QuIC wells were considered positive when their fluorescence crossed the T_{stdev} within the 33-hour cutoff period.

3.3. Amplification of Residual PrP^{Sc} from Treated Samples using PMCA

To complement RT-QuIC findings and further investigate the presence of residual prion seeding activity following chemical treatment, PMCA was used to allow for visualization of PrP^{Sc} if any seed remains present after treatment. Prior to amplification, PrP^{Sc} was enriched from treated samples using NaPTA precipitation to improve sensitivity and reduce background interference. PMCA was then conducted to compare amplification profiles between control and EALC-treated samples, with particular attention to differences in the timing and intensity of PrP^{Sc} signal emergence. This data offers additional insight into the effectiveness of each treatment and the potential for residual prion activity.

3.3.1. NaPTA Precipitation of PrP^{Sc}

Initial NaPTA precipitation and Western blot analysis were performed directly on post-treatment samples at the same dilutions used for RT-QuIC (1:1 to 1:1000 [v/v]) without PMCA amplification (Figure 12). Based on visual analysis of Western blot results, PrP^{Sc} was detected in the PBS-treated 1:1 (v/v) sample,

which exhibited a strong triplet banding pattern between 20–30 kDa, indicating a high concentration of PrP^{Sc} retained in the sample following treatment. Faint bands were also visible in the 1:50 (v/v) dilution, suggesting that although the protein concentration was lower, residual PrP^{Sc} remained detectable. No signal was observed in the 1:500 or 1:1000(v/v) dilutions, indicating that the quantity of PrP^{Sc} present was below T_{stdev} for this assay. Though given that RT-QuIC could detect residual seeding activity in samples treated at the 1:1000 (v/v) dilutions and knowing that RT-QuIC has much higher sensitivity than Western blotting (Atarashi, 2023), it became clear that amplification of aggregates present within treated samples was required to improve PrP^{Sc} detection via Western blot. Based on this, NaPTA precipitation was performed after treatment, and several rounds of PMCA followed to increase sensitivity and improve downstream detection.

The normal brain homogenate (NBH) negative control showed no bands, confirming assay and antibody specificity, while the NBH non-PK control showed a strong signal, indicating total PrP^{C} content. The positive infected brain homogenate (IBH) control displayed the expected PrP^{Sc} banding pattern between 20 and 30 kDa, validating the assay and transfer efficiency (Figure 12).

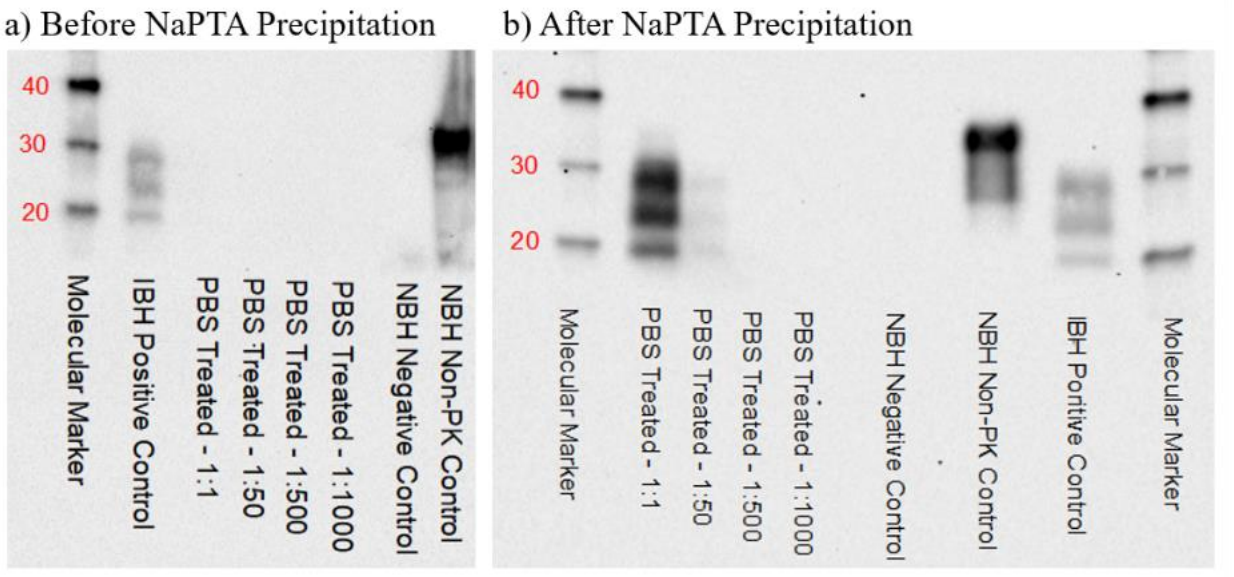

Figure 12. Western blot detection of NaPTA precipitated PrP^{Sc} in PBS mock-treated control samples at various treatment dilutions. a) Samples of 15% CWD-positive brain homogenate were mock-treated

with PBS at several treatment dilutions (1:1 to 1:1000 [v/v]) for 1 hour at room temperature and examined directly. b) Samples of 15% CWD-positive brain homogenate were mock-treated with PBS at several treatment dilutions (1:1 to 1:1000 [v/v]) for 1 hour at room temperature. After treatment, samples were NaPTA precipitated, PK treated (100 μg/mL), subject to electrophoresis followed by immunoblotting, and finally imaged. Controls include PK and non-PK treated normal brain homogenate (NBH), as well as CWD-positive infected brain homogenate (IBH). Molecular weight markers (kDa) are as indicated.

3.3.2. PMCA of EALC-Treated and Control PrP^{Sc}

To increase the sensitivity of detection for low levels of residual PrP^{Sc} following chemical treatment, samples were subjected to PMCA. As previous RT-QuIC results demonstrated anywhere from partial to complete suppression of seeding activity depending on the treatment, PMCA was used to complement these results and to assess whether any residual PrP^{Sc} remained amplifiable following exposure to selected chemicals. Western blot analysis of PMCA results may also provide insight into the mechanisms of chemical inactivation responsible for the effects seen.

Preliminary experiments were done to establish the PMCA assay. In contrast to the blots seen in Figure 12, Figure 13 shows the same 1:1000 (v/v) NaPTA-precipitated CWD PrP^{Sc} samples after undergoing three rounds of PMCA. In round 1, faint bands were observed across all 3 dilutions, indicating that PMCA resulted in sufficient amplification for detection. In round 2, the PrP^{Sc} signal became more evident, with the presence of bands around the expected ~20–30 kDa region. This is consistent with the characteristic migration profile of protease-resistant PrP^{Sc}, even though bands were not as clear as with non-PMCA samples (Figure 12). By round 3, signal intensity increased dramatically, with darker and more defined bands appearing in the examined dilutions original seed dilutions. Of note, the band appearance for round 3, dilution 1, appears unusually faint. One potential explanation for the absence of a detectable band for this sample is pipetting or loading error during Western blot preparation. Another possible reason for this could be experimental variability, such as loss of seeding activity or uneven amplification, which may have contributed to the lack of detectable PrP^{Sc} in this replicate. These results highlight the enhanced detection

limit of Western blot by PMCA, confirming its use to detect any PrP^{Sc} that remains following EALC treatment.

Interestingly, the banding profile of PMCA amplified samples differed from the typical PrP^{Sc} triplet pattern observed in non-amplified samples. Instead, PMCA samples displayed more smeared bands, and the classical three-band architecture was not distinguishable (Figure 13). Notably, an additional high molecular weight band appeared above 30 kDa in the PMCA samples, which was not observed in the corresponding non-PMCA lanes, as seen in Figure 12, despite both being PK-treated.

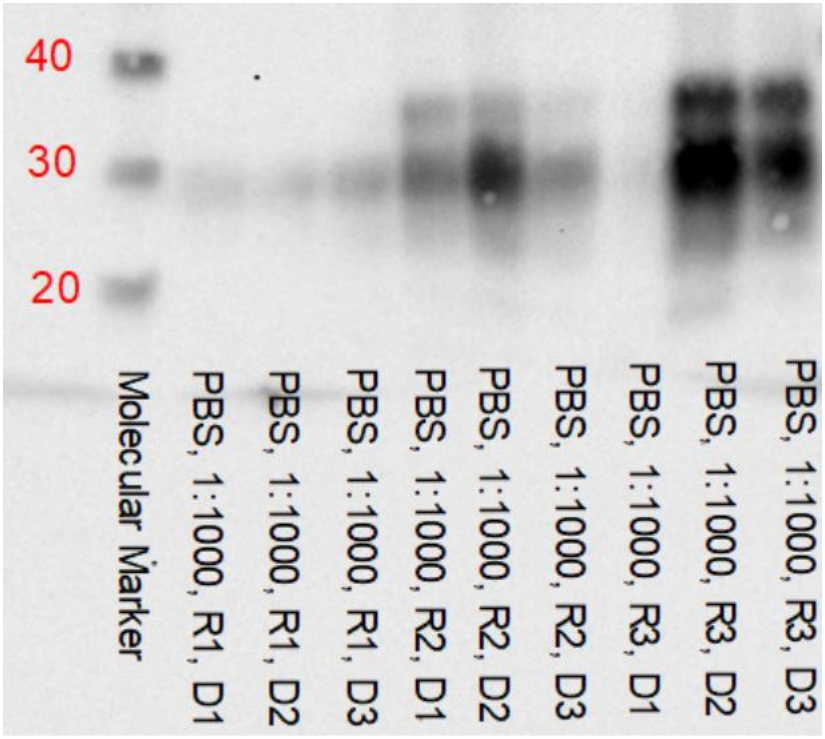

Figure 13. Western blot detection of three 10-fold serial dilutions of PBS mock-treated NaPTA precipitated PrP^{Sc} after three rounds of PMCA. Samples of CWD-positive elk brain homogenate were mock-treated with PBS at a 1:1000 (v/v) dilution for 1 hour, subjected to NaPTA precipitation, and amplified through three successive rounds of PMCA. At the end of each round (R1–R3), 10 µL of amplified material was digested with proteinase K, electrophoresed, and immunoblotted for PrP^{Sc} detection. Molecular weight markers (kDa) are indicated.

Next, PMCA was used to amplify and analyze the effects of EALCs to inactivate PrP^{Sc}. For Catholyte 4 and Anolyte 2, NaPTA-precipitated samples treated with each chemical at a 1:1000 (v/v) ratio were subjected to three rounds of PMCA and analyzed by Western blot (Figure 14). Compared to the PBS mock-treated control samples (Figure 12), which produced detectable PrP^{Sc} presence as early as round 1 and strong, visually striking bands by round 3, the chemically treated samples showed reduced amplification efficiency. In Catholyte 4-treated samples, PrP^{Sc} bands were largely absent in round 1 and only faintly visible in the second round, suggesting a substantial loss of seeding activity, particularly shortly after treatment. Anolyte 2-treated samples displayed a slightly bolder amplification profile, with stronger bands beginning to emerge by round 2 and becoming more distinct by round 3, although still less intense than PBS controls. These results indicate that both Catholyte 4 and Anolyte 2 reduced PrP^{Sc} seeding activity, with Catholyte 4 showing the most decreased seeding activity across all dilutions and PMCA rounds. This correlates with the suppression observed via RT-QuIC detection of treated samples.

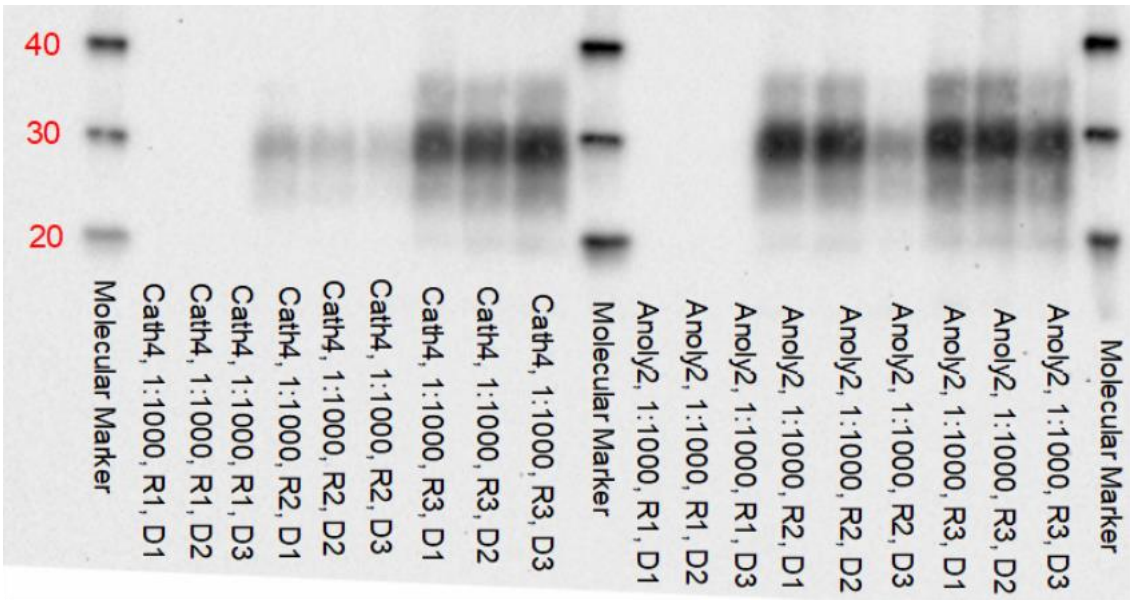

Figure 14. Western blot detection of three 1-fold serial dilutions of Catholyte 4 and Anolyte 2 treated NaPTA precipitated PrP^{Sc} after three rounds of PMCA. CWD-positive elk brain homogenate was treated for 1 hour with either Catholyte 4 or Anolyte 2 at a 1:1000 (v/v) ratio, then subjected to NaPTA precipitation and three successive rounds of PMCA. After each round (R1–R3), 10 µL of amplified product

from three serial dilutions (D1–D3) was PK-digested, run on electrophoresis, and immunoblotted to visualize residual protease-resistant PrP^{Sc}. Molecular weight markers (kDa) are shown for reference.

Comparison of CAC-717 and BrioHOCl (Figure 15) to PBS mock-treated controls (Figure 13) highlights differences in residual PrP^{Sc} seeding activity following treatment. Compared to PBS controls, CAC-717-treated samples showed reduced bands throughout all rounds and dilutions, with a very weak banding appearance by round 3. This shows not only a high level of reduction of seeding activity, but this reduction is maintained through multiple rounds of amplification. BrioHOCl-treated samples also show a reduced ability to amplify through PMCA, with bands appearing only in one dilution of round 2, but becoming distinct by the end of round 3.

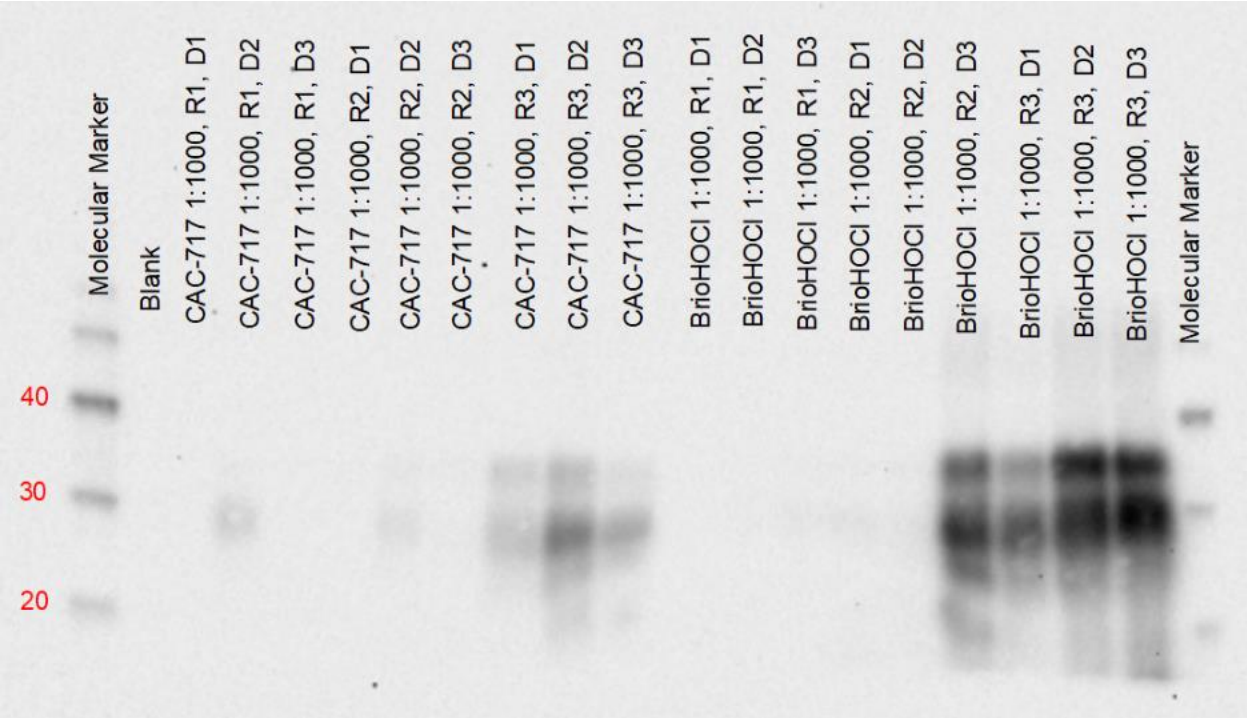

Figure 15. Western blot detection of three 10-fold serial dilutions of CAC-717 and BrioHOCl-treated NaPTA-precipitated PrP^{Sc} after three rounds of PMCA. CWD-positive elk brain homogenate was treated for 1 hour with either CAC-717 or BrioHOCl at a 1:1000 (v/v) brain homogenate: chemical ratio, followed by NaPTA precipitation and three rounds of PMCA. At the end of each round (R1–R3), 10 µL of

amplified material from three serial dilutions (D1–D3) was digested with PK and processed for analysis using Western blot. Molecular weight markers (kDa) are shown for reference.

Compared to PBS mock-treated controls (Figure 13), which displayed clear PrP^{Sc} amplification from round 1, both NaOH and bleach treatments significantly reduced seeding activity (Figure 16). NaOH-treated samples showed the most complete inactivation, with no detectable PrP^{Sc} across all samples, except round 3, dilution 3, which produced one very faint band. Bleach-treated samples demonstrated some residual activity, with faint bands appearing in round 3, though still much less prominent and consistent than PBS controls. These results support the results seen via RT-QuIC and justify the use of conventional decontaminants as strong anti-prion chemicals.

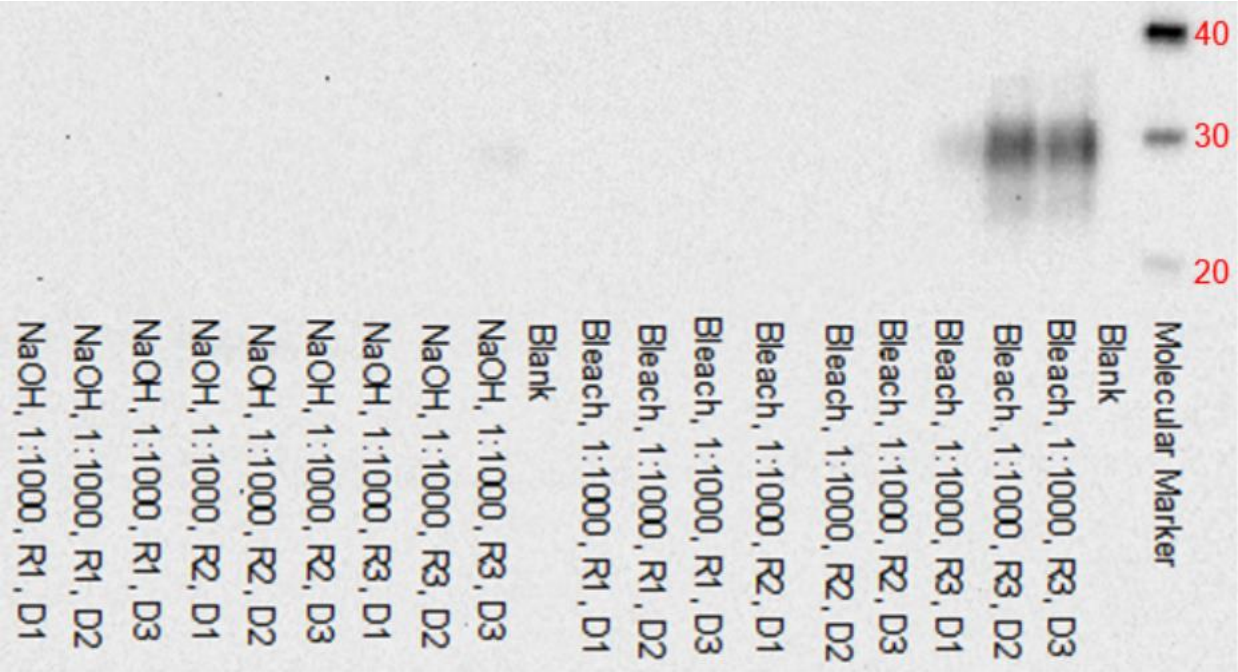

Figure 16. Western blot detection of three dilutions of 2N NaOH and 40% bleach-treated NaPTA-precipitated PrP^{Sc} after three rounds of PMCA. CWD-positive elk brain homogenate was treated for 1 hour with 2N NaOH or 40% bleach at a 1:1000 (v/v) ratio. Proteins from each sample were then selectively precipitated using NaPTA, and PMCA was run for three rounds. At the end of each PMCA round (R1–R3),

10 µL of amplified material from three serial dilutions (D1–D3) was digested with PK and analyzed using Western blot. Molecular weight markers (kDa) are shown for reference.

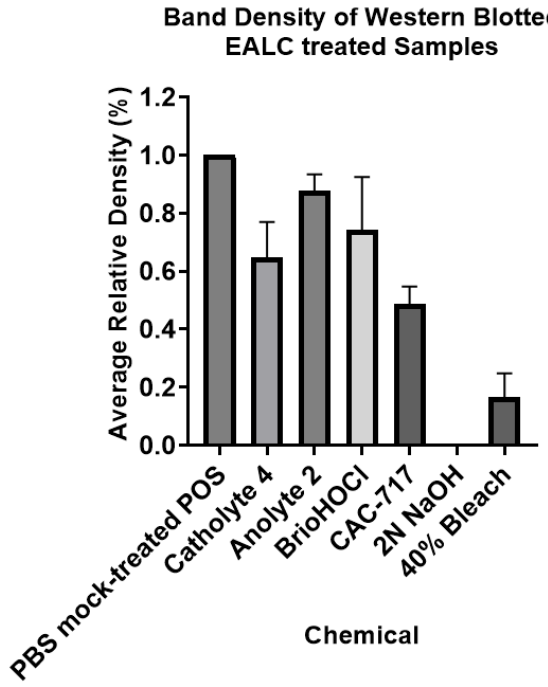

Figure 17. Densitometric bar graphs of PrP^{Sc} bands following Western blot assessment of EALC-treated samples. Western blot band intensities from CWD-positive brain homogenate treated with EALCs or conventional chemicals were quantified using densitometry and normalized to the PBS mock-treated positive control (set as 1.0). Data represents the mean and standard error obtained from the second dilution of the third PMCA round from three independent experiments. Unpaired t-tests with Welch's correction were performed to compare each treatment group to the PBS mock-treated positive control. Treatment with 2N NaOH and 40% bleach resulted in a complete and highly significant reduction compared to PBS controls ($p < 0.0001$ and $p = 0.0097$, respectively). Catholyte 4 and CAC-717 also showed significant reductions ($p = 0.044$ and $p = 0.013$, respectively), whereas Anolyte 2 and BrioHOCl did not differ significantly from PBS ($p > 0.05$).

These results show that the tested EALCs and conventional treatments varied in their ability to eliminate PrP^{Sc} seeding activity. While all chemicals showed some level of suppression compared to PBS controls,

clear differences appeared in the degree and consistency of amplification across rounds after treatment (Figure 17). Commercial, conventional decontaminants NaOH and bleach stood out as the most effective, with little to no detectable amplification, even after three rounds. In contrast, CAC-717 and BrioHOCl allowed some PrP^{Sc} to persist and seed, as shown by the faint bands that appeared in later rounds. All together, these results not only support the reliability of RT-QuIC but also demonstrate how PMCA can provide added resolution in distinguishing partial from complete prion inactivation, strengthening the case for select EALCs as promising anti-prion agents.

3.3.3. Differences in Amplification Kinetics Post-Treatment

To assess how chemical treatments impacted the rate of PrP^{Sc} seeding, Western blot results (as seen in Section 3.4.2) from three rounds of PMCA were examined at the 1:1000 (v/v) treatment ratio for each chemical of interest. Differences in the timing of PrP^{Sc} detection can provide insight into residual seeding activity and the extent of prion inactivation by each chemical.

As seen in Table 6, highlighting differences in amplification kinetics and residual seeding activity, the precise dilution and round at which amplification becomes evident as visualized through Western blot depends greatly on which EALC or commercial chemical was being used. PBS mock-treated controls displayed rapid amplification, with PrP^{Sc} detectable within the first round of PMCA, and increasing signal intensity over time. The early and consistent signal that was produced after mock treatment reflects the strong residual capability of seeding activity and serves as a benchmark for examining the effects of other EALCs and chemicals. Catholyte 4-treated samples showed a lack of bands detected in round 1, and only weak signals appeared in rounds 2, becoming more defined during round 3. This suggests partial inactivation with reduced seeding activity. Similarly to samples treated with Catholyte 4, those treated with Anolyte 2 displayed a similar but slightly stronger amplification potential, with PrP^{Sc} absent during round 1, but appearing much more defined after round 2 than PBS or Catholyte samples. By round 3, all samples showed a high concentration of PrP^{Sc} as evidenced by increased band density. These results point to a slight

reduction in seeding activity after treatment, but we can see that the chemicals are not able to fully inactivate all PrP^{Sc} seeds as amplification resumes and intensifies over rounds.

BrioHOCl-treated samples also delayed amplification, with no PrP^{Sc} signal observed in round 1. During round 2, amplification became slightly more apparent, but only dilution 3 produced a distinct signal. During round 3, signals became much more apparent, and amplification was undeniable at this point. These results point to a higher level of seeding activity than those seen with experimental EALCs, Catholyte 4 and Anolyte 2, but PrP^{Sc} seeds were not eliminated and seeding resumed at a high rate after just a few rounds of amplification. In CAC-717-treated samples, amplification was more strongly inhibited, with faint signals appearing only in one dilution for rounds 1 and 2, and present yet indistinct bands for round 3.

NaOH treatment demonstrated the most potent effects of all chemicals examined, with no detectable PrP^{Sc} in rounds 1 or 2 and only a single very faint and unclear band emerging in round 3, which may reflect a small amount of residual PrP^{Sc} that was unable to be previously amplified, or experimental variability. Bleach-treated samples also resulted in distinct inhibition of seeding activity throughout, with bands apparent only during round 3 of PMCA.

Table 6. Summary of PrP^{Sc} amplification across three PMCA rounds by chemical treatment and dilution.

	Dilution	Absence (✗) or Presence (✓) of PrP^{Sc} by Round		
Chemical		**Round 1**	**Round 2**	**Round 3**
PBS mock-treatmnent	1	✓	✓	✓
	2	✓	✓	✓
	3	✓	✓	✓
Catholyte 4	1	✗	✓	✓
	2	✗	✓	✓
	3	✗	✓	✓
Anolyte 2	1	✗	✓	✓
	2	✗	✓	✓

	3	✗	✓	✓
BrioHOCl	1	✗	✗	✓
	2	✗	✗	✓
	3	✗	✓	✓
CAC-717	1	✗	✗	✓
	2	✓	✓	✓
	3	✗	✗	✓
NaOH	1	✗	✗	✗
	2	✗	✗	✗
	3	✗	✗	✓
Bleach	1	✗	✗	✓
	2	✗	✗	✓
	3	✗	✗	✓

Western blot detection of PrP^{Sc} was assessed at three seed dilutions (D1–D3) following PMCA amplification of NaPTA-precipitated, chemically treated CWD-positive elk brain homogenate. Each sample underwent three PMCA rounds (R1–R3), and the presence (✓) or absence (✗) of PrP^{Sc} was visually determined from immunoblots. PBS mock-treated samples served as positive controls.

Overall, mock treatment using PBS showed rapid and distinct amplification, strong NaOH and bleach showed the most distinct suppression, with delayed PrP^{Sc} detection. All other chemicals (Catholyte 4, Anolyte 2, BrioHOCl, and CAC-717) demonstrated varied impacts on PrP^{Sc}.

3.4. Correlation Between RT-QuIC and PMCA Findings

To investigate the correlation between RT-QuIC and PMCA to detect PrP^{Sc} from CWD-positive samples of brain homogenate after decontamination with selected chemicals, results from both assays were directly compared. Results from RT-QuIC, as indicated by relative seeding activity measured through changes in CT values, were compared against the round number at which amplification was observed via Western blot following PMCA.

Figure 18 illustrates the relationship between RT-QuIC CT values and the round at which PMCA amplification of PrP^{Sc} was first detected for each chemical treatment tested. The PBS mock-treated brain homogenate control showed the lowest CT values, which correspond with early PMCA detection as seen in round 1. Alternatively, samples that were treated with bleach and NaOH resulted in the highest CT values and demonstrated delayed detection using PMCA, signifying significant reductions in prion seeding capability.

EALCs Catholyte 4, Anolyte 2, BrioHOCl, and CAC-717 showed variable CT values (20–40 hrs) and differing PMCA detection rounds depending on the specific chemical treatment, reflecting partial efficacy in prion inactivation, or differences in their underlying mechanisms of action and interaction with PrP^{Sc} during amplification assays. Among the chemical treatments tested, Anolyte 2 and BrioHOCl showed a notable difference between the timing of seeding activity detectable by RT-QuIC and PMCA. Both treatments resulted in relatively low RT-QuIC CT values (18.4 and 10.4 hrs, respectively), suggesting that PrP^{Sc} seeding activity was still present and detectable early during the assay. However, corresponding PMCA results indicated delayed PrP^{Sc} amplification, with detection only appearing by round 2. This difference implies that while low levels of seeding activity remain after treatment (as seen via RT-QuIC), they may be insufficient to trigger immediate amplification in PMCA.

Directly comparing CT values of RT-QuIC and round number of PMCA (Figure 18) demonstrates a pattern of correlation between increased RT-QuIC CT values and delayed PMCA detection, supporting the idea that both methods are capturing similar changes in PrP^{Sc} seeding activity and can be used together to evaluate the effectiveness of prion-inactivating treatments.

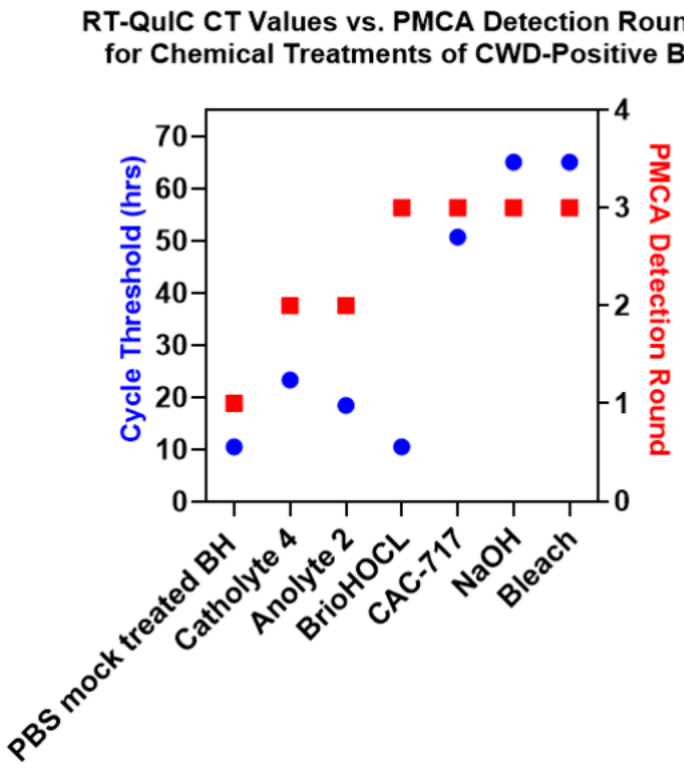

Figure 18. Correlation between RT-QuIC CT values (blue circles, left axis) and detection round number of PMCA (red squares, right axis) following treatment of CWD-positive elk brain homogenate with selected EALCs and conventional disinfectants. CWD-positive elk brain homogenate was treated for 1 hour at a 1:1000 (v/v) ratio, then assessed using RT-QuIC or PMCA. Higher CT values reflect lower prion seeding activity, and higher PMCA detection rounds indicate delayed amplification and reduced seeding efficiency. Each CT value represents the mean of 8 replicates.

4.0 Discussion

4.1. Effects of EALCs: Seeding Inhibition and Treatment Efficacy as Interpreted using RT-QuIC

The purpose of this thesis was to evaluate the potential of the selected EALCs as environmentally friendly decontaminants against infectious prions, with a particular focus on CWD-associated PrP^{Sc}. By comparing experimental catholytes and anolytes alongside commercially available EALCs and classical decontaminants, this study aimed to investigate which chemicals were most effective against CWD-infected brain homogenate and contaminated steel wires as well as the potential mechanisms of action.

4.1.1. Interpretation of Seeding Activity of EALC Treated Samples

To understand how EALCs may be helpful in field and industrial settings, in-vitro preliminary testing to evaluate the inactivation potential of these liquid chemicals against PrP^{Sc}-positive brain homogenate provided initial insight into their effects. As examined using RT-QuIC, results indicate a treatment-dependent hierarchy in PrP^{Sc} inactivation potential among chemicals. An extended lag phase, marked by elevated CT values following treatment, was interpreted as resulting from reduced PrP^{Sc} seeding activity and potential chemical efficacy (Wilham et al, 2010). Across all EALC treatments, a common trend emerged demonstrating that prion inactivation is highly variable and dependent on the chemical and concentration at which it was being used and the composition of the sample matrix. However, when comparing results across homogenate and solid surfaces (steel wire), important differences in inactivation potential and reliability emerged, highlighting the complexity of PrP^{Sc} inactivation attempts.

A serial dilution gradient of CWD-positive elk brain homogenate was used to obtain a concentration gradient to validate the sensitivity and specificity of the RT-QuIC assay before testing chemically treated samples. By correlating CT values of treated brain homogenate with those seen in this untreated dilution series, the approximate fold-reduction in prion seeding activity caused by each treatment can be inferred (Hughson et al, 2016). The data presented in Figure 6 demonstrates a strong dose-dependent relationship between PrP^{Sc} concentration and RT-QuIC amplification kinetics. CWD-positive brain homogenate

dilutions at 10^{-2} have been observed to contain sufficient inhibitors (such as lipids and proteases) to suppress detectable fluorescence via RT-QuIC (Yilmaz et al, 2024), and this is supported by the results seen in Figure 6. Typical sigmoidal kinetics include a lag phase, exponential phase, and plateau phase characteristic of RT-QuIC amyloid amplification, which were seen from the 10^{-3} to 10^{-8} dilutions, complementing the progressively increasing CT values at lower concentrations. Though the 10^{-9} dilution did not produce any CT values within the assay cutoff period, weak ThT fluorescence signals were still observed (Figure 6b), likely reflecting spontaneous aggregation of recPrP rather than PrP^{Sc} seeding, as has been previously reported under conditions of high dilution (Yilmaz et al, 2024; Hughson et al, 2016).

Confirming that the treatment ratio did not affect RT-QuIC detection or sensitivity, mock-treated PBS samples, as seen in Figure 7, show no significant impact on the CT value of differentially treated samples.

Commercial decontaminants showed greater capability to inactivate PrP^{Sc} overall than experimental EALCs. Unsurprisingly, both 2N NaOH and 40% bleach eliminated RT-QuIC detectable fluorescence at all treatment ratios, supporting their use as gold-standard decontaminants. Their efficacy likely results from aggressive denaturation and hydrolytic cleavage of PrP^{Sc} aggregates, rendering the protein non-functional as a seed (Bauman et al, 2006). BrioHOCl and CAC-717 demonstrated dose-dependent effects. BrioHOCl showed little efficacy in reducing PrP^{Sc} seeding activity, with slight CT value increases at higher treatment ratios. However, at some ratios (1:1, 1:100, 1:500 [v/v]), it was unsuccessful in delaying amplification compared to PBS controls and instead increased it. This limited effect may be due to strain-specific differences in PrP^{Sc} conformational stability, as previous work examining BrioHOCl for anti-prion activity was done using CWD from infected mule deer (Hughson et al, 2016) while this study focused on elk. However, these two species have been shown to have distinct structural differences between their C-terminals, possibly impacting the stability of the protein (Slapšak et al, 2019). CAC-717 was more effective, especially at the 1:1000 (v/v) ratio, producing one of the highest CT shifts among all chemicals tested. It successfully reduced the number of replicates classified as positive, as seen in Table 4. CAC-717 is known to generate hydroxide ions and maintain a high pH, which can disrupt proteins, but prions have shown a

particular resistance to damage from these conditions unless their core β-sheet structure is entirely disrupted (Sakudo et al, 2020). Overall, CAC-717 showed good promise in inactivating PrP^{Sc} and may pose as a suitable decontamination option for areas of low prion exposure.

When examining the effects on direct homogenates of CWD-positive elk brain, Catholyte 4 was the experimental EALC responsible for producing the most effective and consistent suppression of PrP^{Sc}, particularly at the highest treatment ratio of 1 part brain homogenate to 1000 parts chemical (v/v). Under these conditions, CT values suggest upwards of a 1000-fold reduction in seeding activity. Between EALC classes, overall anolytes were less effective than catholytes. Of anolytes, Anolyte 2 still demonstrated a statistically significant decrease in seeding activity at the highest treatment ratio, with CT values demonstrating a 100-fold reduction. These results suggest that under controlled, in-vitro conditions, some EALCs can disrupt PrP^{Sc} seeding and reduce the formation of aggregates detectable via RT-QuIC.

While Catholyte 4 and Anolyte 2 proved to be the most promising EALCs in reducing PrP^{Sc} seeding activity, the remaining catholytes and anolytes demonstrated variable and more limited efficiency. Trends seen in Table 4 suggest Catholytes 1–3 produced slight but consistent increases in CT values relative to PBS-treated controls, particularly at higher treatment ratios, indicating a concentration-dependent effect, but failing to eliminate detectable PrP^{Sc}. Among the anolytes, most (Anolytes 1, 3, 4, and 5) induced minimal changes in CT values across treatment ratios. Interestingly, some anolytes at several treatment ratios consistently appeared to accelerate aggregation, with CT values averaging lower than the PBS control, suggesting a potential increase in PrP^{Sc} seeding activity. This may be explained by the components within the anolyte EALCs that stabilize partially unfolded PrP conformers or encourage nucleation, similar to interactions seen boeckerafter exposure to cofactors such as polyanions and metallic ions (Chang et al, 2023; Polano et al, 2008). These findings highlight the importance of characterizing chemical efficacy and unintended effects due to specific EALC formulations.

To simulate real environmental contamination, examination of the EALCs was conducted using steel wire, which is a well-established model for assessing prion surface adherence and resistance to inactivation

(Simmons et al, 2024; Orrú et al, 2024; Mori et al, 2016; Zobeley et al, 1999). Before treatment, the steel wire washing protocol was validated to confirm that no detectable PrP^{Sc} was being leached into the wash solutions, ensuring that any detectable RT-QuIC signal was due to surface-bound prions or that the absence of signal was not due to the detachment of PrP^{Sc} during washes. This was followed by binding control experiments, which quantified the CT values of elk PrP^{Sc} sorbed onto stainless steel. This phenomenon has been previously documented and attributed to the protein's hydrophobic and electrostatic interactions with metal surfaces (Toni et al, 2017).

When 2N NaOH and 40% were used to treat stainless PrP^{Sc}-contaminated steel wire, there was no evidence of amplification in any replicate, as expected. Though these chemicals provide consistent decontamination, their harshness limits practical use in many field or equipment settings, as previously discussed.

When the same group of EALCs was applied to PrP^{Sc} sorbed onto steel wire, the kinetics and consistency of inactivation changed. Catholyte 4 and Anolyte 2 performed better than other EALCs, and their effects were more inactivating when used to treat steel wire than when applied directly to brain homogenate. This may be due to several factors. First, the total quantity of PrP^{Sc} present on the steel wire is lower overall than that in raw brain homogenate, reducing the burden on the chemical to achieve complete inactivation. More importantly, the adsorption between PrP^{Sc} and the steel wire may contribute to conformational or structural changes in the protein and aggregate, which has been alluded to in previous studies (Giles et al, 2017; Fichet et al, 2004). Despite their success, the persistence of some residual seeding activity even after treatment, particularly at lower dilutions, as has been previously seen in other studies attempting to decontaminate PrP^{Sc} (Orrú et al, 2024; Booth et al, 2021; Herzog et al, 2025), reinforces the need for thorough assessment of possible persistent infectivity and highlights the resilience of PrP^{Sc}.

4.1.2. Comparative Analysis and Biological Significance of Catholyte and Anolyte Effects

The differences in prion inactivation efficacy between catholytes and anolytes observed in this study demonstrate the importance of chemical class and their specific properties when determining treatment

outcomes. While both categories of experimental EALCs demonstrated some capacity to reduce PrP^{Sc} seeding activity, catholytes consistently showed more reliable and dramatic inhibitory effects compared to anolytes when assessed by RT-QuIC.

As previously discussed, the catholyte and anolyte that produced the most notable anti-PrP^{Sc} activity of all that were tested were Catholyte 4 and Anolyte 2, respectively. Though these EALCs were dominant in their decontamination potential, they could not eliminate all seeding activity, and residual PrP^{Sc} amplification was noted in both brain homogenate and steel wire samples. The contrasting performance between catholytes and anolytes suggests fundamental differences in how each class of EALC interacts with PrP^{Sc}. While both classes are produced through electrolysis, they differ in their chemical characteristics, such as pH, redox potential, and ROS content. In this study, catholytes are strongly alkaline, while anolytes are acidic and oxidative, and contain HOCl and other reactive chlorine derivatives (Guo et al, 2024; Kim et al, 2019). These differences influence PrP^{Sc}'s structural stability and aggregation state through distinct mechanisms, which will be discussed further in Section 4.2. The greater consistency observed with catholytes suggests that alkaline conditions may better promote destabilization or partial degradation of prion aggregates, particularly in brain homogenate exposure (Hirata et al, 2010). Although acidic anolytes can neutralize upon contact with biological material (Boecker et al, 2023), the initial low pH exposure may still passively promote prion amyloid fibril formation, as acidic conditions have been shown to enhance aggregation under certain circumstances (Lee & Chang, 2019; van der Kamp & Daggett, 2010; Gerber et al, 2008), potentially counteracting the intended inactivation effect.

While any prion decontamination attempt aims to inactivate PrP^{Sc} entirely, this is not always realistic due to the resistant nature of prions. Even so, chemicals that produce even partial inhibition of seeding activity may still hold important biological relevance, particularly in natural environments, such as soil, vegetation, and equipment surfaces, where the amount of PrP^{Sc} that is concentrated is likely much lower than would be possible to obtain in laboratory settings (Saunders et al, 2008). An increase in RT-QuIC CT values, as observed with treatments like Catholyte 4, Anolyte 2, or CAC-717, still reflect a meaningful reduction in

the concentration or structural integrity of PrP^{Sc} and may potentially lower the infectivity below the threshold required for horizontal transmission. As such, using moderately effective but safe and scalable decontaminants may represent a practical solution that minimizes environmental persistence and disease propagation while avoiding corrosive or toxic chemicals unsuitable for widespread field applications.

4.1.3. Concentration-Dependent Effectiveness of Commercially Available EALCs

BrioHOCl and CAC-717 showed clear chemical concentration-dependent effects on PrP^{Sc} seeding activity. While both demonstrated prion-inactivating potential, their mechanisms and effectiveness differed significantly, especially at higher treatment ratios.

BrioHOCl showed very modest and consistent minor reductions in seeding activity for some treatment ratios but also demonstrated accelerated seeding activity compared to PBS controls at other ratios. These findings are consistent with its known activity as a stabilized HOCl solution, demonstrating antimicrobial efficacy through oxidative damage to proteins, lipids, and nucleic acids (Block & Rowan, 2020). However, its oxidative potential may be limited by short-lived reactive species or neutralization by the high content of tissue in brain homogenates (Teng et al, 2018). The observed effectiveness of BrioHOCl in this study was much less promising than the results initially described by Hughson et al. (2018), which inspired the inclusion of BrioHOCl in our current investigation of EALCs. In that study, BrioHOCl effectively reduced prion seeding activity by between 10^3 and 10^6-fold from contaminated brain homogenate and eliminated infectivity from steel wire. However, the specific formula that BrioTech™ used to manufacture the BrioHOCl as described by Hughson (2018), although marked under the same trade name, was not the same that was used by the company in 2023 when the BrioHOCl used in this study was purchased. Consequently, the chemical composition and concentration of reactive HOCl or free chlorine may differ between these formulations and batches, potentially explaining the reduced efficacy observed here.

Regardless of the treatment ratio, the data obtained for BrioHOCl revealed a minimal effect on PrP^{Sc} seeding activity as indicated by relatively stable RT-QuIC CT values across the tested treatment ratios. Unlike the

distinctive concentration-dependent effects observed with other EALCs, BrioHOCl exhibited minor and statistically insignificant increases in CT values compared to PBS mock-treated controls, indicating incomplete inactivation. This suggests that the active oxidative species within this BrioHOCl formulation may rapidly decline or be neutralized in the presence of CWD-positive brain homogenate, limiting its effectiveness based on matrix interactions, regardless of treatment concentration. Additionally, the lack of concentration-dependent efficacy may reflect differences in reactive chlorine species' chemical formulation or stability compared to previously studied BrioHOCl formulations (Hughson et al., 2018).

In contrast to the relatively minor effects on seeding activity seen using commercially available BrioHOCl, CAC-717 showed a much greater ability to increase T_{stdev} and demonstrated a clear dose-dependent relationship. This relationship was observed after treatment with CAC-717, both in brain homogenate and steel wire-bound prion models, and it suggests a threshold-driven mechanism of PrP^{Sc} inactivation. This mechanism is likely reliant on the cumulative structural interactions between the chemical and PrP^{Sc}, possibly due to alkaline-induced denaturation of prion proteins or the adsorption and structural modifications by mesoscopic crystals within CAC-717 (Sakudo et al, 2025), which may explain the required minimum sufficient contact time and concentration to demonstrate clear anti-PrP^{Sc} effects. The mesoscopic structures present within CAC-717, composed of carbon and calcium, may function similarly to soil mineral particles, such as montmorillonite, which have been reported to adsorb prions and influence their structural properties and infectivity (Booth et al, 2021). These observations reinforce the need to consider the physicochemical properties of the EALC's composition and the dose at which it is applied when designing effective prion decontamination techniques.

These findings show that not all commercially available EALCs perform equally, even under identical conditions. Although BrioHOCl was originally selected based on promising results from earlier studies, the results shown here appeared to have limited impact on PrP^{Sc} seeding activity, possibly due to changes in chemical composition since the original product was evaluated. In contrast, CAC-717 demonstrated a strong dose-dependent effect.

4.1.4. Implications of Complete Seeding Inhibition by Conventional Treatments

The complete inhibition of seeding activity after treatment with concentrated NaOH and bleach supports the longstanding and well-supported regimen of these classical prion decontamination techniques. In this study, 2N NaOH and 40% bleach consistently eliminated seeding activity as measured via RT-QuIC. They were equally as effective when used against infected brain homogenates as when used against contaminated steel wire. This absence of detectable RT-QuIC signal indicates a total loss of seeding-competent PrP^{Sc}, indicating that these treatments can eliminate biologically active PrP^{Sc} under the tested conditions.

When examining RT-QuIC results, complete inhibition of amplification is highly significant, as this assay's sensitivity allows it to detect extremely low concentrations of prion seeds. Since there was a consistent lack of amplification across all replicates, it can be suggested that the treated samples likely fall below the threshold for initiating template-directed fibril formation. Given that there has been a positive correlation that has been demonstrated between RT-QuIC results and infectivity in vivo (Høy-Petersen et al, 2025; Baranová et al, 2024; Mok et al, 2021), it is fair to assume that samples treated with NaOH and bleach no longer pose a substantial infectious risk and that horizontal transmission of disease would be prevented. However, it is worth noting that while RT-QuIC provides a reliable method for quantifying seeding activity, it cannot directly measure infectivity, and in vivo bioassay confirmation would still be required.

As previously mentioned, despite their effectiveness, the practicality of using NaOH and bleach is often limited by their harsh, corrosive, and hazardous properties. These chemicals are highly damaging to many surfaces and equipment and toxic to living tissues, making them unrealistic for use in sensitive environments such as medical equipment, field tools, or porous substrates where material integrity must be preserved. If improperly handled, these chemicals' harsh pH and oxidative properties also pose risks to human and animal health and the environment.

Therefore, the results demonstrated here confirm a critical trade-off between potency and practicality. While NaOH and bleach remain good options for decontamination in high-risk or controlled settings such

as laboratory environments or decontamination of disposable materials, there remains a clear need for alternative chemicals that are effective but also more applicable to diverse environments with minimal side effects. This is the gap the experimental EALCs tested for this study aimed to fill.

4.2. Effects of EALCs: Residual PrP^{Sc} Detection as Interpreted using PMCA

4.2.1. Comparison of PrP^{Sc} Amplification Kinetics Post-Treatment

This study also conducted PMCA to support the results obtained using RT-QuIC. Following PMCA, the kinetics of PrP^{Sc} amplification revealed differences in residual seeding activity after treatment from the selected EALCs, providing important validation and further insight into each chemical's efficacy.

According to previous studies, RT-QuIC and PMCA results are generally agreeable in terms of specificity and detection of prion seeding activity, but they differ in sensitivity, strain compatibility, and practical application, meaning a perfect comparison between the assays is not always possible. Despite this, there is generally a positive correlation between the two assays. (Thomas et al, 2024; McNulty et al, 2019; Haley et al, 2017).

When samples were mock-treated with PBS, PrP^{Sc} was apparent after the first round of PMCA, indicating that amplification was not disrupted, and took place rather rapidly. This steady signal appearance is consistent with prior studies showing that even small quantities of PrP^{Sc} can reliably seed further misfolding during PMCA under optimized conditions (Eraña et al., 2020). Understanding how brain homogenate is treated at a ratio of 1:1000 (v/v) serves as a benchmark for assessing the extent to which various EALC treatments under the same conditions delayed or suppressed amplification.

As expected, treatment with conventional decontamination, 2N NaOH and 40% bleach resulted in the strongest prion inhibiting effects of all examined chemicals. No bands were detected in rounds 1 or 2 for either treatment, while a very faint signal appeared in round 3, dilution 3, for NaOH-treated samples, and weak amplification was observed in bleach-treated samples also during round 3. These signals were significantly delayed and diminished relative to PBS controls. While no amplification was observed via

RT-QuIC in samples treated with NaOH and bleach, the variation likely reflects the difference in amplification mechanisms and sensitivity between the two assays. RT-QuIC relies on recombinant PrP and is optimized for rapid detection of seeding-competent aggregates (Orrú et al, 2015), whereas PMCA uses brain-derived PrP^{C} and includes mechanical disruption that may facilitate detection of low-abundance or structurally altered PrP^{Sc} species (Eraña et al, 2020).

CAC-717-treated samples exhibited a more distinct suppression of amplification, with faint bands detected by the third round of PMCA, and a complete absence of signal across most dilutions. This delayed and inconsistent amplification supports the previous suggestion that CAC-717 may interfere with PrP^{Sc} on a structural level, limiting the availability or effectiveness of remaining seeds. The disruption in seeding activity after treatment supports this model and suggests that, under optimized conditions, CAC-717 may offer more consistent reduction in prion activity than other EALCs tested. These results are further supported by the previously discussed RT-QuIC results, which revealed significantly delayed CT values following CAC-717 treatment and a notable decrease in positive wells at the 1:1000 (v/v) dilution. RT-QuIC detected residual seeding activity in only 2 out of 8 replicates at this ratio, like the low and inconsistent band intensity in PMCA. The consensus between assays for CAC-717-treated samples strengthens the conclusion that it may be more effective than other EALCs in reducing PrP^{Sc} seeding activity by delaying amplification onset and reducing the overall quantity or structural integrity of active seeds.

After treatment with BrioHOCl, results amplified through PMCA display a different kinetic profile. While amplification was impacted as seeding activity was absent in round 1 and essentially undetectable in round 2, it became consistent and much more intense in round 3, suggesting that residual PrP^{Sc} required multiple amplification cycles to seed enough for detection. This implies that BrioHOCl-treated samples retain more intact seeds than those treated with CAC-717, though still suppressed after the initial treatment. From a kinetic standpoint, BrioHOCl appears to impair PrP^{Sc}'s ability to convert substrate temporarily. However, this can be overcome with repeated rounds of sonication during PMCA, suggesting partial rather than permanent protein disruption. This is consistent with RT-QuIC results, where BrioHOCl-treated samples

displayed relatively low CT values (comparable to or even lower than PBS controls at specific ratios), indicating that while seeding activity was initially present, the chemical may have affected the efficiency or accessibility of seeds rather than inactivating them entirely.

While Catholyte 4 and Anolyte 2 treatments were not successful in inhibiting amplification entirely, they were successful in delaying the round at which amplification began, suggesting that while some PrP^{Sc} survived treatment, aggregation required more time and the introduction of additional CWD TgElk substrate to amplify to detectable levels. In Catholyte 4-treated samples, bands were undetectable or weak in rounds 1 and 2, respectively, but appeared distinctly by round 3. Anolyte 2 treatment resulted in similar results, in which bands were undetectable during the first round of PMCA but became much denser and more distinctive during the second round compared to Catholyte 4 treatment. These results suggest partial inactivation of PrP^{Sc} likely by the disruption of its templating efficiency, consistent with previous studies showing that chemical stressors can impair the conformation and accessibility of prion seeds, consequently slowing their ability to induce conversion (Shim et al, 2022; Heinzer et al, 2024). This is also consistent with the results reported in Section 4.2, where, when assessed through RT-QuIC kinetics, experimental EALC-treated samples demonstrated delayed CT values. Still, these delays were insufficient to classify the sample as negative. This observation is also supported by the results seen post-PMCA amplification, where lower RT-QuIC CT values correspond to stronger band intensity and earlier detection in PMCA, which reinforces the ability of Anolyte 2, which, while partially inhibitory, leaves behind more amplifiable PrP^{Sc} than Catholyte 4.

This similarity between kinetic delay seen using RT-QuIC and the reduced biochemical amplification using PMCA highlights the benefits of combining both assays to assess the presence of residual PrP^{Sc} and their relative seeding efficiency. In this study, Catholyte 4 appears more effective than Anolyte 2 at suppressing PrP^{Sc} seeding activity, not solely because of a longer lag before detection, but due to the lower quantity or quality of seeding-competent aggregates that survive treatment.

Differences in the findings between RT-QuIC and PMCA can be attributed to their different biochemical environments and substrate compositions. RT-QuIC uses a truncated recombinant prion protein (recPrP) from Syrian Hamster (residues 90–231), which is highly purified and lacks native post-translational modifications. When used in RT-QuIC substrate, recPrP favours the formation of amyloid fibrils and enables real-time detection via ThT fluorescence, offering high specificity but potentially limited sensitivity to certain prion strains (Bistaffa et al, 2019). PMCA uses brain homogenate from transgenic mice expressing elk PrP, providing a full-length, post-translationally modified substrate that more closely mimics the naturally found environment. This allows PMCA to amplify native-like PrP^{Sc} conformers with greater strain specificity and sensitivity but introduces a greater likelihood of variability and background noise (Eraña et al, 2020; Brandel et al, 2019). Similar findings have been reported in previous studies, where PMCA detected residual prion seeding activity in samples deemed negative by RT-QuIC or infectivity bioassays (Thomas et al, 2024; Davenport et al, 2018). These results do not necessarily imply the persistence of infectious prions but rather demonstrate the increased sensitivity of PMCA for some sample types and its practicality in identifying trace quantities of partially inactivated or misfolded PrP aggregates. Therefore, the same sample may exhibit slightly different result kinetics between these assays, as was seen during this study.

4.2.2. Insights into Altered PrP^{Sc} Molecular Profiles after PMCA Amplification

Western blot analysis of NaPTA-precipitated PrP^{Sc} following PMCA revealed differences in the banding profiles of EALC-treated samples compared to mock-treated controls. In untreated or PBS-treated controls, PrP^{Sc} was observed between 19 and 30 kDa and its appearance was constant, consistent with protease-resistant core fragments. In treated samples, however, this banding profile was disrupted. Many exhibited smeared, diffuse, and higher molecular weight bands, suggesting structural changes to PrP^{Sc} aggregates or demonstrating the existence of intermediate conformers during amplification. These changes indicate that chemical treatment may influence PrP^{Sc}'s state of aggregation, potentially explaining the change in biochemical properties and seeding behaviour.

One of the most prominent results was the appearance of high molecular weight bands (>30 kDa) in PMCA-amplified samples, apparent in almost all treated samples by the third round. These bands were absent in non-PMCA, PBS-treated controls despite being PK-treated, indicating that the changes were a product of PMCA-induced aggregation rather than simple incomplete digestion. This suggests that treatment may lead to the formation of PrP^{Sc} that retains seeding activity but differs in size, structure, and protease accessibility from untreated PrP^{Sc}. Similar situations have been observed previously using immunoblotting techniques, where certain prion strains exhibit distinct biochemical profiles, including accumulating higher molecular weight protease-resistant PrP^{Sc}. For example, Klingeborn et al. (2006) demonstrated that different mouse-adapted scrapie strains produced strain-specific PrP^{Sc} banding patterns due to their altered sensitivity to PK, with some strains showing additional higher molecular weight bands, likely reflecting conformational or aggregation state differences. The loss of the classical triplet banding pattern and the appearance of smeared bands may also indicate heterogeneous PrP^{Sc} populations, possibly reflecting differing chemical cleavage sites due to conformational changes, or changes in the accessibility of PK-sensitive regions after treatment. This could happen if chemical treatment introduces partial unfolding, oxidation, or aggregation states that either mask necessary epitopes or produce misfolded intermediates distinct from native PrP^{Sc}. These changes were distinctly more apparent after PMCA, suggesting that repeated amplification cycles may favour the propagation of altered prion conformers, a phenomenon described in previous strain adaptation studies (Kim et al, 2010; Deleault et al, 2012).

As mentioned, on a Western blot, PK-treated PrP^{Sc} typically appears as a triplet of bands between ~19 and 30 kDa, representing the different glycoforms of the protease-resistant core of the protein. The uppermost band, around ~27 and 30 kDa, corresponds to diglycosylated PrP^{Sc} with two N-linked glycans attached, one at each glycosylation site. The middle band between ~23 and 25 kDa represents monoglycosylated PrP^{Sc}, which contains only a single glycan at either site. The lowest band falls between ~19 and 21 kDa and is what remains of any unglycosylated PrP^{Sc} and represents the core fragment of the protein resistant to PK digestion (Huang et al, 2006). Alterations to this typical triplet banding pattern following chemical

treatment and PMCA amplification can provide valuable insight into the mechanisms of PrP^{Sc} inactivation or modification.

In this study, the diglycosylated band was consistently the most prominent across all samples, including untreated and chemically treated conditions. This is consistent with what is typically observed in CWD and many other prion diseases, where the diglycosylated isoform tends to dominate the glycoform ratio (Heisey et al, 2009). The persistence and intensity of this upper band across treated samples suggests that diglycosylated PrP^{Sc} may be the most stable and protease-resistant of the glycoforms, possibly due to steric protection offered by its dual glycans (Schilling et al, 2023). Notably, the dominance of this band even after treatment implies that residual seeding activity is primarily associated with the diglycosylated isoform, which may be more resilient to chemical inactivation. This could help explain why certain treatments, while reducing overall signal intensity, still allow amplification to resume over time.

Interestingly, while all samples were subjected to identical PK digestion and amplification conditions, the uppermost PrP^{C} band (~33 to 35 kDa) remained detectable in all experimental and commercial EALC-treated samples but was absent in bleach-treated samples. The persistence of this upper band implies that EALCs and commercial chemicals (e.g., BrioHOCl, CAC-717) can partially disrupt the protein's sensitivity to PK digestion. Mechanistically, several things may be happening, including oxidation of amino acid side chains or modification of glycan linkages, ultimately leading to destabilization of the protein's overall structure, resulting in heterogeneous PrP^{Sc} aggregates that interact differently during PMCA and electrophoresis. The smearing or broadening of the band may also indicate aggregation of chemically altered PrP^{Sc} species or the propagation of non-native conformers during amplification (Eraña et al, 2024). It is also possible that the epitope recognized by the P4 antibody becomes disrupted, leading to this appearance. Further investigation is needed to determine the specific mechanism of action responsible for the effects seen from each EALC. In contrast to the results seen with other treatments, bleach-treated samples were unique in showing a complete absence of the upper band across all dilutions and PMCA

rounds. This suggests that bleach not only disrupts PrP^{Sc} structure but can also degrade some of the most PK-resistant and structurally sturdy glycoforms.

In summary, the molecular profiles of PrP^{Sc} observed after EALC treatment and PMCA amplification reveal that chemical treatment does more than simply suppress amplification kinetics, but it can induce structural changes that alter protease resistance, glycoform state, and molecular weight. The only treatment that resulted in complete loss of all detectable PrP^{Sc} bands was 2N NaOH, followed in order of effectiveness by 40% Bleach, CAC-717, BrioHOCl, Catholyte 4, and Anolyte 2. While PrP^{Sc} remained detectable after EALC and commercial treatments, its altered band appearance and the persistence of high molecular weight bands suggest, at a minimum, that some partial disruption of the protein's structure is taking place, and the potential formation of non-native conformers is possible. PMCA consistently amplified these changes. This highlights the need for further studies into the precise mechanisms of EALCS, possibly through tools such as mass spectrometry for examining protein structure.

4.3. Proposed Mechanisms of Action for Prion Inactivation by EALCs

4.3.1. Differences in EALC Classes (Catholytes vs. Anolytes vs. Commercial Agents)

The fluctuating performance of the different EALCs observed in this study can potentially be explained, in part, by differences in chemical class composition. While all EALCs are generated through electrolysis of mineral-enriched water, the resulting catholyte and anolyte fractions differ substantially in pH, oxidation-reduction potential, and ionic content. These characteristics are likely responsible for differences in PrP^{Sc} inactivation efficiency.

The complete inactivation of PrP^{Sc} observed following bleach treatment in this study is consistent with its well-documented oxidative mechanism of action. In aqueous solution, the active ingredient in bleach, sodium hypochlorite, exists in equilibrium between OCl^- and HOCl, with HOCl being the more reactive species. HOCl targets susceptible amino acid side chains within PrP^{Sc}, leading to oxidation, chlorination, and disruption of critical hydrogen bonding and hydrophobic interactions that stabilize the protein's β-

sheet–rich conformation (Hawkins et al, 2003), therefore preventing the protein from seeding further amyloid formation. Similar inactivation was seen after treatment with 2N NaOH. At high molarity, NaOH creates a strongly alkaline environment capable of disrupting the hydrogen bonding and hydrophobic interactions that stabilize PrP^{Sc}'s β-sheet-rich structure (Bauman et al, 2006).

Catholytes are typically alkaline electro-activated solutions and can influence prion stability due to their high pH, which promotes protein destabilization through denaturation and base-induced hydrolysis (Aider, 2023). In this study, Catholyte 4, derived from a KCl solution, consistently produced the most significant delay in PrP^{Sc} amplification across RT-QuIC and PMCA. In contrast, Catholyte 1, generated from water and Na^+ ions, and Catholyte 3, containing NaCl and Na^+ ions, showed less consistent effects, indicating that sodium-based catholytes may be less potent than potassium-based catholytes in destabilizing PrP^{Sc}. Catholyte 2, containing $CaCl_2$ and Ca^{2+} ions, also demonstrated limited efficacy.

Unlike catholytes, anolytes are acidic and often contain oxidative species such as Cl^- ions, HOCl, or free chlorine (Aider, 2023). While anolytes were less effective overall, Anolyte 2, composed of NaCl and Cl^- ions, could be recognized for its ability to delay amplification to a higher degree than other experimental anolytes. This suggests that some anolytes derived from sodium can exert sufficient oxidative stress or conformational pressure on PrP^{Sc} to alter its seeding potential, even under low pH conditions. Other anolytes, such as Anolyte 1 (composed of water with Cl^- ions), Anolyte 3 (derived from $CaCl_2$ and Cl^- ions), Anolyte 4 (sodium acetate based), and Anolyte 5 (KCl-based), showed variable effects with no chemical demonstrating clear superiority, highlighting the impact of ionic composition and oxidative potential in prion inactivation. It has previously been shown that in vivo, acidic environments, like endosomes or lysosomes, promote PrP^C to PrP^{Sc} conversion (Majumder & Chakrabarti, 2017). This is partly because low pH can destabilize the native α-helical structure of PrP^C, making it more prone to misfolding into β-sheet-rich oligomers (Tian & Viles, 2022). In vitro, however, the situation is more complex. While low pH can also destabilize proteins, PrP^{Sc} is already highly stable, especially in its aggregated form. So, simply treating PrP^{Sc} with a low pH does not guarantee degradation or inactivation.

Among the commercially available chemical agents tested, BrioHOCl and CAC-717 demonstrated partial prion inactivation under some conditions, but likely through distinct mechanisms reflecting their chemical composition and pH profiles.

BrioHOCl is a stabilized solution of HOCl, a reactive chlorine species generated through electrolysis. HOCl has long been known to be a potent oxidizing agent known to disrupt microbial membranes and denature proteins by targeting nucleophilic amino acid side chains such as methionine, cysteine, and tryptophan (Hawkins et al, 2003). While widely effective against a broad range of bacteria, viruses, and fungi, prions are considerably more resistant to oxidative stress, and there is currently no direct evidence that HOCl alone can fully inactivate PrP^{Sc} (Boecker et al, 2023). In this study, BrioHOCl treatment successfully produced delayed amplification kinetics in RT-QuIC and altered Western blot banding profiles after PMCA. These effects suggest that HOCl may partially denature or alter the structure of the protein. This is enough to impair, but not eliminate, seeding activity. Mechanistically, BrioHOCl likely destabilizes PrP^{Sc} aggregates, reducing templating efficiency during early amplification cycles. This is supported by the delayed appearance of PrP^{Sc} bands in PMCA rounds 2 and 3, and by what has previously been established in literature (Hughson et al, 2016). In practice, HOCl may be helpful in other prion-inactivating approaches, especially when combined with other decontamination methods such as heat or autoclaving, which could enhance its overall impact.

CAC-717 is a calcium bicarbonate-based electro-activated solution with a high pH (~12.3) and strong redox potential. Its effects are believed to be due to alkaline hydrolysis and oxidative stress, a dual mechanism that can compromise protein stability more effectively than through oxidation alone. The high alkalinity of CAC-717 promotes cleavage of peptide bonds and may interfere with hydrogen bonding and β-sheet formation that are critical for PrP^{Sc} structural integrity and seeding activity (Sakudo et al, 2020, 2025; Kirisawa et al, 2022; Onodera et al, 2022).

These findings highlight that prion inactivation may be affected by the characteristics of the class of chemicals used for PrP^{Sc} inactivation. The differences in performance among catholytes, anolytes, and

commercial chemicals reveal the complexity of destabilizing PrP^{Sc}. It suggests that complete inactivation may require specific chemical formulas or multiple treatments. Recognizing these differences may help create EALCs that exploit specific chemical traits for their PrP^{Sc} inactivating properties as effectively as traditional decontaminants like NaOH or bleach.

4.3.2. Chemical Composition and pH Effects on PrP^{Sc} Aggregates

The susceptibility of PrP^{Sc} aggregates to chemical inactivation depends largely on environmental pH and the ionic makeup of treatment chemicals. These factors can change the structural integrity of prion aggregation by impacting hydrogen bonding, electrostatic interactions, and backbone stability. (Hosszu et al, 2020; Lee & Chang, 2019; van der Kamp & Daggett, 2010). In general, extreme pH conditions can induce conformational changes by disrupting the forces that stabilize β-sheet structures within PrP^{Sc}, as mentioned, but the effectiveness of these changes depends on whether the treatment conditions enable irreversible structural damage.

Under basic conditions, such as those created by catholyte solutions or NaOH, an increased hydroxide ion concentration has been shown to promote hydrolysis of peptide bonds and alter the ionization states of amino acid side chains (Whitaker & Feeney, 1983). This can weaken the hydrogen bonding networks that maintain the β-sheet-rich structure characteristic of PrP^{Sc}. Additionally, deprotonation of polar residues under high pH can increase electrostatic repulsion between domains of the fibrils (Zhou & Pang, 2019), under which the same mechanisms can be thought to destabilize aggregates. These combined effects likely explain why strongly alkaline treatments produced the most remarkable delays in amplification in this study, as PrP^{Sc} aggregation under these conditions would exhibit reduced and delayed seeding efficiency.

Acidic conditions, such as those created by anolyte EALCs, can disrupt PrP^{Sc} seeding through protein denaturation, which can partially unfold protein domains or alter aggregate arrangements (Peretz et al, 2006). However, for existing PrP^{Sc} fibrils, low pH alone is not sufficient for complete denaturation because these aggregates are held together by strong hydrophobic bonds and β-sheets that remain stable (Appel et

al, 2006). This may explain why anolytes, despite containing oxidative properties, demonstrated a more limited effect than catholytes. The ability of certain anolytes, such as Anolyte 2, to suppress seeding activity suggests that pH-driven destabilization should be used in tandem with other methods for prion decontamination instead of relying on its abilities.

The chemical composition of EALCs also determines their buffering capacity and the nature of their ROS, which can affect interactions between PrP^{Sc} molecules. For example, the presence of potassium or calcium ions can alter aggregation dynamics by influencing charge shielding, while chloride-based EALCs may trigger oxidative reactions that complement pH effects to destabilize the protein (Toni et al, 2017; Concha-Marambio et al, 2014). The differences in PrP^{Sc} inactivation seen between EALC chemistries likely reflect a combination of these properties rather than pH alone, highlighting the complexity of treating highly resistant prion proteins.

Together, this supports the idea that pH acts as a primary factor of conformational stress and variability of PrP^{Sc} after treatment, but complete inactivation is likely to generally require additional mechanisms or inactivation steps.

4.3.3. Role of Surface Chemistry and Matrix Interactions

Prion inactivation efficacy is highly influenced by the physical and chemical environment in which PrP^{Sc} is targeted. Interaction with surfaces and surrounding matrices can affect prion stability, accessibility to treatments, and overall resistance of PrP^{Sc} to degradation. These factors are relevant when comparing contaminated solid surfaces like stainless steel with biological material like brain homogenate. PrP^{Sc} exhibits strong affinity for solid surfaces, particularly metals, through hydrophobic and electrostatic interactions that drive adsorption (Konold et al, 2015). Once bound to metal, it has been shown that aggregates can adopt a flattened or partially unfolded conformation, different from their structure in tissues, and potentially exposing otherwise hidden regions to inactivation attempts (Migliorini et al, 2018). This structural rearrangement, combined with the reduction in competing organic molecules, likely explains why

EALCs demonstrated greater suppression of amplification on steel wire compared to brain homogenate in this study. When prions are surface-bound, treatment agents can interact more directly with exposed protein domains, and localized microenvironments at the steel interface may promote chemical accessibility.

In brain homogenate, a complex organic matrix mix poses challenges when attempting chemical inactivation. Proteins, lipids, DNA and RNA, and other biomolecules have been thought to be responsible for increasing the difficulty of the chemical in penetrating tissues, reducing the effective concentration available for prion modification. This effect has been previously seen in inactivation attempts (Williams et al, 2019; Baune et al, 2023; Yilmaz et al, 2024) and is reflected in this study by the inhibitory effects observed in RT-QuIC at lower dilutions of brain homogenate, such as 10^{-2}, where excessive matrix complexity likely interfered with assay kinetics and chemical accessibility. In experimental settings such as those tested for this study, this inhibitory effect is not hard to overcome, and dilution of the original sample is typically successful in eliminating inhibitory effects as measured through traditional prion assays. In environmental contexts, such as those the experimental EALCs in this study aim to target, large, tissue-dense hotspots of infection are unlikely to be as concentrated with PrP^{Sc} as what is reported in laboratory environments. In nature, the concentration of PrP^{Sc} is likely more similar to the conditions modelled in our steel wire experiments, making these results a more practical reflection of real-world decontamination potential.

These findings highlight how strongly the surrounding environment influences prion inactivation. Whether sourced from a biomolecule-rich matrix like brain homogenate or attached to surfaces like soil or steel, PrP^{Sc} does not exist independently, and its surroundings can influence its structure, accessibility, and chemical treatment. The results from this study suggest that surface-bound prions, particularly on stainless steel, are more susceptible to EALC inactivation than those within tissue homogenates. While certain EALCs under laboratory conditions show promise, ensuring effective environmental decontamination will require strategies that account for these interactions in real-world settings.

4.4. Environmental and Practical Considerations

4.4.1. Suitability of EALCs for Environmental Decontamination Applications

EALCs were developed as safer, more environmentally friendly alternatives to conventional prion decontaminants such as NaOH and bleach. Their non-toxic by-products, which are composed primarily of water and salts, and their reduced corrosivity, make them good candidates for prion decontamination in wildlife habitats and sensitive environments. The results of this study support their use for these purposes. Specifically, Catholyte 4 and Anolyte 2 demonstrated measurable reductions in PrP^{Sc} seeding activity in brain homogenate and stainless-steel surfaces, with inhibitory effects reaching up to 1000-fold decreases in amplification kinetics under certain conditions.

In addition to their environmental applications, EALCs, especially HOCl-based formulations, are considered safe for use on human skin. These solutions usually have a neutral pH or are slightly acidic and mimic the natural antimicrobial agents made by the human immune system. Due to this, they are non-toxic, non-irritating, and safe for repeated use, even on sensitive skin or open wounds. HOCl has been previously used in wound care, hand sanitizers, and skin disinfectants, and is formulated to avoid oxidative damage and ensure it is safe for use on skin (Boecker et al, 2023). When manufactured and applied correctly, EALCs offer a safe option for environmental decontamination.

In addition to their promising properties, EALCs are relatively inexpensive to produce. They are typically generated by passing a dilute salt solution through an electrolysis cell, which is a process that can be scaled from small portable units to large industrial systems. Unlike NaOH or bleach, which require careful transport and handling due to their hazardous nature, EALCs can be made on-site using readily available materials, reducing logistical and regulatory risks (Aider et al, 2012). In a relatively simple process, combined with the low cost of raw materials and minimal energy requirements, EALCs offer a cost-effective alternative to traditional chemical disinfectants. These advantages, combined with their safety,

efficacy, and environmental compatibility, further enforce the strong potential of EALCs as practical and sustainable decontaminants for widespread environmental use.

4.4.2. Considerations for Use on Surfaces, Equipment, and Soils

The practical use of EALCs for PrP^{Sc} decontamination requires consideration of substrate type, environmental conditions, and operational constraints. The properties of the contaminated surface, such as whether it is non-porous equipment, porous organic materials, or soil, strongly influence the impact of chemical inactivation of PrP^{Sc}.

One of the most promising areas of use for EALCs is the decontamination of surfaces such as stainless steel, concrete, and plastic, as well as equipment commonly used in cervid management. In this study, EALCs demonstrated greater inhibition of PrP^{Sc} seeding on stainless steel than brain homogenate, as discussed in Section 4.3.3. Unlike conventional agents such as NaOH and bleach, EALCs are considerably less corrosive, which minimizes the risk of structural damage during repeated cleaning cycles, and this factor is quite important for industry professionals concerned about preserving expensive infrastructure and tools. Despite this, limitations remain for applications to porous or irregular surfaces like soil, wood, or certain rock types. These surfaces may restrict penetration of the chemicals or create environments that protect prions from direct contact (Pritzkow et al, 2018). Further investigation into the effects of EALCs on these materials when contaminated is necessary to understand their potential applications.

In the natural environment, soil is one of the most likely sites for contamination. Extensive evidence shows that soil components, particularly clay minerals like montmorillonite, can adsorb prions with high affinity, induce conformational stabilization, and significantly hinder chemical degradation (Johnson et al., 2006; Cooke et al., 2006; Booth et al., 2021). Humic substances in soil have also been found to interfere with detection and may provide additional protection against inactivation (Smith et al., 2014). These findings are similar to the matrix effect observed with brain homogenate in this work, reinforcing that both the source material of PrP^{Sc} and surface adsorption can shield the protein from chemical effects. While EALCs

such as Catholyte 4 and Anolyte 2 demonstrated promising results under laboratory conditions, it is reasonable to anticipate more challenges when treating soil-bound prions. Effective soil decontamination may require higher chemical volumes, longer contact times, or repeated applications, which introduce potential logistical and ecological considerations.

Though EALCs show promise in controlled in-vitro studies, verification of successful decontamination of complex environmental materials remains difficult, and each of these materials presents a specific set of challenges when adapting conventional prion detecting assays. Soils, for example, present challenges as they maintain a reducing extraction efficiency and can physically shield aggregates from exposure, while simultaneously containing inhibitory compounds that interfere with assay performance (Smith et al, 2011). In this study, RT-QuIC and PMCA addressed these limitations on a small scale by promoting highly sensitive detection of residual seeding activity after treatment. However, applying these detection and decontamination techniques to large-scale environmental surveillance remains impractical, highlighting the critical need to improve effective inactivation methods and reliable field assays.

4.4.3. Comparison to Conventional Decontaminants (e.g., NaOH, Bleach)

While the primary objective of this study was to investigate the potential of EALCs as alternatives to conventional decontaminants, it is important to recognize that concentrated NaOH and bleach have a much stronger ability to inactivate prions when used in controlled conditions. Both chemicals have successfully eliminated PrP^{Sc} infectivity when applied at high concentrations and prolonged contact times (Williams et al, 2019; Giles et al., 2008). In this study, NaOH and bleach-treated samples showed minimal residual amplification during PMCA and no detectable seeding activity in RT-QuIC.

While EALCs such as Catholyte 4 and Anolyte 2 effectively reduced seeding activity by several log-fold under certain conditions, they did not achieve the same degree of inactivation as NaOH and bleach. Even after treatment, residual PrP^{Sc} was still detectable in PMCA after multiple amplification rounds. This aligns

with previous literature, which emphasizes that prion inactivation often requires highly aggressive and harsh treatments due to the unique structural stability of PrP^{Sc} (Concha-Marambio et al, 2014).

Despite these differences, EALCs remain attractive for field use where traditional chemicals may be impractical or dangerous. Rather than serving as a replacement for NaOH or bleach, EALCs may offer a complementary method for decontamination, suitable for mitigating environmental contamination or for use in wildlife management practices, provided that their efficacy is optimized for use.

4.5. Study Limitations of Using RT-QuIC and PMCA Assays

This study used two in vitro amplification techniques, RT-QuIC and PMCA, to detect and evaluate residual prion seeding activity following chemical treatment. Though both assays offer advantages over conventional detection methods, they also present limitations that must be considered.

One of the primary concerns regarding RT-QuIC is its strain-dependent sensitivity, as it has been shown that certain prion strains may not seed efficiently under standard assay conditions, leading to false negatives. This is partly due to the use of recombinant PrP^{C} as a substrate, which lacks native post-translational modifications such as glycosylation and GPI anchoring, which may affect its ability to interact with some PrP^{Sc} conformers (Atarashi, 2023; Vascellari et al, 2012). Additionally, RT-QuIC detects the ability of prions to seed amyloid formation, which has been shown to correlate with infectivity, but amyloid formation is not a direct indicator of disease per se. Therefore, a positive RT-QuIC result cannot be used to guarantee infection, and similarly, a negative result does not rule out the presence of infectious prions (Caughey et al, 2017). RT-QuIC is also sensitive to assay environmental conditions and changes in pH, salt concentration, and shaking parameters, which can significantly influence the kinetics and efficiency of amplification (Atarashi et al, 2011). Collectively, these factors limit the RT-QuIC's ability to serve as a standalone validation tool for all prion inactivation studies.

For this project, some preliminary work was done using soil as an environmental matrix. However, it quickly became evident how challenging it can be to optimize environmental samples for RT-QuIC analysis.

While RT-QuIC is highly effective for sample types like brain tissues or cerebral spinal fluid (Moško et al, 2021), applying it to assess complex substrates such as soil is far less straightforward. Other studies have demonstrated that detecting soil-bound prions is possible but often requires extensive optimization and specialized protocols to remove assay inhibitors (Grunklee et al, 2025; Genovesi et al, 2007). Achieving that level of optimization was beyond this project's practical scope, reflecting an important limitation of RT-QuIC. Despite its sensitivity, not all sample types can be readily assessed without significant modifications to the assay.

PMCA complements RT-QuIC by amplifying residual PrP^{Sc} over multiple rounds, simulating the natural conversion processes in-vitro. Despite this, PMCA shares similar limitations of RT-QuIC. PMCA is also subject to strain-dependent sensitivity, as it may preferentially propagate certain prion strains over others, which could result in incomplete detection profiles after treatment (Castilla et al, 2008). Though unlike RT-QuIC, the products of PMCA are widely recognized to be infectious and have been shown to transmit disease with a sensitivity comparable to those of animal bioassays (Wang et al, 2021). However, repeated sonication cycles during PMCA introduce a risk of spontaneous aggregation of the substrate in the absence of seeds, which can lead to false positives (Makarava et al, 2020); hence, only the first three PMCA rounds for this study are used. Due to its high sensitivity, PMCA is also highly susceptible to cross-contamination, which can compromise assay reliability if sufficient controls are not in place (Cosseddu et al, 2011). On a technical level, PMCA is also considerably more complex and time-consuming, requiring specialized equipment and more hands-on labour, making it less practical for routine diagnostics compared to RT-QuIC, though it does remain ideal for investigations into infectivity, preserving prion strain characteristics, amplifying low-titer or peripheral samples, or validating inactivation protocols.

While both assays show high sensitivity and offer valuable insights into residual seeding activity, they cannot fully confirm whether treated material remains infectious after treatment. For any decontamination method to be considered thorough, in vivo studies must be conducted using animal models to confirm total loss of infectivity, which is beyond the scope of this study.

5.0 Conclusions

This study set out to investigate the efficacy of environmentally friendly EALCs for the inactivation of CWD PrP^{Sc}. The primary objective was to assess whether selected EALCs could significantly reduce or eliminate PrP^{Sc} seeding activity in both CWD-infected brain homogenates and surface-bound contamination models. The secondary objective involved investigating potential mechanistic changes to PrP^{Sc} following treatment. To complete these objectives, the primary assays of interest were RT-QuIC and PMCA.

Across all experiments, conventional disinfectants sodium hydroxide and bleach consistently eliminated detectable prion seeding activity under the tested conditions. Among the EALCs tested, Catholyte 4 and CAC-717 were the most effective in reducing PrP^{Sc} seeding activity, while BrioHOCl and Anolyte 2 showed variable performance, with notably greater reductions in prions sorbed to stainless steel than in brain homogenates. Mechanistically, based on current and previously published literature, it seems as though EALCs may affect the structure or aggregation state of PrP^{Sc} in ways that affect the proteins' ability to initiate amyloid formation, rather than completely degrading or inactivating all present protein. As evidenced through PMCA, even though the EALCs can delay seeding activity, amplification of residual PrP^{Sc} still took place, concluding that complete inactivation of all PrP^{Sc} after treatment with EALCs is not yet possible.

This research fills a gap in abnormal prion decontamination studies by evaluating the effects of multiple EALCs using homogenate and surface-bound prion models using two complementary in vitro amplification assays. The combined approach strengthens the conclusions by verifying treatment effects across independent methodologies and allows for deeper exploration into possible mechanisms of action. The findings suggest that while some EALCs have promising anti-prion potential with significant reduction of PrP^{Sc} seeding activity, their performance is formula- and condition-dependent, and further optimization of these chemicals would be ideal.

6.0 Future Directions

While this study provides valuable insight into the prion-inactivating potential of EALCs, several avenues for future investigations could strengthen the conclusions formed from current work and further reinforce their practical application.

While this study provides important insights into the ability of EALCs to reduce detectable prion seeding activity in-vitro, the interpretation of these results must be carefully considered when looking to apply EALCs for further investigation. As discussed in Section 4.6.1, both assays detect residual seeding activity in-vitro but cannot fully predict whether treated samples remain infectious in vivo. Since it has been shown that residual infectivity may persist even when amplification is undetectable (Caughey et al, 2017; Lasméza et al, 1997), follow-up studies using animal bioassays remain essential to confirm true prion inactivation. This is particularly relevant for samples treated with the experimental EALCs, as they showed delayed or partial amplification rather than complete suppression, and these conditions could still harbour low levels of pathogenic PrP^{Sc} capable of initiating disease.

In addition to validation via animal bioassay, further mechanistic studies should aim to investigate how EALCs interact with PrP^{Sc} and PrP^{Sc} aggregates on a deeper molecular level. Specifically, better characterization of the structure of the protein after treatment would provide deeper insight into the specific mechanisms underlying each EALC. Advanced imaging techniques like circular dichroism (CD) spectroscopy, Fourier transform-infrared (FT-IR) spectroscopy, cryo-EM, or NMR spectroscopy may be used for this purpose. Any changes seen using these methods could potentially be associated with reductions in infectivity and could help provide evidence of molecular markers of prion inactivation, which could reduce the need for long-term animal bioassays.

In the future, environmental simulation experiments involving more complex and diverse materials should be further explored and combined with in vivo experiments to better reflect real-world contamination scenarios. While this study included a steel wire model, actual environmental conditions where contamination of PrP^{Sc} would be likely to occur often involve many substrates, such as soil, organic debris, and porous materials that can influence the performance of the chemical treatments, as well as detecting the residual PrP^{Sc} seeding activity. Since these chemicals are intended for use in environmental scenarios, future studies should also evaluate meteorological factors, including the temperature of the chemicals during application, the ambient temperature of the environment, sunlight and the humidity of the contaminated materials. Incorporating these matrices into experimental designs, followed by in vivo bioassays to confirm lack of infectivity, would provide a clearer picture of EALC efficacy in field conditions. This would ensure thorough verification, ensuring the chemicals are scientifically validated and practical for wildlife management, agricultural, and industrial settings.

Another area of interest is evaluating EALCs in combination with other decontamination strategies to enhance their overall prion-inactivating potential. This could involve sequential or concurrent use with physical methods such as autoclaving or dry heat, which may help destabilize PrP^{Sc} aggregates and improve chemical penetration (Sakudo et al, 2020). Extended contact times or repeated chemical applications could allow for more complete disruption of resistant PrP^{Sc} that might survive a single treatment. To improve overall inactivation, pairing EALCs with other methods, such as enzyme-based treatments (Saunders et al, 2010) or other prion-inactivating cleaners (Heinzer et al, 2024; Sakudo et al, 2020; Race & Raymond, 2004) could also be explored. These techniques have shown promise for their anti-PrP^{Sc} properties in the past, so their use in combination with EALC treatment could result in additive or synergistic effects by targeting different structural features or stability mechanisms of PrP^{Sc}. It is possible that these integrated approaches have the potential to overcome the limitations of a single treatment and may be particularly useful for decontaminating complex or heavily contaminated materials, where achieving thorough penetration and contact with all potentially infectious material is challenging. Evaluating these combined strategies under

laboratory and simulated environmental conditions would provide critical insight into their feasibility, efficacy, and practicality for large-scale or field applications.

7.0 Appendices

7.1. Bactericidal Efficacy of EALCs

To preliminarily evaluate the effectiveness of EALCs as broad-spectrum disinfectants, their bactericidal activity was assessed using two representative bacterial species: gram-positive *Listeria monocytogenes* and gram-negative *Pseudomonas aeruginosa*. These organisms were selected based on their differing structural features, environmental relevance, and varying resistance profiles and serve as model microorganisms for evaluating the antimicrobial capacity of the EALCs. In addition, this model could be used to assess the stability or shelf-life of the selected EALCs in the future.

7.1.1. Bacterial Strains and Culture Conditions

The QUANTOM Tx Microbial Cell Counter (Logos Biosystems) was used to determine total and viable cell counts for *Listeria monocytogenes* (ATCC 7644) and *Pseudomonas aeruginosa*. Cultures of *L. monocytogenes* were grown on brain heart infusion (BHI) agar and in BHI broth, with the agar plate incubated at 30°C and the broth culture incubated overnight in a rotating incubator. *P. aeruginosa* was cultured under similar conditions but with Lysogeny Broth (LB) as the growth medium and an incubation temperature of 37°C.

Bacterial colonies were suspended in PBS and adjusted to an approximate concentration of 10^9 CFU/mL based on standard comparisons. A serial dilution was performed to 10^{-8}, with the 10^{-1} dilution selected for cell counting. Agar-derived cells were suspended in PBS for total staining or Viable Cell Buffer for viable staining. Overnight cultures were centrifuged, resuspended in PBS, and then diluted to 10^{-1}. Four sample conditions were analyzed: (1) total stain from agar, (2) total stain from overnight culture, (3) viable stain from agar, and (4) viable stain from overnight culture.

Total cell counts were performed using the QUANTOM™ Total Cell Staining Kit (Logos Biosystems). Bacterial samples were mixed with the staining enhancer and total stain, incubated at 37°C for 30 minutes, and then combined with cell loading buffer before loading onto the counting slide.

Viable cell counts were examined using the QUANTOM™ Viable Cell Staining Kit (Logos Biosystems). The viable cell staining dye was added to each sample and incubated at 37°C for 2-3 hours. Following incubation, a cell loading buffer was added, and the mixture was loaded onto the counting slide for analysis.

7.1.2. Treatment of Listeria monocytogenes and Pseudomonas aeruginosa

For both *L. monocytogenes* and *P. aeruginosa*, 25 µL of the respective bacterial suspension at the intended dilution was treated with 225 µL of the EALC treatment (10% v/v). Each treated sample was placed into a 1.5 mL microcentrifuge tube and incubated for one hour at room temperature.

7.1.3. Drop Plate Method for Viability Assessment

Following the incubation, five 20 µL drops of each treated suspension were plated onto BHI agar for *L. monocytogenes* and onto LB agar for *P. aeruginosa*. Plates inoculated with *L. monocytogenes* were incubated at 30°C overnight, while those with *P. aeruginosa* were incubated at 37°C overnight. Colonies were counted and photographed the following day to assess the effectiveness of the EALC treatment.

7.1.4. Quantification of Bactericidal Effects

To quantify the bactericidal activity of each EALC treatment, colony-forming units (CFUs) were manually counted from each of the five 20 µL drops plated per condition. Counts were recorded for each drop, and the average number of colonies per drop was calculated. This value was used to estimate the bacterial concentration (CFU/mL) for each treatment using the formula:

$$CFU/mL = \frac{Mean\ colony\ count}{0.02\ mL}\ x\ Dilution\ Factor$$

Where 0.02 mL corresponds to the volume of each drop plated.

Viable bacterial counts from treated samples were compared to PBS-treated controls and bactericidal activity was expressed as the $\log_{10}$ reduction in CFU/mL, calculated as:

$$LogReduction = Log10CFU/mL_{control} - \log 1\,0CFU/mL_{treatment}$$

A log reduction of ≥3 was considered indicative of significant bactericidal activity, corresponding to a 99.9% reduction in viable bacteria.

For bacterial viability testing via drop plate assay, CFU counts were first log-transformed using the equation $\log_{10}(CFU + 1)$ to normalize the data and allow for meaningful comparisons in the presence of zero values. At a chosen dilution (typically 10^{-6}), log-transformed CFU values for each treatment group were compared to PBS-treated controls. If normality and equal variance assumptions were satisfied, data were analyzed using one-way ANOVA with Tukey's test. If not, the Kruskal–Wallis test with Dunn's multiple comparisons test was applied. Log reductions in CFU/mL were also calculated as descriptive measures of bactericidal efficacy but were not statistically tested directly.

7.1.5. Viability of L. monocytogenes Post-Treatment

This section presents the quantification of *L. monocytogenes* (ATCC 7644) following treatment.

The data was obtained using the QUANTOM Tx Microbial Cell Counter. It compares microbial counts from colonies grown on BHI agar plates and overnight broth cultures. Concentrations are reported as colony-forming units per millilitre (CFU/mL). Total cell counts yielded concentrations of approximately 4.18 x 10^7 cells/mL for colonies grown on BHI agar plates and 8.44 x 10^7 CFU/mL for overnight broth cultures. Viable cell counts were lower, measuring 1.20 x 10^7 CFU/mL for plated colonies and 1.48 x 10^7 CFU/mL for overnight cultures. Therefore, in future experiments, only the viable counts for plated colonies were used to represent bacterial concentrations.

The effectiveness of selected EALCs against *L. monocytogenes* was evaluated using a standard drop plate assay. As shown in Table 7, PBS control samples showed abundant colonies at higher dilutions, with colony counts decreasing at lower dilutions from 1.20 x 10^3. Treatment with 2N NaOH, 3% bleach, and BrioHOCl inhibited bacterial growth at all tested dilutions, indicating strong bactericidal efficacy. All tested catholytes and most anolytes (A1, A2, A3, A5) also fully prevented colony growth. CAC-717 displayed limited bactericidal activity, with observable colony growth at intermediate dilutions of 1.40 x 10^2 and 1 x 10^1.

Anolyte 4 also demonstrated partial efficacy, reducing bacterial growth at intermediate dilutions from 6.00 x 10^2. These results demonstrate the varied bactericidal responses of *L. monocytogenes* to different EALCs, exemplifying the importance of targeted chemical selection when addressing pathogens.

Table 7. Efficacy of a one-hour treatment of EALCs at room temperature against *L. monocytogenes*.

Chemical	Estimated Concentration before Treatment (CFU/mL)	Concentration after Treatment (CFU/mL)
PBS mock-treated POS Control	> 1.20 x 10^3	TMTC
	1.20 x 10^2	1.20 x 10^3
	1.20 x 10^1	2.00 x 10^2
	1.20 x 10^0	3.00 x 10^1
2N NaOH	1.20 x 10^7—1.20 x 10^0	0
3% Bleach	1.20 x 10^7—1.20 x 10^0	0
BrioHOCl	1.20 x 10^7—1.20 x 10^0	0
CAC-717	> 1.20 x 10^2	TMTC
	1.20 x 10^1	1.40 x 10^2
	1.20 x 10^0	1.00 x 10^1
Catholyte 1	1.20 x 10^7—1.20 x 10^0	0
Catholyte 2	1.20 x 10^7—1.20 x 10^0	0
Catholyte 3	1.20 x 10^7—1.20 x 10^0	0
Catholyte 4	1.20 x 10^7—1.20 x 10^0	0
Anolyte 1	1.20 x 10^7—1.20 x 10^0	0
Anolyte 2	1.20 x 10^7—1.20 x 10^0	0
Anolyte 3	1.20 x 10^7—1.20 x 10^0	0
Anolyte 4	> 1.20 x 10^5	TMTC
	1.20 x 10^4	6.00 x 10^2
	1.20 x 10^3	2.00 x 10^1
	1.20 x 10^2	1.00 x 10^1
	1.20 x 10^1—1.20 x 10^0	0
Anolyte 5	1.20 x 10^7—1.20 x 10^0	0

TMTC = Too Many to Count

PBS mock-treated positive controls allowed substantial bacterial growth at higher dilutions, gradually decreasing at lower dilutions. No bacterial growth was observed after treatments with 2N NaOH, 3% bleach, BrioHOCl, Catholytes 1, 2, 3, and 4, and Anolytes 1, 2, 3, and 5. Anolyte 4 and CAC-717 showed partial bactericidal activity, reducing bacterial growth at higher dilutions but failing to eliminate it at higher bacterial concentrations.

Statistical analysis was conducted using Fisher's exact test to evaluate whether treatment with EALCs resulted in significantly reduced bacterial growth relative to PBS controls. Results showed that treatments with NaOH, 3% bleach, BrioHOCl, all catholytes, and several anolytes (A1, A2, A3, A5), respectively, each significantly inhibited the growth of *L. monocytogenes* compared to PBS ($p < 0.001$ for all comparisons), supporting the results from the visual drop plate assessment. CAC-717 and Anolyte 4 did not significantly differ from PBS at intermediate dilutions ($p > 0.05$).

7.1.6. Viability of P. aeruginosa Post-Treatment

To evaluate the impact of treatment on *P. aeruginosa* (ATCC 27853), total and viable cell populations were measured using the same methods used in Section 3.1.1 for *L. monocytogenes*. *P. aeruginosa* was quantified using the QUANTOM Tx Microbial Cell Counter to quantify both total and viable cells in agar-derived colonies and overnight cultures. The growth on LB plates resulted in total cell counts reaching 6.70×10^7 cells/mL for colonies and 3.70×10^7 cells/mL for broth cultures. Viable cell counts were lower at 9.90×10^6 cells/mL and 8.72×10^6 cells/mL, respectively. As with *L. monocytogenes*, only the viable counts for plated colonies were used to represent bacterial concentrations in future experiments.

To better understand how each chemical affected the survival of *P. aeruginosa*, colony counts were performed across serial dilutions following a one-hour treatment at room temperature. The PBS control showed higher bacterial growth with visible colonies detected at nearly all dilutions. Treatment using most EALCS, including all catholytes and anolytes, 2N NaOH, 3% bleach, and BrioHOCl inhibited colony growth. The only exception was CAC-717, which allowed for limited survival at intermediate

concentrations after treatment. Some colony growth was seen as 1.00×10^1 CFU/mL, comparable to the level of growth seen in the PBS control. This suggests that while CAC-717 may overall reduce the survival of most bacteria, it cannot be guaranteed to fully eliminate *P. aeruginosa* under these conditions.

Table 8. Efficacy of a one-hour treatment with EALCs at room temperature against *P. aeruginosa*.

Chemical	Estimated Concentration before Treatment (CFU/mL)	Concentration after Treatment (CFU/mL)
PBS mock-treated POS Control	$> 9.90 \times 10^2$	TMTC
	9.90×10^1	2.10×10^2
	9.90×10^0	2.00×10^1
	9.90×10^{-1}	1.00×10^1
2N NaOH	9.90×10^6—9.90×10^{-1}	0
3% Bleach	9.90×10^6—9.90×10^{-1}	0
BrioHOCl	9.90×10^6—9.90×10^{-1}	0
CAC-717	$> 9.90 \times 10^1$	0
	9.90×10^0	1.00×10^1
	9.90×10^{-1}	0
Catholyte 1	9.90×10^6—9.90×10^{-1}	0
Catholyte 2	9.90×10^6—9.90×10^{-1}	0
Catholyte 3	9.90×10^6—9.90×10^{-1}	0
Catholyte 4	9.90×10^6—9.90×10^{-1}	0
Anolyte 1	9.90×10^6—9.90×10^{-1}	0
Anolyte 2	9.90×10^6—9.90×10^{-1}	0
Anolyte 3	9.90×10^6—9.90×10^{-1}	0
Anolyte 4	9.90×10^6—9.90×10^{-1}	0
Anolyte 5	9.90×10^6—9.90×10^{-1}	0

TMTC = Too Many to Count

Concentrations are presented as CFU/mL. A standard drop plate assay was also used to evaluate the effects of EALCs on *P. aeruginosa*. PBS control samples grew dense and distinct colonies across nearly all dilutions, with countable colonies detected down to intermediate dilutions, and complete inhibition only at the lowest dilution. Of all EALCs, CAC-717 exhibited only partial antimicrobial efficacy. All other EALCs, including 2N NaOH, 3% bleach, and BrioHOCl, effectively eliminated all viable *P. aeruginosa* across every dilution tested.

Fisher's exact test was used to determine whether EALC treatment significantly reduced bacterial viability compared to the PBS control. Chemicals that achieved complete inactivation of *P. aeruginosa* (NaOH, bleach, BrioHOCl, all catholytes and anolytes) were all significantly more effective than PBS ($p < 0.001$). Even though CAC-717 did not eliminate all growth at one dilution, overall, it also significantly differed from PBS at the same dilution ($p < 0.001$), indicating that its partial reduction in viable cells was sufficiently statistically distinguishable from untreated conditions.

7.1.7. Comparative Susceptibility of L. monocytogenes and P. aeruginosa to EALCs

Listeria monocytogenes (Gram-positive) and *Pseudomonas aeruginosa* (Gram-negative) were chosen for this study because they (i) represent the two bacterial cell wall structures, (ii) are recognized biofilm formers that show heightened tolerance to oxidative and alkaline disinfection techniques (Rohilla et al, 2024; Kim et al, 2016), and (iii) are considered challenging organisms to disinfect (U.S. Environmental Protection Agency, 2024; World Health Organization, 2018). Examining the susceptibility of these bacteria to the EALCs provides a quick, inexpensive, and relatively safe model to preliminarily gauge the broad-spectrum antimicrobial effects of the chemicals before proceeding to high-containment prion experiments. By establishing bactericidal efficacy against resilient bacterial species, this assay is an important screening step to prioritize EALCs with the most significant potential for environmental decontamination applications.

A side-by-side comparison of the drop-plate data shows that *P. aeruginosa* was slightly more susceptible to the EALC panel than *L. monocytogenes*. All acidic and oxidizing chemicals (BrioHOCl and anolytes)

and alkaline and reductive (catholytes, CAC-717, 2 N NaOH, 3 % bleach) solutions achieved complete disinfection of both organisms at every dilution tested. Still, only *L. monocytogenes* retained detectable levels after exposure to Anolyte 4 ($6x10^2$ CFU mL^{-1} at 10^{-3}) and CAC-717 ($1.4x10^2$ CFU mL^{-1} at 10^{-6}), whereas *P. aeruginosa* was fully eradicated by Anolyte 4 and showed merely trace survival with CAC-717 (10 CFU mL^{-1} at 10^{-6}). Fisher's exact tests confirmed that both partial failures were statistically distinguishable from the PBS control, yet the higher residual counts for *L. monocytogenes* indicate a modest, but repeatable, resistance edge.

The observed difference in susceptibility between bacterial species is likely reflective of their different species-specific cell-envelope types. *L. monocytogenes* is gram-positive and possesses a thick, highly cross-linked peptidoglycan cell membrane that can buffer pH and scavenge reactive chlorine species (Bucur et al, 2018). The cell membrane of *P. aeruginosa* is gram-negative and thin, and under the same conditions, it becomes rapidly permeabilized, increasing the amount of damage done to the cells (da Cruz Nizer et al., 2020).

Overall, these results demonstrate that EALCs can effectively target resilient bacterial species, providing preliminary evidence of their potential to act against other resistant pathogens. This supports their selection for subsequent evaluation against CWD prions in the present study.

7.1.8. Proposed Mechanisms of Action Responsible for Observed Bactericidal Effects of EALCs

EALCs exert their antimicrobial activity through two chemically distinct pathways formed during electrolysis. Acidic anolytes contain a high amount of free available chlorine, mainly in the form of HOCl. In contrast, alkaline, strongly reductive catholytes contain many hydroxide ions and oxidative species (Nyamende et al, 2023).

The primary bactericidal pathway for acidic EALCs involves HOCl-mediated oxidation. Because HOCl is electrically neutral and only ~1.5 Å in diameter, it crosses the cell membrane relatively easily. Once inside, it oxidizes membrane lipids, unfolds proteins, and induces irreversible protein aggregation. It produces

toxic secondary reactive oxygen species (ROS), all cumulating to result in the deadly loss of membrane integrity and enzyme function (Dianty et al, 2023; Andrés et al, 2022). For alkaline EALCs such as catholytes, extreme pH (> 11) hydrolyses ester linkages in cell membrane phospholipids, converting fatty acids to more water-soluble lipids and causing rapid membrane breakdown. Such high alkalinity also disrupts peptidoglycan cross-linkages and denatures surface proteins (Ndjomgoue-Yossa et al, 2022).

As mentioned, the observations described in Results section 3.1 can likely be attributed to each bacterial species' membrane structure and stress response capacity. The porous, outer-membrane-free peptidoglycan mesh of *L. monocytogenes* does not offer much resistance to neutral HOCl and secondary ROS, allowing these oxidants to reach and disrupt the cytoplasmic membrane almost immediately (Bucur et al., 2018). Contrarily, *P. aeruginosa* initially benefits from a thick outer membrane that slows oxidant ingress and from inducible catalase, peroxidase, and efflux systems that detoxify reactive chlorine species (da Cruz Nizer et al., 2020). This physical barrier delays but does not prevent damage. Once it becomes destabilized by a high oxidation-reduction potential (ORP) and alkaline pH, the cell's internal components become vulnerable, and both organisms are ultimately eliminated within the one-hour EALC treatment.

7.1.9. Relevance to Environmental Decontamination Applications

L. monocytogenes and *P. aeruginosa*, two microorganisms uncommonly recognized as "difficult to disinfect," are good models to provide preliminary proof-of-concept that EALCs can meet broad-spectrum disinfection requirements within realistic contact times for use in practical settings.

EALCs also demonstrate excellent compatibility with the operational needs of wildlife-management sites, abattoirs, and mobile decontamination units, making them good contenders for all-purpose cleaners. Because they are generated on-site from simple ingredients derived from salt and water, there is no need to transport or store large volumes of hazardous chemicals, and spent solutions quickly revert to benign NaCl and H_2O, minimizing potential secondary side effects on the environment (Gnatko et al, 2011). High ORP anolytes and strongly alkaline catholytes target a wide variety of cellular components including lipids,

proteins, and nucleic acids, encompassing the possible diversity of contaminants that could be found in farming environments and on processing surfaces (Dianty et al, 2023). Importantly, our one-hour EALC exposure achieved statistically significant bacterial reductions for most concentrations tested, supporting further research examining their potential as prion inactivating chemicals.

Previous research examining material compatibility has shown that repeated applications of electrolyzed water on stainless steel only resulted in minimal corrosion (Ayebah & Hung, 2005), supporting the practicality of these chemicals for routine use on equipment such as metal tools, transport trailers, or wildlife necropsy benches (Aider et al, 2012). Due to the relatively safe nature of EALCS, there is an opportunity for the delivery format of EALCs to be optimized to their ideal location. This could include low-pressure fogging for stalls and transport trucks, immersion baths for small instruments and tools, and pre-saturated wipes for hunters' knives or sampling probes. In addition to the other benefits of EALCs over traditional decontaminants, the solutions are also non-flammable, produce no toxic chlorine gas at working concentrations, and generally do not require extensive safe handling measures, broadening the possibility of uses outside high-containment laboratories.

Finally, the same oxidative and alkaline actions that disrupt bacterial membranes also oxidize methionine and tyrosine residues, cleave disulfide bonds, and destabilize the β-sheet-rich fold of PrP^{Sc} (Sakudo et al., 2024). Bacteria and prions can both persist in the environment, often sharing the same contaminated surfaces, soil, or water sources, particularly in agricultural, wildlife, or food-processing settings. If an EALC can inactivate both, it offers a more universal tool for decontamination, capable of addressing multiple hard-to-remove pathogens in a single treatment. Overall, EALCs provide a novel avenue for the environmental decontamination of pathogens that routinely survive conventional disinfectants, proving their practicality, while being an environmentally friendly alternative to classical decontamination methods.

8.0 Bibliography

Abid, K., Soto, C. (2006). The intriguing prion disorders. *Cellular and molecular life sciences: CMLS*, 63(19-20), 2342–2351. https://doi.org/10.1007/s00018-006-6140-5

Acín, C., Bolea, R., Monzón, M., Monleón, E., Moreno, B., Filali, H., Marín, B., Sola, D., Betancor, M., Guijarro, I. M., García, M., Vargas, A., Badiola, J. J. (2021). Classical and Atypical Scrapie in Sheep and Goats. Review on the Etiology, Genetic Factors, Pathogenesis, Diagnosis, and Control Measures of Both Diseases. *Animals*, 11(3), 691. https://doi.org/10.3390/ani11030691

Aider, M., Gnatko, E., Benali, M., Plutakhin, G., Kastyuchik, A. (2012) Electro-activated aqueous solutions: Theory and application in the food industry and biotechnology. *Innovative Food Science Emerging Technologies*, 15, 38-49. https://doi.org/10.1016/j.ifset.2012.02.002

Aider, M. (2023). Electro-activation as emerging technology for proteins extraction from plant materials: Theory and applications. In A. J. Hernández-Álvarez, M. Mondor, M. G. Nosworthy (Eds.), *Green protein processing technologies from plants* (pp. 89-110). Springer. https://doi.org/10.1007/978-3-031-16968-7_4

Alpers M. P. (2008). The epidemiology of kuru: monitoring the epidemic from its peak to its end. *Philosophical transactions of the Royal Society of London. Series B, Biological sciences*, 363(1510), 3707–3713. https://doi.org/10.1098/rstb.2008.0071

Alpers, M. P., Kuru Surveillance Team (2005). The epidemiology of kuru in the period 1987 to 1995. *Communicable diseases intelligence*, 29(4), 391–399.

Alves, R. N., Iglesia, R. P., Prado, M. B., Melo Escobar, M. I., Boccacino, J. M., Fernandes, C. F. L., Coelho, B. P., Fortes, A. C., Lopes, M. H. (2020). A New Take on Prion Protein Dynamics in Cellular Trafficking. *Int J of Mol Sci*, 21(20), 7763. https://doi.org/10.3390/ijms21207763

Andrés, C. M. C., Pérez de la Lastra, J. M., Juan, C. A., Plou, F. J., Pérez-Lebeña, E. (2022). Hypochlorous Acid Chemistry in Mammalian Cells-Influence on Infection and Role in Various Pathologies. *International journal of molecular sciences*, 23(18), 10735. https://doi.org/10.3390/ijms231810735

Animal and Plant Health Agency. (2023, November 21). Exotic species and domestic cats: TSE surveillance statistics. *Government of the United Kingdom*.

https://www.gov.uk/government/publications/exotic-species-and-domestic-cats-tse-surveillance-statistics

Appel, T. R., Lucassen, R., Groschup, M. H., Joncic, M., Beekes, M., Riesner, D. (2006). Acid inactivation of prions: efficient at elevated temperature or high acid concentration. *The Journal of general virology*, *87(*Pt 5), 1385–1394. https://doi.org/10.1099/vir.0.81426-0

Arifin, M. I., Hannaoui, S., Chang, S. C., Thapa, S., Schatzl, H. M., Gilch, S. (2021). Cervid Prion Protein Polymorphisms: Role in Chronic Wasting Disease Pathogenesis. *International journal of molecular sciences*, 22(5), 2271. https://doi.org/10.3390/ijms22052271

Atarashi, R., Sano, K., Satoh, K., Nishida, N. (2011). Real-time quaking-induced conversion: a highly sensitive assay for prion detection. *Prion*, 5(3), 150–153. https://doi.org/10.4161/pri.5.3.16893

Atarashi R. (2023). RT-QuIC as ultrasensitive method for prion detection. *Cell and tissue research*, 392(1), 295–300. https://doi.org/10.1007/s00441-021-03568-8

Atkinson, C. J., Zhang, K., Munn, A. L., Wiegmans, A., Wei, M. Q. (2016). Prion protein scrapie and the normal cellular prion protein. *Prion*, 10(1), 63–82. https://doi.org/10.1080/19336896.2015.1110293

Ayebah, B., Hung, Y-C. (2005). ELECTROLYZED WATER AND ITS CORROSIVENESS ON VARIOUS SURFACE MATERIALS COMMONLY FOUND IN FOOD PROCESSING FACILITIES. *Journal of Food Process Engineering*, 28(3), 247-264. https://doi.org/10.1111/j.1745-4530.2005.00424.x

Baranová, S., Moško, T., Brůžová, M., Haldiman, T., Kim, C., Safar, J. G., Matěj, R., Holada, K. (2024). Detection of prions in matching post-mortem skin and cerebrospinal fluid samples using second-generation real-time quaking-induced conversion assay. Scientific reports, 14(1), 6294. https://doi.org/10.1038/s41598-024-56789-6

Baron, T., Bencsik, A., Biacabe, A. G., Morignat, E., Bessen, R. A. (2007). Phenotypic similarity of transmissible mink encephalopathy in cattle and L-type bovine spongiform encephalopathy in a mouse model. *Emerging infectious diseases*, 13(12), 1887–1894. https://doi.org/10.3201/eid1312.070635

Barria, M. A., Libori, A., Mitchell, G., Head, M. W. (2018). Susceptibility of Human Prion Protein to Conversion by Chronic Wasting Disease Prions. *Emerging infectious diseases*, 24(8), 1482–1489. https://doi.org/10.3201/eid2408.161888

Bartz J. C. (2016). Prion Strain Diversity. *Cold Spring Harbor perspectives in medicine*, 6(12), a024349. https://doi.org/10.1101/cshperspect.a024349

Bauman, P. A., Lawrence, L. A., Biesert, L., Dichtelmüller, H., Fabbrizzi, F., Gajardo, R., Gröner, A., Jorquera, J. I., Kempf, C., Kreil, T. R., von Hoegen, I., Pifat, D. Y., Petteway, S. R., Jr, Cai, K. (2006). Critical factors influencing prion inactivation by sodium hydroxide. *Vox sanguinis*, 91(1), 34–40. https://doi.org/10.1111/j.1423-0410.2006.00790.x

Baune, C., Groveman, B. R., Hughson, A. G., Thomas, T., Twardoski, B., Priola, S., Chesebro, B., Race, B. (2023). Efficacy of Wex-cide 128 disinfectant against multiple prion strains. *PloS one*, 18(8), e0290325. https://doi.org/10.1371/journal.pone.0290325

Bechtel, K., Geschwind, M. D. (2013). Ethics in prion disease. *Progress in neurobiology*, 110, 29–44. https://doi.org/10.1016/j.pneurobio.2013.07.001

Bishop, M. T., Will, R. G., Manson, J. C. (2010). Defining sporadic Creutzfeldt-Jakob disease strains and their transmission properties. *Proceedings of the National Academy of Sciences of the United States of America*, 107(26), 12005–12010. https://doi.org/10.1073/pnas.1004688107

Bistaffa, E., Vuong, T. T., Cazzaniga, F. A., Tran, L., Salzano, G., Legname, G., Giaccone, G., Benestad, S. L., Moda, F. (2019). Use of different RT-QuIC substrates for detecting CWD prions in the brain of Norwegian cervids. *Scientific reports*, 9(1), 18595. https://doi.org/10.1038/s41598-019-55078-x

Block, M. S., Rowan, B. G. (2020). Hypochlorous Acid: A Review. *Journal of oral and maxillofacial surgery : official journal of the American Association of Oral and Maxillofacial Surgeons*, 78(9), 1461–1466. https://doi.org/10.1016/j.joms.2020.06.029

Boecker, D., Zhang, Z., Breves, R., Herth, F., Kramer, A., Bulitta, C. (2023). Antimicrobial efficacy, mode of action and in vivo use of hypochlorous acid (HOCl) for prevention or therapeutic support of infections. *GMS hygiene and infection control*, 18, Doc07. https://doi.org/10.3205/dgkh000433

Bonda, D. J., Manjila, S., Mehndiratta, P., Khan, F., Miller, B. R., Onwuzulike, K., Puoti, G., Cohen, M. L., Schonberger, L. B., Cali, I. (2016). Human prion diseases: surgical lessons learned from iatrogenic prion transmission. *Neurosurgical focus*, 41(1), E10. https://doi.org/10.3171/2016.5.FOCUS15126

Booth, C. J., Lichtenberg, S. S., Chappell, R. J., Pedersen, J. A. (2021). Chemical Inactivation of Prions Is Altered by Binding to the Soil Mineral Montmorillonite. *ACS infectious diseases*, 7(4), 859–870. https://doi.org/10.1021/acsinfecdis.0c00860

Bosques, C. J., Imperiali, B. (2003). The interplay of glycosylation and disulfide formation influences fibrillization in a prion protein fragment. *Proceedings of the National Academy of Sciences of the United States of America*, *100*(13), 7593–7598. https://doi.org/10.1073/pnas.1232504100

Brandel, J. P., Culeux, A., Grznarova, K., Levavasseur, E., Lamy, P., Privat, N., Welaratne, A., Denouel, A., Laplanche, J. L., Haik, S. (2019). Amplification techniques and diagnosis of prion diseases. *Revue neurologique*, 175(7-8), 458–463. https://doi.org/10.1016/j.neurol.2019.06.002

Brown, P., Rau, E. H., Lemieux, P., Johnson, B. K., Bacote, A. E., Gajdusek, D. C. (2004). Infectivity studies of both ash and air emissions from simulated incineration of scrapie-contaminated tissues. *Environmental science & technology*, 38(22), 6155–6160. https://doi.org/10.1021/es040301z

Bucur, F. I., Grigore-Gurgu, L., Crauwels, P., Riedel, C. U., Nicolau, A. I. (2018). Resistance of *Listeria monocytogenes* to Stress Conditions Encountered in Food and Food Processing Environments. *Frontiers in microbiology*, 9, 2700. https://doi.org/10.3389/fmicb.2018.02700

Burgener, K. R., Lichtenberg, S. S., Lomax, A., Storm, D. J., Walsh, D. P., Pedersen, J. A. (2022). Diagnostic testing of chronic wasting disease in white-tailed deer (*Odocoileus virginianus*) by RT-QuIC using multiple tissues. *PloS one*, 17(11), e0274531. https://doi.org/10.1371/journal.pone.0274531

Canadian Food Inspection Agency. (2013, March 21). Overview of Canada's BSE Safeguards. *Government of Canada*. https://inspection.canada.ca/en/animal-health/terrestrial-animals/diseases/reportable/bovine-spongiform-encephalopathy/safeguards

Canadian Food Inspection Agency. (2021, April 22). Sheep genetics and scrapie. *Government of Canada.* https://inspection.canada.ca/en/animal-health/terrestrial-animals/diseases/reportable/scrapie/sheep-genetics-and-scrapie

Canadian Food Inspection Agency. (2023, December 7). National Scrapie Eradication Program. *Government of Canada.* https://inspection.canada.ca/en/animal-health/terrestrial-animals/diseases/reportable/scrapie/nsep

Canadian Food Inspection Agency. (2023, December 7). Bovine spongiform encephalopathy. *Government of Canada*. https://inspection.canada.ca/en/animal-health/terrestrial-animals/diseases/reportable/bovine-spongiform-encephalopathy

Canadian Food Inspection Agency. (2023, September 9). Bovine spongiform encephalopathy: Atypical and classical. *Government of Canada*. https://inspection.canada.ca/en/animal-health/terrestrial-animals/diseases/reportable/bovine-spongiform-encephalopathy/bse-atypical-and-classical

Canadian Food Inspection Agency. (2024, February 8). Chronic wasting disease of deer and elk. *Government of Canada*. https://inspection.canada.ca/en/animal-health/terrestrial-animals/diseases/reportable/cwd

Cassmann, E. D., Moore, S. J., Smith, J. D., Greenlee, J. J. (2019). Sheep Are Susceptible to the Bovine Adapted Transmissible Mink Encephalopathy Agent by Intracranial Inoculation and Have Evidence of Infectivity in Lymphoid Tissues. *Frontiers in veterinary science*, 6, 430. https://doi.org/10.3389/fvets.2019.00430

Carlson, C. M., Thomas, S., Keating, M. W., Soto, P., Gibbs, N. M., Chang, H., Wiepz, J. K., Austin, A. G., Schneider, J. R., Morales, R., Johnson, C. J., Pedersen, J. A. (2023). Plants as vectors for environmental prion transmission. *iScience*, 26(12), 108428. https://doi.org/10.1016/j.isci.2023.108428

Carrasco, A. E., Appleby, B. S., Cali, I., Okhravi, H. R. (2022). Atypical Case of VV1 Creutzfeldt-Jakob Disease Subtype: Case Report. *Frontiers in neurology*, 13, 875370. https://doi.org/10.3389/fneur.2022.875370

Caughey, B., Orru, C. D., Groveman, B. R., Hughson, A. G., Manca, M., Raymond, L. D., Raymond, G. J., Race, B., Saijo, E., Kraus, A. (2017). Amplified Detection of Prions and Other Amyloids by RT-QuIC in Diagnostics and the Evaluation of Therapeutics and Disinfectants. *Progress in*

molecular biology and translational science, 150, 375–388. https://doi.org/10.1016/bs.pmbts.2017.06.003

Chang, S. C., Hannaoui, S., Arifin, M. I., Huang, Y. H., Tang, X., Wille, H., Gilch, S. (2023). Propagation of PrP^{Sc} in mice reveals impact of aggregate composition on prion disease pathogenesis. *Communications biology*, 6(1), 1162. https://doi.org/10.1038/s42003-023-05541-3

Chen, Z., Guo, J., Ran, N., Zhong, Y., Yang, F., Sun, H. (2023). A family with mental disorder as the first symptom finally confirmed with Gerstmann-Sträussler-Scheinker disease with P102L mutation in PRNP gene - case report. *Prion*, 17(1), 37–43. https://doi.org/10.1080/19336896.2023.2180255

Chen, Z., Kong, Y., Zhang, J., Zou, W. Q., Wu, L. (2024). Genetic and pathological features encipher the phenotypic heterogeneity of Gerstmann-Sträussler-Scheinker disease. *Neurobiology of disease*, 195, 106497. https://doi.org/10.1016/j.nbd.2024.106497

Chen, B., Newnam, G. P., Chernoff, Y. O. (2007). Prion species barrier between the closely related yeast proteins is detected despite coaggregation. *Proceedings of the National Academy of Sciences of the United States of America*, *104*(8), 2791–2796. https://doi.org/10.1073/pnas.0611158104

Chen, L. J., Sawyer, E. B., Perrett, S. (2011). The yeast prion protein Ure2: insights into the mechanism of amyloid formation. *Biochemical Society transactions*, 39(5), 1359–1364. https://doi.org/10.1042/BST0391359

Chitravas, N., Jung, R. S., Kofskey, D. M., Blevins, J. E., Gambetti, P., Leigh, R. J., Cohen, M. L. (2011). Treatable neurological disorders misdiagnosed as Creutzfeldt-Jakob disease. Annals of neurology, 70(3), 437–444. https://doi.org/10.1002/ana.22454

Chu, M., Xie, K., Zhang, J., Chen, Z., Ghorayeb, I., Rupprecht, S., Reder, A. T., Garay, A., Honda, H., Nagayama, M., Shi, Q., Zhan, S., Nan, H., Zhang, J., Guan, H., Cui, L., Guo, Y., Rosa-Neto, P., Gauthier, S., Wang, J., … Wu, L. (2022). Proposal of new diagnostic criteria for fatal familial insomnia. *Journal of neurology*, 269(9), 4909–4919. https://doi.org/10.1007/s00415-022-11135-6

Cobb, N. J., Apostol, M. I., Chen, S., Smirnovas, V., Surewicz, W. K. (2014). Conformational stability of mammalian prion protein amyloid fibrils is dictated by a packing polymorphism within the core region. *The Journal of biological chemistry*, *289*(5), 2643–2650. https://doi.org/10.1074/jbc.M113.520718

Concha-Marambio, L., Diaz-Espinoza, R., Soto, C. (2014). The extent of protease resistance of misfolded prion protein is highly dependent on the salt concentration. *The Journal of biological chemistry*, 289(5), 3073–3079. https://doi.org/10.1074/jbc.M113.513267

Connor, A., Wang, H., Appleby, B. S., Rhoads, D. D. (2019). Clinical Laboratory Tests Used To Aid in Diagnosis of Human Prion Disease. Journal of clinical microbiology, 57(10), e00769-19. https://doi.org/10.1128/JCM.00769-19

Cooke, C. M., Rodger, J., Smith, A., Fernie, K., Shaw, G., Somerville, R. A. (2007). Fate of prions in soil: detergent extraction of PrP from soils. *Environmental science & technology*, 41(3), 811–817. https://doi.org/10.1021/es0618189

Corona, C., Vallino Costassa, E., Iulini, B., Caramelli, M., Bozzetta, E., Mazza, M., Desiato, R., Ru, G., Casalone, C. (2017). Phenotypical Variability in Bovine Spongiform Encephalopathy: Epidemiology, Pathogenesis, and Diagnosis of Classical and Atypical Forms. *Progress in molecular biology and translational science*, 150, 241–265. https://doi.org/10.1016/bs.pmbts.2017.06.015

Cosseddu, G. M., Nonno, R., Vaccari, G., Bucalossi, C., Fernandez-Borges, N., Di Bari, M. A., Castilla, J., Agrimi, U. (2011). Ultra-efficient PrP(Sc) amplification highlights potentialities and pitfalls of PMCA technology. *PLoS pathogens*, 7(11), e1002370. https://doi.org/10.1371/journal.ppat.1002370

Cuillé, J., Chelle, P-L. (1936). La maladie dite “tremblante” du mouton; est-elle inoculable? Compte Rend Acad Sci. 1936;203:1552.

Cunningham, A. A. (1991). Bovine Spongiform Encephalopathy and British Zoos. *Journal of Zoo and Wildlife Medicine*, 22(3), 304–308. http://www.jstor.org/stable/20095161

da Cruz Nizer, W. S., Inkovskiy, V., Overhage, J. (2020). Surviving Reactive Chlorine Stress: Responses of Gram-Negative Bacteria to Hypochlorous Acid. *Microorganisms*, *8*(8), 1220. https://doi.org/10.3390/microorganisms8081220

Davenport, K. A., Hoover, C. E., Denkers, N. D., Mathiason, C. K., Hoover, E. A. (2018). Modified Protein Misfolding Cyclic Amplification Overcomes Real-Time Quaking-Induced Conversion Assay Inhibitors in Deer Saliva To Detect Chronic Wasting Disease Prions. *Journal of clinical microbiology*, 56(9), e00947-18. https://doi.org/10.1128/JCM.00947-18

Deleault, N. R., Walsh, D. J., Piro, J. R., Wang, F., Wang, X., Ma, J., Rees, J. R., Supattapone, S. (2012). Cofactor molecules maintain infectious conformation and restrict strain properties in purified prions. *Proceedings of the National Academy of Sciences of the United States of America*, 109(28), E1938–E1946. https://doi.org/10.1073/pnas.1206999109

Denkers, N. D., Hayes-Klug, J., Anderson, K. R., Seelig, D. M., Haley, N. J., Dahmes, S. J., Osborn, D. A., Miller, K. V., Warren, R. J., Mathiason, C. K., Hoover, E. A. (2013). Aerosol transmission of chronic wasting disease in white-tailed deer. *Journal of virology*, 87(3), 1890–1892. https://doi.org/10.1128/JVI.02852-12

Desai, N., Purzycki, T. (2023). Early Diagnostic Measures to Confirm the Diagnosis of Human Prion Diseases. *Cureus*, 15(5), e39412. https://doi.org/10.7759/cureus.39412

De Vries, K., Cousins, E., Harrison Dening, K. (2021). Palliative care in Creutzfeldt-Jakob disease: looking back, thinking ahead. BMJ supportive palliative care, bmjspcare-2020-002799. Advance online publication. https://doi.org/10.1136/bmjspcare-2020-002799

Dianty, R., Hirano, J., Anzai, I., Kanai, Y., Hayashi, T., Morimoto, M., Kataoka-Nakamura, C., Kobayashi, S., Uemura, K., Ono, C., Watanabe, T., Kobayashi, T., Murakami, K., Kikuchi, K., Hotta, K., Yoshikawa, T., Taguwa, S., Matsuura, Y. (2023). Electrolyzed hypochlorous acid water exhibits potent disinfectant activity against various viruses through irreversible protein aggregation. *Frontiers in microbiology*, *14*, 1284274. https://doi.org/10.3389/fmicb.2023.1284274

Dudas, S., Czub, S. (2017). Atypical BSE: Current Knowledge and Knowledge Gaps. *Food safety*, 5(1), 10–13. https://doi.org/10.14252/foodsafetyfscj.2016028

Duyckaerts, C., Clavaguera, F., Potier, M. C. (2019). The prion-like propagation hypothesis in Alzheimer's and Parkinson's disease. *Current opinion in neurology*, 32(2), 266–271. https://doi.org/10.1097/WCO.0000000000000672

Environment and Protected Areas. (2024, March 21). Chronic Wasting Disease – Updates. *Government of Alberta*. https://www.alberta.ca/chronic-wasting-disease-updates

Eraña, H., Charco, J. M., González-Miranda, E., García-Martínez, S., López-Moreno, R., Pérez-Castro, M. A., Díaz-Domínguez, C. M., García-Salvador, A., Castilla, J. (2020). Detection of Pathognomonic Biomarker PrPSc and the Contribution of Cell Free-Amplification Techniques to

the Diagnosis of Prion Diseases. *Biomolecules*, 10(3), 469. https://doi.org/10.3390/biom10030469

Eraña, H., Sampedro-Torres-Quevedo, C., Charco, J. M., Díaz-Domínguez, C. M., Peccati, F., San-Juan-Ansoleaga, M., Vidal, E., Gonçalves-Anjo, N., Pérez-Castro, M. A., González-Miranda, E., Piñeiro, P., Fernández-Veiga, L., Galarza-Ahumada, J., Fernández-Muñoz, E., Perez de Nanclares, G., Telling, G., Geijo, M., Jiménez-Osés, G., Castilla, J. (2024). A Protein Misfolding Shaking Amplification-based method for the spontaneous generation of hundreds of bona fide prions. *Nature communications*, 15(1), 2112. https://doi.org/10.1038/s41467-024-46360-2

Fichet, G., Comoy, E., Duval, C., Antloga, K., Dehen, C., Charbonnier, A., McDonnell, G., Brown, P., Lasmézas, C. I., Deslys, J. P. (2004). Novel methods for disinfection of prion-contaminated medical devices. *Lancet (London, England)*, 364(9433), 521–526. https://doi.org/10.1016/S0140-6736(04)16810-4

Foliaki, S. T., Lewis, V., Islam, A. M. T., Senesi, M., Finkelstein, D. I., Ellett, L. J., Lawson, V. A., Adlard, P. A., Roberts, B. R., Collins, S. J. (2020). PrPSc Oligomerization Appears Dynamic, Quickly Engendering Inherent M1000 Acute Synaptotoxicity. *Biophysical journal*, 119(1), 128–141. https://doi.org/10.1016/j.bpj.2020.04.040

Ford, M. J., Burton, L. J., Morris, R. J., Hall, S. M. (2002). Selective expression of prion protein in peripheral tissues of the adult mouse. *Neuroscience*, 113(1), 177–192. https://doi.org/10.1016/s0306-4522(02)00155-0

Fułek, M., Hachiya, N., Gachowska, M., Beszłej, J. A., Bartoszewska, E., Kurpas, D., Kurpiński, T., Adamska, H., Poręba, R., Urban, S., Fułek, K., Leszek, J. (2025). Cellular Prion Protein and Amyloid-β Oligomers in Alzheimer's Disease-Are There Connections?. International journal of molecular sciences, 26(5), 2097. https://doi.org/10.3390/ijms26052097

Food and Drug Administration. (2022, May). Recommendations to Reduce the Possible Risk of Transmission of Creutzfeldt-Jakob Disease and Variant Creutzfeldt-Jakob Disease by Blood and Blood Components. *U.S. Department of Health and Human Services*. https://www.fda.gov/media/124156/download

Gajdusek, D. C., Zigas, V. (1957). Degenerative disease of the central nervous system in New Guinea; the endemic occurrence of kuru in the native population. *The New England journal of medicine*, 257(20), 974–978. https://doi.org/10.1056/NEJM195711142572005

Gambetti, P., Parchi, P., Petersen, R. B., Chen, S. G., Lugaresi, E. (1995). Fatal familial insomnia and familial Creutzfeldt-Jakob disease: clinical, pathological and molecular features. *Brain pathology*, 5(1), 43–51. https://doi.org/10.1111/j.1750-3639.1995.tb00576.x

Gavier-Widén, D., Stack, M. J., Baron, T., Balachandran, A., & Simmons, M. (2005). Diagnosis of transmissible spongiform encephalopathies in animals: a review. *Journal of veterinary diagnostic investigation,*. 17(6), 509–527. https://doi.org/10.1177/104063870501700601

Genovesi, S., Leita, L., Sequi, P., Andrighetto, I., Sorgato, M. C., Bertoli, A. (2007). Direct detection of soil-bound prions. *PloS one*, 2(10), e1069. https://doi.org/10.1371/journal.pone.0001069

Georgsson, G., Sigurdarson, S., Brown, P. (2006). Infectious agent of sheep scrapie may persist in the environment for at least 16 years. *Journal of General Virology*, 87(12), 3737–3740. https://doi.org/10.1099/vir.0.82011-0

Gerber, R., Tahiri-Alaoui, A., Hore, P. J., James, W. (2008). Conformational pH dependence of intermediate states during oligomerization of the human prion protein. *Protein science : a publication of the Protein Society*, 17(3), 537–544. https://doi.org/10.1110/ps.073163308

Giles, K., Glidden, D. v., Beckwith, R., Seoanes, R., Peretz, D., DeArmond, S. J., Prusiner, S. B. (2008). Resistance of Bovine Spongiform Encephalopathy (BSE) Prions to Inactivation. *PLoS Pathogens*, 4(11), 1000206. https://doi.org/10.1371/JOURNAL.PPAT.1000206

Gibbs, C. J., Jr, Gajdusek, D. C., Asher, D. M., Alpers, M. P., Beck, E., Daniel, P. M., Matthews, W. B. (1968). Creutzfeldt-Jakob disease (spongiform encephalopathy): transmission to the chimpanzee. *Science*, 161(3839), 388–389. https://doi.org/10.1126/science.161.3839.388

Giles, K., Woerman, A. L., Berry, D. B., Prusiner, S. B. (2017). Bioassays and Inactivation of Prions. *Cold Spring Harbor perspectives in biology*, 9(8), a023499. https://doi.org/10.1101/cshperspect.a023499

Gnatko, E.N., Kravets, V.I., Leschenko, E.V., Omelchenko, A. (2011). Emergence of the Science and Technology of Electroactivated Aqueous Solutions: Applications for Environmental and Food Safety. In: Alpas, H., Berkowicz, S., Ermakova, I. (eds) *Environmental Security and Ecoterrorism*. NATO Science for Peace and Security Series C: Environmental Security. Springer, Dordrecht. https://doi.org/10.1007/978-94-007-1235-5_8

Goldman, J. S., Vallabh, S. M. (2022). Genetic counseling for prion disease: Updates and best practices. *Genetics in medicine*, 24(10), 1993–2003. https://doi-org.proxy.bib.uottawa.ca/10.1016/j.gim.2022.06.003

Gough, K. C., Baker, C. A., Simmons, H. A., Hawkins, S. A., Maddison, B. C. (2015). Circulation of prions within dust on a scrapie affected farm. *Veterinary research*, 46(1), 40. https://doi.org/10.1186/s13567-015-0176-1

Goold, R., McKinnon, C., Tabrizi, S. J. (2015). Prion degradation pathways: Potential for therapeutic intervention. *Molecular and cellular neurosciences*, 66(Pt A), 12–20. https://doi.org/10.1016/j.mcn.2014.12.009

Greenlee J. J. (2019). Review: Update on Classical and Atypical Scrapie in Sheep and Goats. *Veterinary pathology*, 56(1), 6–16. https://doi.org/10.1177/0300985818794247

Groveman, B. R., Williams, K., Race, B., Foliaki, S., Thomas, T., Hughson, A. G., Walters, R. O., Zou, W., Haigh, C. L. (2024). Lack of Transmission of Chronic Wasting Disease Prions to Human Cerebral Organoids. *Emerging infectious diseases*, 30(6), 1193–1202. https://doi.org/10.3201/eid3006.231568

Grunklee, M. K., Lichtenberg, S. S., Rowden, G., Karwan, D. L., Li, E. A., Schwabenlander, M. D., Wolf, T. M. (2025). RT-QuIC optimization for prion detection in soils. *MethodsX*, 14, 103380. https://doi.org/10.1016/j.mex.2025.103380

Grunklee, M. K., Lichtenberg, S. S., Lurndahl, N. A., Schwabenlander, M. D., Karwan, D. L., Li, E. A., Bartz, J. C., Yuan, Q., Larsen, P. A., Wolf, T. M. (2025). Detection of chronic wasting disease prions in soil at an illegal white-tailed deer carcass disposal site. *Prion*, 19(1), 8–19. https://doi.org/10.1080/19336896.2025.2514947

Guo, Y., Lin, K., Gao, X., Zheng, Q., Zhou, T., Zhao, Y. (2024). Disinfection efficacy of slightly acidic electrolyzed water on microorganisms: Application in contaminated waste sorting rooms across varied scenarios. *Journal of Cleaner Production*, 467, 142938. https://doi.org/10.1016/j.jclepro.2024.142938

Hadlow W. J. (2008). Kuru likened to scrapie: the story remembered. *Philosophical transactions of the Royal Society of London. Series B, Biological sciences*, 363(1510), 3644. https://doi.org/10.1098/rstb.2008.4013

Haley, N. J., Richt, J. A. (2017). Evolution of Diagnostic Tests for Chronic Wasting Disease, a Naturally Occurring Prion Disease of Cervids. *Pathogens*, 6(3), 35. https://doi.org/10.3390/pathogens6030035

Hamir, A. N., Kunkle, R. A., Miller, J. M., Bartz, J. C., Richt, J. A. (2006). First and second cattle passage of transmissible mink encephalopathy by intracerebral inoculation. *Veterinary pathology*, 43(2), 118–126. https://doi.org/10.1354/vp.43-2-118

Hara, H., Sakaguchi, S. (2020). N-Terminal Regions of Prion Protein: Functions and Roles in Prion Diseases. *Int J of Mol Sci*, 21(17), 6233. https://doi.org/10.3390/ijms21176233

Harpaz, E., Vuong, T. T., Tran, L., Tranulis, M. A., Benestad, S. L., Ersdal, C. (2023). Inter- and intra-species conversion efficacies of Norwegian prion isolates estimated by serial protein misfolding cyclic amplification. *Veterinary research*, *54*(1), 84. https://doi.org/10.1186/s13567-023-01220-7

Hawkins, C. L., Pattison, D. I., Davies, M. J. (2003). Hypochlorite-induced oxidation of amino acids, peptides and proteins. *Amino acids*, 25(3-4), 259–274. https://doi.org/10.1007/s00726-003-0016-x

Heath, C. A., Barker, R. A., Esmonde, T. F., Harvey, P., Roberts, R., Trend, P., Head, M. W., Smith, C., Bell, J. E., Ironside, J. W., Will, R. G., Knight, R. S. (2006). Dura mater-associated Creutzfeldt-Jakob disease: experience from surveillance in the UK. *Journal of neurology, neurosurgery, and psychiatry*, 77(7), 880–882. https://doi.org/10.1136/jnnp.2005.073395

Heinzer, D., Avar, M., Pfammatter, M., Moos, R., Schwarz, P., Buhmann, M. T., Kuhn, B., Mauerhofer, S., Rosenberg, U., Aguzzi, A., Hornemann, S. (2024). Advancing surgical instrument safety: A screen of oxidative and alkaline prion decontaminants using real-time quaking-induced conversion with prion-coated steel beads as surgical instrument mimetic. *PloS one*, 19(6), e0304603. https://doi.org/10.1371/journal.pone.0304603

Heisey, D. M., Mickelsen, N. A., Schneider, J. R., Johnson, C. J., Johnson, C. J., Langenberg, J. A., Bochsler, P. N., Keane, D. P., Barr, D. J. (2010). Chronic wasting disease (CWD) susceptibility of several North American rodents that are sympatric with cervid CWD epidemics. *Journal of virology*, 84(1), 210–215. https://doi.org/10.1128/JVI.00560-09

Henry, R., Murphy, F. A. (2017). Etymologia: Creutzfeldt-Jakob Disease. *Emerging Infectious Diseases*, 23(6), 956. https://doi.org/eid2306.ET2306

Henry, R., Schonburger, L. B. (2020). Etymologia: Scrapie. *Emerging Infectious Diseases*, 26(6), 1139. https://doi.org/10.3201/eid2606.ET2606

Herzog, L., Reine, F., Castille, J., Passet, B., Moudjou, M., Bonnet, R., Torres, J. M., Rezaei, H., Vilotte, J. L., Béringue, V., Igel, A. (2025). Optimization and evaluation of new decontamination procedures inactivating human prions. *The Journal of hospital infection*, 160, 109–117. https://doi.org/10.1016/j.jhin.2024.12.013

Hilbe, M. M., Soldati, G. G., Zlinszky, K. K., Wunderlin, S. S., Ehrensperger, F. F. (2009). Immunohistochemical study of PrP(Sc) distribution in neural and extraneural tissues of two cats with feline spongiform encephalopathy. *BMC veterinary research*, 5, 11. https://doi.org/10.1186/1746-6148-5-11

Hirata, Y., Ito, H., Furuta, T., Ikuta, K., Sakudo, A. (2010). Degradation and destabilization of abnormal prion protein using alkaline detergents and proteases. *International journal of molecular medicine*, 25(2), 267–270. https://doi.org/10.3892/ijmm_00000340

Holz, C. L., Darish, J. R., Straka, K., Grosjean, N., Bolin, S., Kiupel, M., Sreevatsan, S. (2022). Evaluation of Real-Time Quaking-Induced Conversion, ELISA, and Immunohistochemistry for Chronic Wasting Disease Diagnosis. *Frontiers in veterinary science*, 8, 824815. https://doi.org/10.3389/fvets.2021.824815

Hosszu, L. L. P., Conners, R., Sangar, D., Batchelor, M., Sawyer, E. B., Fisher, S., Cliff, M. J., Hounslow, A. M., McAuley, K., Leo Brady, R., Jackson, G. S., Bieschke, J., Waltho, J. P., Collinge, J. (2020). Structural effects of the highly protective V127 polymorphism on human prion protein. *Communications biology*, 3(1), 402. https://doi.org/10.1038/s42003-020-01126-6

Houston, F., Andréoletti, O. (2018). The zoonotic potential of animal prion diseases. *Handbook of clinical neurology*, 153, 447–462. https://doi.org/10.1016/B978-0-444-63945-5.00025-8

Hoyt, F., Alam, P., Artikis, E., Schwartz, C. L., Hughson, A. G., Race, B., Baune, C., Raymond, G. J., Baron, G. S., Kraus, A., Caughey, B. (2022). Cryo-EM of prion strains from the same genotype of host identifies conformational determinants. *PLoS pathogens*, 18(11), e1010947. https://doi.org/10.1371/journal.ppat.1010947

Høy-Petersen, J., Niedringhaus, K., Henderson, D. M., Armstrong, J. P., Livengood, J., Tewari, D., Gagne, R. B., Gibison, M. (2025). RT-QuIC detection of chronic wasting disease prions in third

eyelids from white-tailed deer. *Scientific Reports*, 15(8946). https://doi.org/10.1038/s41598-025-94146-3

Huang, H., Spencer, J. L., Soutyrine, A., Guan, J., Rendulich, J., Balachandran, A. (2007). Evidence for degradation of abnormal prion protein in tissues from sheep with scrapie during composting. *Canadian journal of veterinary research = Revue canadienne de recherche veterinaire*, 71(1), 34–40.

Huang, H., Spencer, J. L., Guan, J. (2010). In Vitro Microbial Degradation of Abnormal Prions in Central Nervous System from Scrapie Affected Sheep. *The Open Veterinary Science Journal*, 4(1), 20–26. https://doi.org/10.2174/1874318801004010020

Huang, H., Rendulich, J., Stevenson, D., O'Rourke, K., Balachandran, A. (2005). Evaluation of Western blotting methods using samples with or without sodium phosphotungstic acid precipitation for diagnosis of scrapie and chronic wasting disease. *Canadian journal of veterinary research = Revue canadienne de recherche veterinaire*, *69*(3), 193–199.

Hughes, D., Halliday, M. (2017). What Is Our Current Understanding of PrPSc-Associated Neurotoxicity and Its Molecular Underpinnings?. *Pathogens*, 6(4), 63. https://doi.org/10.3390/pathogens6040063

Hughson, A. G., Race, B., Kraus, A., Sangaré, L. R., Robins, L., Groveman, B. R., Saijo, E., Phillips, K., Contreras, L., Dhaliwal, V., Manca, M., Zanusso, G., Terry, D., Williams, J. F., Caughey, B. (2016). Inactivation of Prions and Amyloid Seeds with Hypochlorous Acid. *PLoS Pathogens*, 12(9), e1005914. https://doi.org/10.1371/journal.ppat.1005914

Igel, A., Fornara, B., Rezaei, H., Béringue, V. (2023). Prion assemblies: structural heterogeneity, mechanisms of formation, and role in species barrier. *Cell and tissue research*, 392(1), 149–166. https://doi.org/10.1007/s00441-022-03700-2

Imran, M., Mahmood, S. (2011). An overview of animal prion diseases. *Virology journal*, 8, 493. https://doi.org/10.1186/1743-422X-8-493

Inzalaco, H. N., Bravo-Risi, F., Morales, R., Walsh, D. P., Storm, D. J., Pedersen, J. A., Turner, W. C., Lichtenberg, S. S. (2023). Ticks harbor and excrete chronic wasting disease prions. *Scientific reports*, 13(1), 7838. https://doi.org/10.1038/s41598-023-34308-3

Iram, A., Wang, X., Demirci, A. (2021). Electrolyzed Oxidizing Water and Its Applications as Sanitation and Cleaning Agent. *Food Engineering Reviews*, *13*(2), 411–427. https://doi.org/10.1007/s12393-021-09278-9

Ishida, Y., Tian, T., Brandt, A. L., Kelly, A. C., Shelton, P., Roca, A. L., Novakofski, J., Mateus-Pinilla, N. E. (2020). Association of chronic wasting disease susceptibility with prion protein variation in white-tailed deer (*Odocoileus virginianus*). *Prion*, 14(1), 214–225. https://doi.org/10.1080/19336896.2020.1805288

Jennelle, C. S., Samuel, M. D., Nolden, C. A., Berkley, E. A. (2009). Deer Carcass Decomposition and Potential Scavenger Exposure to Chronic Wasting Disease. *The Journal of Wildlife Management*, 73(5), 655–662. https://doi.org/10.2193/2008-282

Johnson, C. J., Phillips, K. E., Schramm, P. T., McKenzie, D., Aiken, J. M., Pedersen, J. A. (2006). Prions adhere to soil minerals and remain infectious. *PLoS pathogens*, 2(4), e32. https://doi.org/10.1371/journal.ppat.0020032

Kang, H. E., Mo, Y., Abd Rahim, R., Lee, H. M., Ryou, C. (2017). Prion Diagnosis: Application of Real-Time Quaking-Induced Conversion. *BioMed Research International*, 2017. https://doi.org/10.1155/2017/5413936

Katsikaki, G., Dagklis, I. E., Angelopoulos, P., Ntantos, D., Prevezianou, A., Bostantjopoulou, S. (2021). Atypical and early symptoms of sporadic Creutzfeldt–Jakob disease: case series and review of the literature. *International Journal of Neuroscience*, 131(9), 927–938. https://doi.org/10.1080/00207454.2020.1759594

Kim, M. O., Takada, L. T., Wong, K., Forner, S. A., Geschwind, M. D. (2018). Genetic PrP Prion Diseases. *Cold Spring Harbor perspectives in biology*, 10(5), a033134. https://doi.org/10.1101/cshperspect.a033134

Kim, J. I., Cali, I., Surewicz, K., Kong, Q., Raymond, G. J., Atarashi, R., Race, B., Qing, L., Gambetti, P., Caughey, B., Surewicz, W. K. (2010). Mammalian prions generated from bacterially expressed prion protein in the absence of any mammalian cofactors. *The Journal of biological chemistry*, 285(19), 14083–14087. https://doi.org/10.1074/jbc.C110.113464

Kim, H. J., Tango, C. N., Chelliah, R., Oh, D. H. (2019). Sanitization Efficacy of Slightly Acidic Electrolyzed Water against pure cultures of Escherichia coli, Salmonella enterica, Typhimurium,

Staphylococcus aureus and Bacillus cereus spores, in Comparison with Different Water Hardness. *Scientific reports*, 9(1), 4348. https://doi.org/10.1038/s41598-019-40846-6

Kim, S. K., Lee, J. H. (2016). Biofilm dispersion in Pseudomonas aeruginosa. *Journal of microbiology (Seoul, Korea)*, 54(2), 71–85. https://doi.org/10.1007/s12275-016-5528-7

Kirisawa, R., Kato, R., Furusaki, K., Onodera, T. (2022). Universal Virucidal Activity of Calcium Bicarbonate Mesoscopic Crystals That Provides an Effective and Biosafe Disinfectant. *Microorganisms*, 10(2), 262. https://doi.org/10.3390/microorganisms10020262

Kirkwood, J. K., Cunningham, A. A. (1994). Epidemiological observations on spongiform encephalopathies in captive wild animals in the British Isles. *The Veterinary record*, 135(13), 296–303. https://doi.org/10.1136/vr.135.13.296

Klingeborn, M., Wik, L., Simonsson, M., Renström, L. H. M., Ottinger, T., Linné, T. (2006). Characterization of proteinase K-resistant N- and C-terminally truncated PrP in Nor98 atypical scrapie. *The Journal of general virology*, 87(Pt 6), 1751–1760. https://doi.org/10.1099/vir.0.81618-0

Konold, T., Bone, G. E., Clifford, D., Chaplin, M. J., Cawthraw, S., Stack, M. J., Simmons, M. M. (2012). Experimental H-type and L-type bovine spongiform encephalopathy in cattle: observation of two clinical syndromes and diagnostic challenges. BMC veterinary research, 8, 22. https://doi.org/10.1186/1746-6148-8-22

Konold, T., Hawkins, S. A., Thurston, L. C., Maddison, B. C., Gough, K. C., Duarte, A., Simmons, H. A. (2015). Objects in Contact with Classical Scrapie Sheep Act as a Reservoir for Scrapie Transmission. *Frontiers in veterinary science*, 2, 32. https://doi.org/10.3389/fvets.2015.00032

Kupfer, L., Hinrichs, W., Groschup, M. H. (2009). Prion protein misfolding. *Current molecular medicine*, 9(7), 826–835. https://doi.org/10.2174/156652409789105543

Kurt, T. D., Bett, C., Fernández-Borges, N., Joshi-Barr, S., Hornemann, S., Rülicke, T., Castilla, J., Wüthrich, K., Aguzzi, A., Sigurdson, C. J. (2014). Prion transmission prevented by modifying the β2-α2 loop structure of host PrPC. *The Journal of neuroscience: the official journal of the Society for Neuroscience*, 34(3), 1022–1027. https://doi.org/10.1523/JNEUROSCI.4636-13.2014

Kuznetsova, A., McKenzie, D., Banser, P., Siddique, T., Aiken, J. M. (2014). Potential role of soil properties in the spread of CWD in western Canada. *Prion*, 8(1), 92–99. https://doi.org/10.4161/pri.28467

LaFauci, G., Carp, R. I., Meeker, H. C., Ye, X., Kim, J. I., Natelli, M., Cedeno, M., Petersen, R. B., Kascsak, R., Rubenstein, R. (2006). Passage of chronic wasting disease prion into transgenic mice expressing Rocky Mountain elk (Cervus elaphus nelsoni) PrPC. *The Journal of general virology*, 87(Pt 12), 3773–3780. https://doi.org/10.1099/vir.0.82137-0

Lasmézas, C. I., Deslys, J. P., Robain, O., Jaegly, A., Beringue, V., Peyrin, J. M., Fournier, J. G., Hauw, J. J., Rossier, J., Dormont, D. (1997). Transmission of the BSE agent to mice in the absence of detectable abnormal prion protein. *Science*, 275(5298), 402–405. https://doi.org/10.1126/science.275.5298.402

Lee, J., Chang, I. (2019). Structural insight into conformational change in prion protein by breakage of electrostatic network around H187 due to its protonation. *Sci Rep*, 9, 19305. https://doi.org/10.1038/s41598-019-55808-1

Le Roy, D. G., Klein, K. K. (2005). Mad Cow Chaos in Canada: Was It Just Bad Luck or Did Government Policies Play a Role? *Canadian Public Policy / Analyse de Politiques*, 31(4), 381–399.

Levin, J., Schmidt, F., Boehm, C., Prix, C., Bötzel, K., Ryazanov, S., Leonov, A., Griesinger, C., Giese, A. (2014). The oligomer modulator anle138b inhibits disease progression in a Parkinson mouse model even with treatment started after disease onset. *Acta neuropathologica*, 127(5), 779–780. https://doi.org/10.1007/s00401-014-1265-3

Lezmi, S., Bencsik, A., Monks, E., Petit, T., Baron, T. (2003). First case of feline spongiform encephalopathy in a captive cheetah born in France: PrP(sc) analysis in various tissues revealed unexpected targeting of kidney and adrenal gland. *Histochemistry and cell biology*, 119(5), 415–422. https://doi.org/10.1007/s00418-003-0524-5

Li, J., Browning, S., Mahal, S. P., Oelschlegel, A. M., Weissmann, C. (2010). Darwinian evolution of prions in cell culture. *Science*, 327(5967), 869–872. https://doi.org/10.1126/science.1183218

Liato, V., Labrie, S., Aïder, M. (2017). Study of the antibacterial activity of electro-activated solutions of salts of weak organic acids on Salmonella enterica, Staphylococcus aureus and Listeria

monocytogenes. *Journal of industrial microbiology & biotechnology*, *44*(1), 23–33. https://doi.org/10.1007/s10295-016-1859-y

Liberski, P. P., Sikorska, B., Guiroy, D., Bessen, R. A. (2009). Transmissible mink encephalopathy - review of the etiology of a rare prion disease. *Folia neuropathologica*, 47(2), 195–204.

Liberski, P. P., Gajos, A., Sikorska, B., Lindenbaum, S. (2019). Kuru, the First Human Prion Disease. *Viruses*, 11(3), 232. https://doi.org/10.3390/v11030232

Litzroth, A., Cras, P., De Vil, B., Quoilin, S. (2015). Overview and evaluation of 15 years of Creutzfeldt-Jakob disease surveillance in Belgium, 1998-2012. *BMC neurology*, 15, 250. https://doi.org/10.1186/s12883-015-0507-x

Lo, R. Y., Shyu, W. C., Lin, S. Z., Wang, H. J., Chen, S. S., Li, H. (2007). New molecular insights into cellular survival and stress responses: neuroprotective role of cellular prion protein (PrP^{C}). *Molecular neurobiology*, 35(3), 236–244. https://doi.org/10.1007/s12035-007-8003-y

Lugaresi, E., Medori, R., Montagna, P., Baruzzi, A., Cortelli, P., Lugaresi, A., Tinuper, P., Zucconi, M., Gambetti, P. (1986). Fatal familial insomnia and dysautonomia with selective degeneration of thalamic nuclei. *The New England journal of medicine*, 315(16), 997–1003. https://doi.org/10.1056/NEJM198610163151605

Majumder, P., Chakrabarti, O. (2018). Lysosomal Quality Control in Prion Diseases. Molecular neurobiology, 55(3), 2631–2644. https://doi.org/10.1007/s12035-017-0512-8

Makarava, N., Savtchenko, R., Baskakov, I. V. (2017). Methods of Protein Misfolding Cyclic Amplification. *Methods in molecular biology*, 1658, 169–183. https://doi.org/10.1007/978-1-4939-7244-9_13

Manka, S. W., Wenborn, A., Collinge, J., Wadsworth, J. D. F. (2023). Prion strains viewed through the lens of cryo-EM. *Cell and tissue research*, 392(1), 167–178. https://doi.org/10.1007/s00441-022-03676-z

Manson, J. C., Diack, A. B. (2016). Evaluating the Species Barrier. *Food safety*, 4(4), 135–141. https://doi.org/10.14252/foodsafetyfscj.2016022

Mathiason, C. K., Hays, S. A., Powers, J., Hayes-Klug, J., Langenberg, J. (2009). Infectious Prions in Pre-Clinical Deer and Transmission of Chronic Wasting Disease Solely by Environmental Exposure. *PLoS ONE*, 4(6), 5916. https://doi.org/10.1371/journal.pone.0005916

Mathiason, C. K., Nalls, A. V., Seelig, D. M., Kraft, S. L., Carnes, K., Anderson, K. R., Hayes-Klug, J., Hoover, E. A. (2013). Susceptibility of domestic cats to chronic wasting disease. *Journal of virology*, 87(4), 1947–1956. https://doi.org/10.1128/JVI.02592-12

Marín-Moreno, A., Huor, A., Espinosa, J., Douet, J., Aguilar-Calvo, P., Aron, N., Píquer, A., Lugan, S., Lorenzo, P., Tiller, C., Cassard, H., Andreoletti, O.,Torres, J. (2020). Radical Change in Zoonotic Abilities of Atypical BSE Prion Strains as Evidenced by Crossing of Sheep Species Barrier in Transgenic Mice. *Emerging Infectious Disease*s, 26(6), 1130-1139. https://doi.org/10.3201/eid2606.181790.

Marrero-Winkens, C., Sankaran, C., Schätzl, H. M. (2020). From Seeds to Fibrils and Back: Fragmentation as an Overlooked Step in the Propagation of Prions and Prion-Like Proteins. *Biomolecules*, 10(9), 1305. https://doi.org/10.3390/biom10091305

McAlary, L., Plotkin, S. S., Yerbury, J. J., Cashman, N. R. (2019). Prion-Like Propagation of Protein Misfolding and Aggregation in Amyotrophic Lateral Sclerosis. *Frontiers in molecular neuroscience*, 12, 262. https://doi.org/10.3389/fnmol.2019.00262

McDonnell, G., & Burke, P. (2003). The challenge of prion decontamination. *Clinical infectious diseases*, 36(9), 1152–1154. https://doi.org/10.1086/374668

McGlinchey, R. P., Kryndushkin, D., Wickner, R. B. (2011). Suicidal [PSI+] is a lethal yeast prion. *Proceedings of the National Academy of Sciences of the United States of America*, 108(13), 5337–5341. https://doi.org/10.1073/pnas.1102762108

McGuire, L. I., Peden, A. H., Orrú, C. D., Wilham, J. M., Appleford, N. E., Mallinson, G., Andrews, M., Head, M. W., Caughey, B., Will, R. G., Knight, R. S., Green, A. J. (2012). Real time quaking-induced conversion analysis of cerebrospinal fluid in sporadic Creutzfeldt-Jakob disease. *Annals of neurology*, 72(2), 278–285. https://doi.org/10.1002/ana.23589

McNulty, E., Nalls, A. V., Mellentine, S., Hughes, E., Pulscher, L., Hoover, E. A., Mathiason, C. K. (2019). Comparison of conventional, amplification and bio-assay detection methods for a chronic

wasting disease inoculum pool. *PloS one*, 14(5), e0216621. https://doi.org/10.1371/journal.pone.0216621

Miles, S. L., Takizawa, K., Gerba, C. P., Pepper, I. L. (2011). Survival of infectious prions in water. *Journal of Environmental Science and Health. Part A, Toxic/Hazardous Substances Environmental Engineering*, 46(9), 938–943. https://doi.org/10.1080/10934529.2011.586247

Moazami-Goudarzi, K., Andréoletti, O., Vilotte, JL., Beringue, V. (2021). Review on PRNP genetics and susceptibility to chronic wasting disease of Cervidae. *Vet Res*, 52, 128. https://doi.org/10.1186/s13567-021-00993-z

Mok, T. H., Nihat, A., Luk, C., Sequeira, D., Batchelor, M., Mead, S., Collinge, J., Jackson, G. S. (2021). Bank vole prion protein extends the use of RT-QuIC assays to detect prions in a range of inherited prion diseases. Scientific reports, 11(1), 5231. https://doi.org/10.1038/s41598-021-84527-9

Moore, S. J., Vrentas, C. E., Hwang, S., West Greenlee, M. H., Nicholson, E. M., Greenlee, J. J. (2018). Pathologic and biochemical characterization of PrPSc from elk with PRNP polymorphisms at codon 132 after experimental infection with the chronic wasting disease agent. *BMC veterinary research*, 14(1), 80. https://doi.org/10.1186/s12917-018-1400-9

Moreno, J. A., Telling, G. C. (2017). Insights into Mechanisms of Transmission and Pathogenesis from Transgenic Mouse Models of Prion Diseases. *Methods in molecular biology*, 1658, 219–252. https://doi.org/10.1007/978-1-4939-7244-9_16

Mori, T., Atarashi, R., Furukawa, K., Takatsuki, H., Satoh, K., Sano, K., Nakagaki, T., Ishibashi, D., Ichimiya, K., Hamada, M., Nakayama, T., Nishida, N. (2016). A direct assessment of human prion adhered to steel wire using real-time quaking-induced conversion. *Scientific reports*, 6, 24993. https://doi.org/10.1038/srep24993

Moško, T., Galušková, S., Matěj, R., Brůžová, M., Holada, K. (2021). Detection of Prions in Brain Homogenates and CSF Samples Using a Second-Generation RT-QuIC Assay: A Useful Tool for Retrospective Analysis of Archived Samples. *Pathogens*, 10(6), 750. https://doi.org/10.3390/pathogens10060750

Moudjou, M., Castille, J., Passet, B., Herzog, L., Reine, F., Vilotte, J. L., Rezaei, H., Béringue, V., Igel-Egalon, A. (2020). Improving the Predictive Value of Prion Inactivation Validation Methods to

Minimize the Risks of Iatrogenic Transmission With Medical Instruments. *Frontiers in Bioengineering and Biotechnology*, 8. https://doi.org/10.3389/FBIOE.2020.591024/FULL

Murphy, R. G., Scanga, J. A., Powers, B. E., Pilon, J. L., Vercauteren, K. C., Nash, P. B., Smith, G. C., Belk, K. E. (2009). Alkaline hydrolysis of mouse-adapted scrapie for inactivation and disposal of prion-positive material. *Journal of animal science*, 87(5), 1787–1793. https://doi.org/10.2527/jas.2008-1492

Nafe, R., Arendt, C. T., Hattingen, E. (2023). Human prion diseases and the prion protein - what is the current state of knowledge?. *Translational neuroscience*, 14(1), 20220315. https://doi.org/10.1515/tnsci-2022-0315

National CJD research and surveillance network. (2024, July 1). reutzfeldt–Jakob Disease in the United Kingdom by Calendar Year. *University of Edinburgh.* http://www.cjd.ed.ac.uk/sites/default/files/figs.pdf

NDA Staff. (2024, January 10). 41% OF DEER HUNTERS TAKE AT LEAST ONE DEER, BUT STATES RANGE FROM 18 TO 71%. *National Deer Association*. https://deerassociation.com/41-of-deer-hunters-take-at-least-one-deer

Ndjomgoue-Yossa, A. C., Nanseu-Nijiki, C. P., Ngameni, E. (2022). Effect of pH on *Escherichia coli* Removal by Electrocoagulation and Elimination Kinetics after Treatment. *Journal of Chemistry*, 5249368. https://doi.org/10.1155/2022/5249368

Ness, A., Aiken, J., McKenzie, D. (2023). Sheep scrapie and deer rabies in England prior to 1800. *Prion*, 17(1), 7–15. https://doi.org/10.1080/19336896.2023.2166749

Nyamende, N, E., Belay, Z, A., Caleb, O, J. (2023). Recent advances in electrolyzed water treatments: Mechanisms of action and its effect on browning, bioactive compounds, and disinfection of fresh-cut fruit and vegetables–A review. *Food Chemistry Advances*, 3, 100569. https://doi.org/10.1016/j.focha.2023.100569

Onodera, T., Sakudo, A., Iwamaru, Y., Yokoyama, T., Haritani, M., Sugiura, K., Shimakura, H., Haga, T., Onishi, R., Furusaki, K. (2022). Calcium bicarbonate as an antimicrobial, antiviral, and prion-inhibiting agent (Review). *Biomedical reports*, 17(1), 57. https://doi.org/10.3892/br.2022.1540

Orrú, C. D., Groveman, B. R., Hughson, A. G., Zanusso, G., Coulthart, M. B., Caughey, B. (2015). Rapid and sensitive RT-QuIC detection of human Creutzfeldt-Jakob disease using cerebrospinal fluid. *mBio*, 6(1). https://doi.org/10.1128/MBIO.02451-14

Orrú, C. D., Groveman, B. R., Hughson, A. G., Barrio, T., Isiofia, K., Race, B., Ferreira, N. C., Gambetti, P., Schneider, D. A., Masujin, K., Miyazawa, K., Ghetti, B., Zanusso, G., Caughey, B. (2024). Sensitive detection of pathological seeds of α-synuclein, tau and prion protein on solid surfaces. *PLoS pathogens*, 20(4), e1012175. https://doi.org/10.1371/journal.ppat.1012175

Otero, A., Duque Velásquez, C., Johnson, C., Herbst, A., Bolea, R., Badiola, J. J.,Aiken, J., McKenzie, D. (2019). Prion protein polymorphisms associated with reduced CWD susceptibility limit peripheral PrP^{CWD} deposition in orally infected white-tailed deer. *BMC veterinary research*, 15(1), 50. https://doi.org/10.1186/s12917-019-1794-z

Panes, J. D., Saavedra, P., Pineda, B., Escobar, K., Cuevas, M. E., Moraga-Cid, G., Fuentealba, J., Rivas, C. I., Rezaei, H., Muñoz-Montesino, C. (2021). PrP^{C} as a Transducer of Physiological and Pathological Signals. *Frontiers in molecular neuroscience*, 14, 762918. https://doi.org/10.3389/fnmol.2021.762918

Pauly, T., Bolakhrif, N., Kaiser, J., Nagel-Steger, L., Gremer, L., Gohlke, H., Willbold, D. (2022). Met/Val129 polymorphism of the full-length human prion protein dictates distinct pathways of amyloid formation. *The Journal of biological chemistry*, 298(10), 102430. https://doi.org/10.1016/j.jbc.2022.102430

Petigara, M., Dridi, C., Unterschultz, J. (2011). The Economic Impacts of Chronic Wasting Disease and Bovine Spongiform Encephalopathy in Alberta and the Rest of Canada. *Journal of Toxicology and Environmental Health, Part A*, 74(22–24), 1609–1620. https://doi.org/10.1080/15287394.2011.618987

Peretz, D., Supattapone, S., Giles, K., Vergara, J., Freyman, Y., Lessard, P., Safar, J. G., Glidden, D. V., McCulloch, C., Nguyen, H. O., Scott, M., Dearmond, S. J., Prusiner, S. B. (2006). Inactivation of prions by acidic sodium dodecyl sulfate. *Journal of virology*, 80(1), 322–331. https://doi.org/10.1128/JVI.80.1.322-331.2006

Plummer, I. H., Johnson, C. J., Chesney, A. R., Pedersen, J. A., Samuel, M. D. (2018). Mineral licks as environmental reservoirs of chronic wasting disease prions. *PloS one*, 13(5), e0196745. https://doi.org/10.1371/journal.pone.0196745

Poggiolini, I., Saverioni, D., Parchi, P. (2013). Prion protein misfolding, strains, and neurotoxicity: an update from studies on Mammalian prions. *International journal of cell biology*, 2013, 910314. https://doi.org/10.1155/2013/910314

Pritzkow, S., Morales, R., Moda, F., Khan, U., Telling, G. C., Hoover, E., Soto, C. (2015). Grass plants bind, retain, uptake, and transport infectious prions. *Cell reports*, 11(8), 1168–1175. https://doi.org/10.1016/j.celrep.2015.04.036

Pritzkow, S., Morales, R., Lyon, A., Concha-Marambio, L., Urayama, A., Soto, C. (2018). Efficient prion disease transmission through common environmental materials. *The Journal of biological chemistry*, 293(9), 3363–3373. https://doi.org/10.1074/jbc.M117.810747

Pritzkow, S., Gorski, D., Ramirez, F., Soto, C. (2021). Prion Dissemination through the Environment and Medical Practices: Facts and Risks for Human Health. *Clinical microbiology reviews*, 34(4), e0005919. https://doi.org/10.1128/CMR.00059-19

Prusiner S. B. (1982). Novel proteinaceous infectious particles cause scrapie. *Science*, 216(4542), 136–144. https://doi.org/10.1126/science.6801762

Prusiner S. B. (1998). Prions. *Proceedings of the National Academy of Sciences of the United States of America*, 95(23), 13363–13383. https://doi.org/10.1073/pnas.95.23.13363

Prusiner S. B. (2013). Biology and genetics of prions causing neurodegeneration. *Annual review of genetics*, 47, 601–623. https://doi.org/10.1146/annurev-genet-110711-155524

Race, B., Meade-White, K. D., Miller, M. W., Barbian, K. D., Rubenstein, R., LaFauci, G., Cervenakova, L., Favara, C., Gardner, D., Long, D., Parnell, M., Striebel, J., Priola, S. A., Ward, A., Williams, E. S., Race, R., Chesebro, B. (2009). Susceptibilities of nonhuman primates to chronic wasting disease. *Emerging infectious diseases*, 15(9), 1366–1376. https://doi.org/10.3201/eid1509.090253

Raymond, G. J., Zhao, H. T., Race, B., Raymond, L. D., Williams, K., Swayze, E. E., Graffam, S., Le, J., Caron, T., Stathopoulos, J., O'Keefe, R., Lubke, L. L., Reidenbach, A. G., Kraus, A., Schreiber, S. L., Mazur, C., Cabin, D. E., Carroll, J. B., Minikel, E. V., Kordasiewicz, H., Vallabh, S. M. (2019). Antisense oligonucleotides extend survival of prion-infected mice. *JCI insight*, 5(16), e131175. https://doi.org/10.1172/jci.insight.131175

Rikhvanov, E. G., Romanova, N. V., Chernoff, Y. O. (2007). Chaperone effects on prion and nonprion aggregates. *Prion*, 1(4), 217–222. https://doi.org/10.4161/pri.1.4.5058

Rohilla, A., Kumar, V., Ahire, J. J. (2024). Unveiling the persistent threat: recent insights into *Listeria monocytogenes* adaptation, biofilm formation, and pathogenicity in foodborne infections. *Journal of food science and technology*, 61(8), 1428–1438. https://doi.org/10.1007/s13197-023-05918-6

Rossi, M., Baiardi, S., Parchi, P. (2019). Understanding Prion Strains: Evidence from Studies of the Disease Forms Affecting Humans. *Viruses*, 11(4), 309. https://doi.org/10.3390/v11040309

Sakudo, A., Ano, Y., Onodera, T., Nitta, K., Shintani, H., Ikuta, K., Tanaka, Y. (2011). Fundamentals of prions and their inactivation (review). *International journal of molecular medicine*, 27(4), 483–489. https://doi.org/10.3892/ijmm.2011.605

Sakudo A. (2020). Inactivation Methods for Prions. *Current issues in molecular biology*, 36, 23–32. https://doi.org/10.21775/cimb.036.023

Sakudo, A., Anraku, D., Itarashiki, T. (2020). Inactivation of Prions by Low-Temperature Sterilization Technology Using Vaporized Gas Derived from a Hydrogen Peroxide-Peracetic Acid Mixture. *Pathogens*, 10(1), 24. https://doi.org/10.3390/pathogens10010024

Sakudo, A., Iwamaru, Y., Furusaki, K., Haritani, M., Onishi, R., Imamura, M., Yokoyama, T., Yoshikawa, Y., Onodera, T. (2020). Inactivation of Scrapie Prions by the Electrically Charged Disinfectant CAC-717. Pathogens. 9(7), 536. https://doi.org/10.3390/pathogens9070536

Sakudo, A., Yamashiro, R., Onodera, T. (2022). Recent Advances in Prion Inactivation by Plasma Sterilizer. *International journal of molecular sciences*, 23(18), 10241. https://doi.org/10.3390/ijms231810241

Sakudo, A., Furusaki, K., Onishi, R., Onodera, T., Yoshikawa, Y. (2025). A Review of CAC-717, a Disinfectant Containing Calcium Hydrogen Carbonate Mesoscopic Crystals. *Microorganisms*, 13(3), 507. https://doi.org/10.3390/microorganisms13030507

Saunders, S. E., Bartelt-Hunt, S. L., Bartz, J. C. (2008). Prions in the environment: occurrence, fate and mitigation. *Prion*, 2(4), 162–169. https://doi.org/10.4161/pri.2.4.7951

Saunders, S. E., Bartelt-Hunt, S. L., Bartz, J. C. (2012). Occurrence, transmission, and zoonotic potential of chronic wasting disease. *Emerging infectious diseases*, 18(3), 369–376. https://doi.org/10.3201/eid1803.110685

Saunders, S. E., Bartz, J. C., Vercauteren, K. C., Bartelt-Hunt, S. L. (2010). Enzymatic digestion of chronic wasting disease prions bound to soil. *Environmental science & technology*, 44(11), 4129–4135. https://doi.org/10.1021/es903520d

Schilling, K. M., Jorwal, P., Ubilla-Rodriguez, N. C., Assafa, T. E., Gatdula, J. R. P., Vultaggio, J. S., Harris, D. A., Millhauser, G. L. (2023). N-glycosylation is a potent regulator of prion protein neurotoxicity. *The Journal of biological chemistry, 299(9), 1*05101. https://doi.org/10.1016/j.jbc.2023.105101

Schmitz, M., Zafar, S., Silva, C. J., Zerr, I. (2014). Behavioral abnormalities in prion protein knockout mice and the potential relevance of PrP(C) for the cytoskeleton. *Prion*, *8*(6), 381–386. https://doi.org/10.4161/19336896.2014.983746

Schramm, P. T., Johnson, C. J., Mathews, N. E., McKenzie, D., Aiken, J. M., Pedersen, J. A. (2006). Potential Role of Soil in the Transmission of Prion Disease. *Reviews in Mineralogy and Geochemistry*, 64(1), 135-152. https://doi.org/10.2138/rmg.2006.64.5

Serio T. R. (2018). [PIN+]ing down the mechanism of prion appearance. *FEMS yeast research*, 18(3), foy026. https://doi.org/10.1093/femsyr/foy026

Sigurdson, C. J., Miller, M. W. (2003). Other animal prion diseases. *British medical bulletin*, 66, 199–212. https://doi.org/10.1093/bmb/66.1.199

Silva, C. J., Vázquez-Fernández, E., Onisko, B., Requena, J. R. (2015). Proteinase K and the structure of PrPSc: The good, the bad and the ugly. *Virus research*, 207, 120–126. https://doi.org/10.1016/j.virusres.2015.03.008

Simmons, M. M., Chaplin, M. J., Konold, T., Casalone, C., Beck, K. E., Thorne, L., Everitt, S., Floyd, T., Clifford, D., Spiropoulos, J. (2016). L-BSE experimentally transmitted to sheep presents as a unique disease phenotype. *Veterinary research*, *47*(1), 112. https://doi.org/10.1186/s13567-016-0394-1

Simmons, S. M., Payne, V. L., Hrdlicka, J. G., Taylor, J., Larsen, P. A., Wolf, T. M., Schwabenlander, M. D., Yuan, Q., Bartz, J. C. (2024). Rapid and sensitive determination of residual prion infectivity from prion-decontaminated surfaces. *mSphere*, 9(9), e0050424. https://doi.org/10.1128/msphere.00504-24

Sitammagari, K. K., Masood, W. (2024, January 30). Creutzfeldt Jakob disease. StatPearls [Internet]. https://www.ncbi.nlm.nih.gov/books/NBK507860/

Shim, K. H., Sharma, N., An, S. S. A. (2022). Prion therapeutics: Lessons from the past. *Prion*, *16*(1), 265–294. https://doi.org/10.1080/19336896.2022.2153551

Slapšak, U., Salzano, G., Ilc, G., Giachin, G., Bian, J., Telling, G., Legname, G., Plavec, J. (2019). Unique Structural Features of Mule Deer Prion Protein Provide Insights into Chronic Wasting Disease. *ACS omega*, 4(22), 19913–19924. https://doi.org/10.1021/acsomega.9b02824

Smith, C. B., Booth, C. J., Wadzinski, T. J., Legname, G., Chappel, R., Johnson, C. J., Pedersen, J. A. (2014). Humic substances interfere with detection of pathogenic prion protein. *Soil Biology and Biochemistry*. 68, 309-316. https://doi.org/10.1016/j.soilbio.2013.10.005

Smith, C. B., Booth, C. J., Pedersen, J. A. (2011). Fate of prions in soil: a review. Journal of environmental quality, 40(2), 449–461. https://doi.org/10.2134/jeq2010.0412

Soto, C., Pritzkow, S. (2018). Protein misfolding, aggregation, and conformational strains in neurodegenerative diseases. Nature neuroscience, 21(10), 1332–1340. https://doi.org/10.1038/s41593-018-0235-9

Soto, C., Satani, N. (2011). The intricate mechanisms of neurodegeneration in prion diseases. *Trends in molecular medicine*, 17(1), 14–24. https://doi.org/10.1016/j.molmed.2010.09.001

Stanley B. Prusiner – Biographical. NobelPrize.org. Nobel Prize Outreach AB 2024. Thu. 23 May 2024. https://www.nobelprize.org/prizes/medicine/1997/prusiner/biographical/

Stefani, M., Rigacci, S. (2013). Protein folding and aggregation into amyloid: the interference by natural phenolic compounds. *International journal of molecular sciences*, 14(6), 12411–12457. https://doi.org/10.3390/ijms140612411

Šulskis, D., Šneiderienė, G., Žiaunys, M., Smirnovas, V. (2023). The seeding barrier between human and Syrian hamster prion protein amyloid fibrils is determined by β2-α2 loop sequence elements.

International journal of biological macromolecules, 238, 124038. https://doi.org/10.1016/j.ijbiomac.2023.124038

Sun, Y., Jack, K., Ercolani, T., Sangar, D., Hosszu, L., Collinge, J., Bieschke, J. (2023). Direct Observation of Competing Prion Protein Fibril Populations with Distinct Structures and Kinetics. *ACS nano*, 17(7), 6575–6588. https://doi.org/10.1021/acsnano.2c12009

Taylor D. M. (1993). Inactivation of SE agents. *British medical bulletin*, *49*(4), 810–821. https://doi.org/10.1093/oxfordjournals.bmb.a072648

Taylor D. M. (2000). Inactivation of transmissible degenerative encephalopathy agents: A review. *Veterinary journal*, 159(1), 10–17. https://doi.org/10.1053/tvjl.1999.0406

Teferedegn, E. Y., Yaman, Y., Un, C. (2020). Five novel PRNP gene polymorphisms and their potential effect on Scrapie susceptibility in three native Ethiopian sheep breeds. *BMC veterinary research*, 16(1), 122. https://doi.org/10.1186/s12917-020-02336-0

Teng, Z., Luo, Y., Alborzi, S., Zhou, B., Chen, L., Zhang, J., Zhang, B., Millner, P., Wang, Q. (2018). Investigation on chlorine-based sanitization under stabilized conditions in the presence of organic load. *International journal of food microbiology*, 266, 150–157. https://doi.org/10.1016/j.ijfoodmicro.2017.11.027

Thomas, C. M., Salamat, M. K. F., Almela, F., Cooper, J. K., Ladhani, K., Arnold, M. E., Bougard, D., Andréoletti, O., Houston, E. F. (2024). Longitudinal detection of prion infection in preclinical sheep blood samples compared using 3 assays. *Blood*, 144(18), 1962–1973. https://doi.org/10.1182/blood.2024024649

Thorn, R. M., Lee, S. W., Robinson, G. M., Greenman, J., Reynolds, D. M. (2012). Electrochemically activated solutions: evidence for antimicrobial efficacy and applications in healthcare environments. *European journal of clinical microbiology & infectious diseases : official publication of the European Society of Clinical Microbiology*, *31*(5), 641–653. https://doi.org/10.1007/s10096-011-1369-9

Tian, Y., Viles, J. H. (2022). pH Dependence of Amyloid-β Fibril Assembly Kinetics: Unravelling the Microscopic Molecular Processes. *Angewandte Chemie (International ed. in English)*, 61(48), e202210675. https://doi.org/10.1002/anie.202210675

Toni, M., Massimino, M. L., De Mario, A., Angiulli, E., Spisni, E. (2017). Metal Dyshomeostasis and Their Pathological Role in Prion and Prion-Like Diseases: The Basis for a Nutritional Approach. *Frontiers in neuroscience*, 11, 3. https://doi.org/10.3389/fnins.2017.00003

True, H. L., Lindquist, S. L. (2000). A yeast prion provides a mechanism for genetic variation and phenotypic diversity. *Nature*, 407(6803), 477–483. https://doi.org/10.1038/35035005

U. S. Centres for Disease Control and Prevention. (2024, May 13). About Variant Creutzfeldt-Jakob Disease (vCJD). *U.S. Department of Health and Human Services.* https://www.cdc.gov/variant-creutzfeldt-jakob/about/index.html

U.S. Environmental Protection Agency. (2024, August 21). Efficacy test methods, test criteria, and labeling guidance for antimicrobial products with claims against biofilm on hard, non-porous surfaces. *EPA.gov*. Retrieved June 17, 2025, from https://www.epa.gov/pesticide-analytical-methods/efficacy-test-methods-test-criteria-and-labeling-guidance

van der Kamp, M. W., Daggett, V. (2010). Influence of pH on the human prion protein: insights into the early steps of misfolding. *Biophysical journal*, 99(7), 2289–2298. https://doi.org/10.1016/j.bpj.2010.07.063

Vascellari, S., Orrù, C. D., Hughson, A. G., King, D., Barron, R., Wilham, J. M., Baron, G. S., Race, B., Pani, A., Caughey, B. (2012). Prion seeding activities of mouse scrapie strains with divergent PrPSc protease sensitivities and amyloid plaque content using RT-QuIC and eQuIC. *PloS one*, 7(11), e48969. https://doi.org/10.1371/journal.pone.0048969

Vaske, J.J., Needham, M. D., Newman, P, Manfredo, M.J., Petchenik,J. (2006). Potential for conflict index: Hunters' responses to chronic wasting disease. *Wildlife Society Bulletin*, 34, 44- 50. https://doi.org/10.2193/0091-7648(2006)34[44:PFCIHR]2.0.CO;2

Wang, Z., Qin, K., Camacho, M. V., Cali, I., Yuan, J., Shen, P., Greenlee, J., Kong, Q., Mastrianni, J. A., Zou, W. Q. (2021). Generation of human chronic wasting disease in transgenic mice. *Acta neuropathologica communications*, 9(1), 158. https://doi.org/10.1186/s40478-021-01262-y

Wang, F., Pritzkow, S., Soto, C. (2023). PMCA for ultrasensitive detection of prions and to study disease biology. *Cell and tissue research*, 392(1), 307–321. https://doi.org/10.1007/s00441-022-03727-5

Watson, N., Brandel, J. P., Green, A., Hermann, P., Ladogana, A., Lindsay, T., Mackenzie, J., Pocchiari, M., Smith, C., Zerr, I., Pal, S. (2021). The importance of ongoing international surveillance for Creutzfeldt-Jakob disease. *Nature reviews*. Neurology, 17(6), 362–379. https://doi.org/10.1038/s41582-021-00488-7

Weissmann, C., Büeler, H. (2004). A mouse to remember. *Cell*, *116*(2 Suppl), S111–S113. https://doi.org/10.1016/s0092-8674(04)00032-7

Westergard, L., Christensen, H. M., Harris, D. A. (2007). The cellular prion protein (PrP(C)): its physiological function and role in disease. *Biochimica et biophysica acta*, 1772(6), 629–644. https://doi.org/10.1016/j.bbadis.2007.02.011

Whitaker, J. R., Feeney, R. E. (1983). Chemical and physical modification of proteins by the hydroxide ion. *Critical reviews in food science and nutrition,* 19(3), 173–212. https://doi.org/10.1080/10408398309527375

Wickner, R. B., Edskes, H. K., Shewmaker, F., Nakayashiki, T. (2007). Prions of fungi: inherited structures and biological roles. *Nature reviews. Microbiology*, 5(8), 611–618. https://doi.org/10.1038/nrmicro1708

Wilham, J. M., Orrú, C. D., Bessen, R. A., Atarashi, R., Sano, K., Race, B., Meade-White, K. D., Taubner, L. M., Timmes, A., Caughey, B. (2010). Rapid end-point quantitation of prion seeding activity with sensitivity comparable to bioassays. *PLoS pathogens*, 6(12), e1001217. https://doi.org/10.1371/journal.ppat.1001217

Wille, H., Requena, J. R. (2018). The Structure of PrP^{Sc} Prions. *Pathogens, 7*(1), 20. https://doi.org/10.3390/pathogens7010020

Williams, E. S., Young, S. (1980). Chronic wasting disease of captive mule deer: a spongiform encephalopathy. *Journal of wildlife diseases*, 16(1), 89–98. https://doi.org/10.7589/0090-3558-16.1.89

Williams, K., Hughson, A. G., Chesebro, B., Race, B. (2019). Inactivation of chronic wasting disease prions using sodium hypochlorite. *PloS one*, 14(10), e0223659. https://doi.org/10.1371/journal.pone.0223659

World Organization for Animal Health (OIE). (2023, May 30). *Bovine spongiform encephalopathy.* https://www.woah.org/en/disease/bovine-spongiform-encephalopathy/

World Health Organization. (2018, February 20). *Listeriosis*. https://www.who.int/news-room/fact-sheets/detail/listeriosis

Wulf, M., Senatore, A. Aguzzi, A. (2017) The biological function of the cellular prion protein: an update. *BMC Biol*, 15(34). https://doi.org/10.1186/s12915-017-0375-5

Wyatt, J. M., Pearson, G. R., Smerdon, T. N., Gruffydd-Jones, T. J., Wells, G. A., Wilesmith, J. W. (1991). Naturally occurring scrapie-like spongiform encephalopathy in five domestic cats. *The Veterinary record*, 129(11), 233–236. https://doi.org/10.1136/vr.129.11.233

Wyckoff, A. C., Kane, S., Lockwood, K., Seligman, J., Michel, B., Hill, D., Ortega, A., Mangalea, M. R., Telling, G. C., Miller, M. W., Vercauteren, K., Zabel, M. D. (2016). Clay Components in Soil Dictate Environmental Stability and Bioavailability of Cervid Prions in Mice. *Frontiers in microbiology*, 7, 1885. https://doi.org/10.3389/fmicb.2016.01885

Yamaguchi, K., Kamatari, Y. O., Ono, F., Shibata, H., Fuse, T., Elhelaly, A. E., Fukuoka, M., Kimura, T., Hosokawa-Muto, J., Ishikawa, T., Tobiume, M., Takeuchi, Y., Matsuyama, Y., Ishibashi, D., Nishida, N., Kuwata, K. (2019). A designer molecular chaperone against transmissible spongiform encephalopathy slows disease progression in mice and macaques. *Nature biomedical engineering*, 3(3), 206–219. https://doi.org/10.1038/s41551-019-0349-8

Yilmaz, G., Morrill, T., Pilot, W., Ward, C., Mitchell, G., Soutyrine, A., Dan, H., Lin, M., Guan, J. (2024). Optimization of RT-QuIC Assay Duration for Screening Chronic Wasting Disease in White-Tailed Deer. *Veterinary sciences*, 11(2), 60. https://doi.org/10.3390/vetsci11020060

Zafar, S., Younas, N., Shafiq, M., Zerr, I. (2019). Prion Protein Strain Diversity and Disease Pathology. *IntechOpen*. doi: 10.5772/intechopen.80702

Zerr, I., Schmitz, M. (2021, January 7). Genetic Prion Disease. *National Library of Medicine*. https://www.ncbi.nlm.nih.gov/books/NBK1229/

Zhang, J., Chu, M., Tian, Z., Xie, K., Cui, Y., Liu, L., Meng, J., Yan, H., Ji, Y. M., Jiang, Z., Xia, T. X., Wang, D., Wang, X., Zhao, Y., Ye, H., Li, J., Wang, L., Wu, L. (2022). Clinical profile of fatal familial insomnia: phenotypic variation in 129 polymorphisms and geographical regions. *Journal*

of neurology, neurosurgery, and psychiatry, 93(3), 291–297. https://doi.org/10.1136/jnnp-2021-327247

Zhao, M. M., Feng, L. S., Hou, S., Shen, P. P., Cui, L., Feng, J. C. (2019). Gerstmann-Sträussler-Scheinker disease: A case report. *World journal of clinical cases*, *7*(3), 389–395. https://doi.org/10.12998/wjcc.v7.i3.389

Zhou, H. X., Pang, X. (2018). Electrostatic Interactions in Protein Structure, Folding, Binding, and Condensation. *Chemical reviews,* 118(4), 1691–1741. https://doi.org/10.1021/acs.chemrev.7b00305

Zobeley, E., Flechsig, E., Cozzio, A., Enari, M., Weissmann, C. (1999). Infectivity of scrapie prions bound to a stainless steel surface. *Molecular medicine*, 5(4), 240–243.